The role of CCM proteins in β1 Integrin-Klf2-Egfl7-mediated angiogenesis

D i s s e r t a t i o n

zur Erlangung des akademischen Grades

d o c t o r r e r u m n a t u r a l i u m

(Dr. rer. nat.)

im Fach Biologie

eingereicht an der

Lebenswissenschaftlichen Fakultät

der Humboldt-Universität zu Berlin

von

Marc Andreas Renz

Präsident der Humboldt-Universität zu Berlin

Prof. Dr. Jan-Hendrik Olbertz

Dekanin/Dekan der Lebenswissenschaftlichen Fakultät

Prof. Dr. Richard Lucius

Gutachter/innen:
1. Prof. Dr. Harald Saumweber
2. Prof. Dr. Salim Seyfried
3. Prof. Dr. Michael Bader

Tag der mündlichen Prüfung: 04.12.2015

TABLE OF CONTENTS

Summary

Angiogenesis is critical to most physiological processes and many pathological conditions. This process is controlled by physical interactions between the extracellular matrix (ECM) and endothelial cells. Klf2, a blood flow–sensitive transcription factor, promotes VEGF-dependent angiogenesis during zebrafish cardiovascular development. However, the mechanism by which biophysical stimuli regulate Klf2 expression and control angiogenesis remains largely unknown.

In my study, I show that elevated *klf2* mRNA levels underlie the molecular and morphogenetic cardiovascular defects in zebrafish *ccm* mutants. Furthermore, I demonstrate that these defects are mediated by enhanced *egfl7* expression and angiogenesis signaling. My study also revealed that Klf2 expression is regulated by the extracellular matrix-binding receptor β1 integrin in the absence of blood flow. The CCM protein complex and its associated β1 integrin-regulatory protein ICAP-1 prevents increased angiogenesis signaling in endothelial cells by limiting β1 integrin-mediated expression of Klf2.

ln sum, my work uncovered a novel β1 integrin-Klf2-Egfl7 signaling pathway, which is regulated by the cerebral cavernous malformations (CCM) proteins.

Zusammenfassung

Angiogenese ist entscheidend für die meisten physiologische Prozesse und viele pathologische Umstände. Dabei wird Angiogenese durch die Interaktion zwischen der extrazellulären Matrix (ECM) und endothelialen Zellen reguliert. Während der kardiovaskulären Entwicklung im Zebrafisch fördert Klf2, ein blutstrom-sensitiver Transkriptionsfaktor, die VEGF-abhängige Angiogenese. Der Mechanismus, bei dem biophysikalische Reize die Klf2 Expression regulieren und Angiogenese kontrollieren, ist größtenteils unbekannt.

In meiner Studie zeige ich, dass erhöhte *klf2* mRNA Expression den molekularen und morphogenetischen kardiovaskulären Defekten in Zebrafisch *ccm* Mutanten zugrundeliegen. Desweiteren zeige ich, dass diese Defekte durch verstärkte *egfl7*-Expression und Angiogenese vermittelt werden. Meine Studie zeigt ausserdem, dass die Klf2-Expression unabhängig vom Blutstrom durch den Extrazellularmatrix-bindenden Rezeptor β1 Integrin reguliert wird. Der CCM-Protein-Komplex, zusammen mit dem ihm verbundenden Integrin-regulierenden Protein ICAP-1 verhindert ein verstärktes Angiogenese-Signal in endothelialen Zellen, indem es die β1 Integrin-abhängige Klf2 Expression begrenzt.

Zusammenfassend zeigt meine Arbeit einen neuen β1 Integrin-Klf2-Egfl7 Signalweg, der durch zerebrale kavernöse malformations (CCM) Proteine reguliert wird.

1 Introduction

1.1 Cerebral Cavernous Malformation

1.1.1 CCM proteins in the human pathology

Cerebral cavernous malformations (CCMs) are vascular lesions within low blood flow venous capillary beds. They are characterized by mulberry-like clusters of thin-walled, enlarged blood vessels arranged to densely packed sinusoids without intervening neural parenchyma (Introduction Fig. 1) (Fischer et al., 2013). Ultrastructural analyses of CCMs revealed ruptures and damages in the luminal endothelium due to a lack of endothelial junctions and detachements between the endothelium and basal lamina. Furthermore, these lesions lack supporting subendothelial cells such as smooth muscle

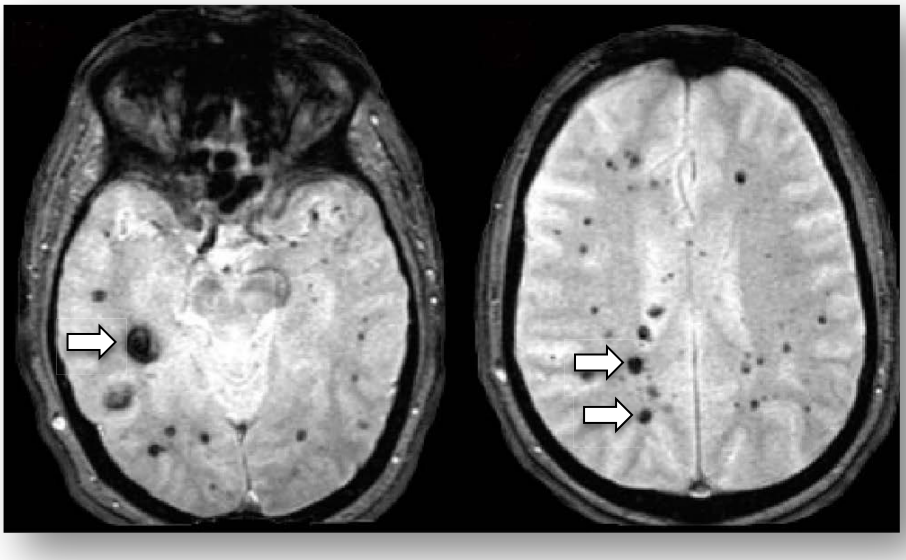

Introduction Figure 1
Magnetic Resonance Imaging (MRI) of multiple cerebral cavernous malformations in human patients (white arrows, adapted from Cooper et al., 2008)

cells, elastic tissue, or astrocytic foot processes (Clatterbuck et al., 2001; Tanriover et al., 2013). Primarily, CCMs are found within the neurovasculature of the central

nervous system, where they can cause headaches, seizure, and neurological deficits caused by cerebral hemorrhages (Dobyns et al., 1987; Gil-Nagel et al., 1995), but they can also occur in the skin (Eerola et al., 2000; Labauge et al., 1999).

CCMs have a prevalence of approximately 0,5% of the entire population (Otten et al., 1989). CCMs may occur in both sporadic or familial forms. The sporadic form accounts for 80% of CCMs and is mostly associated with a single CCM formation. In contrast, most of the familial cases develop multiple CCMs (Krisht et al., 2010; Riant et al., 2010). Familial CCMs are autosomal-dominant and are associated with heterozygous germline loss-of-function due to a mutation in at least one of the three genes, CCM1 (Laberge-le Couteulx et al., 1999; Sahoo et al., 1999), CCM2 (Denier et al., 2004; Liquori et al., 2003), or CCM3 (Bergametti et al., 2005). A „second hit“, or Knudsonian mutation is needed for a somatic loss-of-function of the second allele (Akers et al., 2009; Gault et al., 2005; Pagenstecher et al., 2009). The total loss-of-function of any of these genes may then result in CCM lesions.

1.1.2 Structure and functions of CCM proteins

1.1.2.1 KRIT1 (Krev interaction trapped 1)/ CCM1

In human and mouse, KRIT1 is a 736 amino acid protein that consists of a N-terminal Nudix domain, three canonical NPxY/F motifs and a C-terminal FERM (band 4.1, ezrin, radixin, moesin) domain (Introduction Fig. 2) (Gingras et al., 2013; Li et al., 2012; Liu et al., 2013). It was identified in a yeast two-hybrid screen as an interaction partner of the small GTPase Krev-1 (Rap1) (Serebriiskii et al., 1997). During early embryogenesis, KRIT1 is broadly expressed with a preference to endothelial cells (Guzeloglu-Kayisli et al., 2004). Intracellularly, KRIT1 was found in different cellular compartments, including cell-cell junctions in endothelial cells (Glading et al., 2007; Zawistowski et al., 2005). The subcellular localization of KRIT1 appears to be dependent on its conformational organization (Beraud-Dufour et al., 2007; Francalanci et al., 2009). It has been suggested that intramolecular binding of the NPxY/F motifs with its FERM domain results in a „closed“ conformation which allows KRIT1 to bind to microtubules (Beraud-Dufour et al., 2007). KRIT1 is then transported along

microtubules to the plasma membrane. There, activated Rap1 binds to KRIT1 and causes an „open“ conformation thereby enabling the relocalization of KRIT1 to the membrane and the stabilization of adherence junctions (Liu et al., 2011). Junctional stability is achived by the association of KRIT1 with components of the adherence junctions (β-catenin, α-catenin, VE-cadherin, AF 6 and p120-catenin) (Glading et al., 2007). Loss of KRIT1 results in a translocation of β-catenin to the nucleus and a transcriptional up-regulation of β-catenin target genes. Rap1 binding stabilizes KRIT1 and prevents the dissociation of β-catenin from the junctional complex (Introduction Fig. 7) (Glading et al., 2010). In zebrafish, knock-down of Rap1b leads to intracranial hemorrhage due to damaged endothelial junctions. Intriguingly, combinatorial minor reduction of Rap1b and Krit1 results in intracranial hemorrhage, indicating that both genes act in a common pathway (Gore et al., 2008). However, proteomic analysis showed that Rap1 was not found in the CCM complex suggesting that KRIT1 and Rap1 act in an independent complex (Hilder et al., 2007). In addition, loss of KRIT1 resulted in defective endothelial cell polarity by impairing localization of the TIAM-PAR3-PKCζ complex, vascular lumen formation, and directed cell migration (Lampugnani et al., 2010). These findings are similiar to human vascular lesions, where endothelial cells are loosely connected to each other (Clatterbuck et al., 2001).

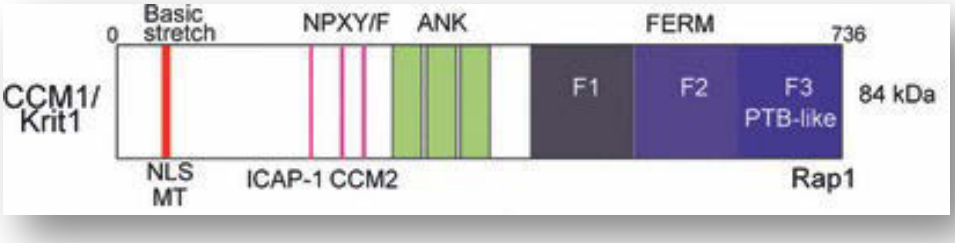

Introduction Figure 2

Structural domains and interaction partners of KRIT1/CCM1. Krit1 comprises a C-terminal FERM (band 4.1, ezrin, radixin, moesin) domain and three N-terminal NPXY/F motifs. ANK: Ankyrin domain, NLS: Nuclear Localization Signal, MT: microtubules, PTB: PhosphoTyrosineBinding domain. (adapted from Faurobert and Albiges-Rizo, 2010)

Several lines of evidences suggested that the formation of CCM lesions could be driven by aberrant angiogenesis (Jung et al., 2003). Loss of KRIT1 reduces the

expression of the Notch target genes *DLL4*, *HEY1*, and *HEY2* and leads to enhanced sprouting formation in endothelial cells (Wustehube et al., 2010). Conversely, KRIT1 overexpression leads to increased expression of HEY1 and DLL4, arguing for a modulation of angiogenesis by a KRIT1-Notch signaling cascade.

Another binding partner of KRIT1 is the integrin cytoplasmic domain associated protein-1 (ICAP-1) (Introduction Fig. 3). ICAP-1 is a negative regulator of β1 integrin signaling (Liu et al., 2013; Millon-Fremillon et al., 2008). New data shows that KRIT1 stabilizes ICAP-1 in endothelial cells and prevents increased β1 integrin signaling. ICAP-1 levels are reduced upon loss of KRIT1 resulting in increased β1 integrin activation and actin stress fiber formation (Faurobert et al., 2013). Conversely, KRIT1

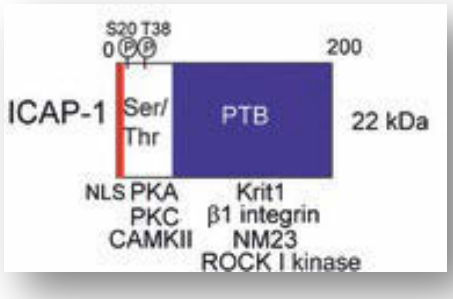

Introduction Figure 3

Structural domains and interaction partners of ICAP-1. ICAP-1 bears a Ser/Thr riche N-terminal NLS motif and phosphorylation sites for Calmodulin-dependent kinase II, Protein kinase A and C. (adapted from Faurobert and Albiges-Rizo, 2010)

and the cytoplasmic tail of β1 integrin compete for the same binding site of ICAP-1. Hence, binding of KRIT1 to ICAP-1 prevents the inhibition of β1 integrin activation (Liu et al., 2013).

Blood vessels in CCM lesions are frequently characterized by a loss of junctional stability, vessel integrity, loss of cell polarity, and increased endothelial cell proliferation. These are hallmarks of a process known as endothelial-mesenchymal transition (EndMT). Recent data showed that the loss of KRIT1 or PDCD10 (CCM3) results in EndMT due to inreased BMP6-SMAD signaling in endothelial cells (Maddaluno et al., 2013). Intriguingly, this signaling pathway is also up-regulated in human patient material with a loss of KRIT1 or CCM2 (Maddaluno et al., 2013).

1.1.2.2 CCM2/ Malcavernin

CCM2 consists of a N-terminal PTB domain (Liquori et al., 2003) and C-terminal harmonin-homology domain (HHD) (Introduction Fig. 4) (Fischer et al., 2013) and was identified in a yeast two-hybrid screen as a scaffold for the MEKK3/MKK3 complex (Uhlik et al., 2003). The MEKK3/MKK3 complex is required to restore cell volume and morphology upon osmotic shock by activation of its downstream target p38 MAPK.

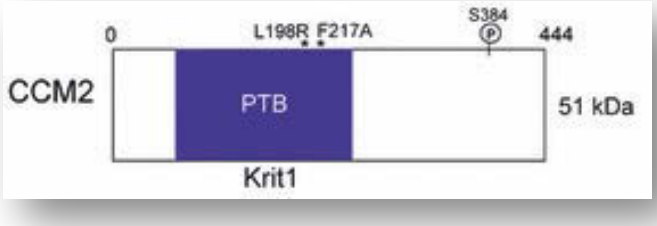

Introduction Figure 4

Structural domains and interaction partners of CCM2. The CCM2 PTB domain interacts with a Krit1 NPXY/F motif. (adapted from Faurobert and Albiges-Rizo, 2010)

P38 MAPK activates actin reorganization and stabilization by inducing the F-actin cap binding protein HSP27 (Heat Shock Protein 27). Upon osmotic shock, the CCM2-MEKK3 complex is recruited to membrane ruffles to interact with Rac1 and F-actin. Therefore, the CCM2-MEKK3 complex reorganizes actin polymerization in a RAC1-dependent manner (Uhlik et al., 2003). Proteomic analysis revealed a direct interaction between CCM2, Rac and MEKK3 (Hilder et al., 2007). Interestingly, the loss of CCM2 does not the affect p38 MAPK pathway, but rather the JNK (c-Jun N-terminal kinase), MKK4, MKK7 pathway (Whitehead et al., 2009). Reduction of *CCM2* transcript levels increased the phosphorylation of JNK and its upstream targets MKK4 and MKK7 via increased RhoA levels. Intriguingly, elevated RhoA levels are a common feature after RNA-interference-mediated knock-down of any of the CCM proteins (Crose et al., 2009; Glading et al., 2007; Stockton et al., 2010; Whitehead et al., 2009) and inhibition of RhoA-ROCK signaling abolished RhoA-dependent actin stress fiber formation in heterozygous *Krit1* or *Ccm2* mice, and CCM-deficient cells (Borikova et al., 2010; Stockton et al., 2010; Whitehead et al., 2009). Co-immunoprecipitation assays showed that CCM2 interacts with the E3 ubiquitin ligase Smad ubiquitin regulatory factor 1

(SMURF1) through a PTB/NPXY interaction. This interaction leads to proteosomal RhoA degradation required for normal endothelial cell function (Crose et al., 2009).

Besides direct interaction of CCM2 with Rac1 and RhoA, it has been suggested that CCM2 is also involved in Cdc42 activation during vascular lumenization (Kleaveland et al., 2009; Whitehead et al., 2009). Cdc42 and Rac1 mediate lumen formation via the regulation of components of the cytoskeletal signaling (Pak2 and Pak4), and the cell polarity complex (Par3 and Par6) (Koh et al., 2008). CCM2 loss-of-function studies in zebrafish and mice revealed a failure of vascular lumen formation, although vacuoles are normally formed in the intersegmental vessels in zebrafish. In contrast, CCM2-depleted HUVECs exhibit decreased numbers of vacuoles and lumen formation in a 3D *in vitro* culture (Whitehead et al., 2009). These results imply that CCM2 acts at different levels in vascular lumen formation. Further investigations are needed to solve these conflicting results.

As mentioned above, KRIT1 and ICAP-1 complexes in the regulation of β1 integrin dependent stress fiber formation (Introduction Fig. 7). Since KRIT1 and ICAP-1 have a NLS motif, both are able to shuttle between the nucleus and the cytosol and activate transcriptional programs and cellular proliferation (Fournier et al., 2005; Francalanci et al., 2009; Zawistowski et al., 2005). *In vitro* assays showed that CCM2 can bind to KRIT1-ICAP-1 in a ternary complex to inhibit the nuclear translocation of KRIT1-ICAP-1 (Francalanci et al., 2009; Zawistowski et al., 2005) and therefore transcriptional activation of downstream target genes.

It has been shown that CCM2 induces cell death in neuroblastoma or medullablastoma by binding to the receptor tyrosine kinase TrkA in nerve cells (Harel et al., 2009) and subsequently recruiting a complex composed of CCM3/PDCD10 and STK25 (Costa et al., 2012).

The identification of CCM2-like (CCM2L), a CCM2 paralogue, allowed further insights into the role of CCM proteins in cardiovascular developement (Zheng et al., 2012). CCM2L is expressed in activated endothelial cells during cardiovascular development. Loss of CCM2L reduced endocardial growth factor expression and phenocopied the zebrafish Ccm2 phenotype. Overexpression of CCM2 partially rescues the CCM2L phenotype (Rosen et al., 2013). Moreover, CCM2L completely blocks CCM2-mediated junctional stability and competes with CCM2 for binding to KRIT1.

The contribution of CCM2L in human CCM pathology is still unknown and needs to be elucidated.

1.1.2.3 CCM3/ PDCD10 (Programmed cell death 10)

In human, CCM3 is a 212 amino acid protein that consists of a N-terminal dimerization domain (Introduction Fig. 5) (Kean et al., 2011; Li et al., 2010) and a C-terminal focal adhesion targeting-homology (FAT-H) domain. (Li et al., 2010). CCM3 can interact with CCM2 with its FAT-H domain to build the ternary KRIT1-CCM2-CCM3 complex

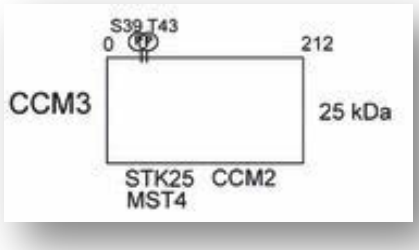

Introduction Figure 5

Structural domains and interaction partners of CCM3. CCM3 interacts with MST4, STK24, STK25, and CCM2. (adapted from Faurobert and Albiges-Rizo, 2010)

(Hilder et al., 2007). Furthermore, CCM3 heterodimerizes with several members of the germinal center kinase III protein family, including MST4/MASK, STK24/MST3 and STK25/YSK1/SOK1 (Sugden et al., 2013; Xu et al., 2013; Zhang et al., 2013a) within the striating interacting phosphatase and kinase (STRIPAK) complex to promote Golgi assembly and polarization (Fidalgo et al., 2010; Kean et al., 2011). CCM3-depletion in SaOS2 cells impaired directed cell migration due to a failure of correct Golgi repositioning towards the leading edge (Fidalgo et al., 2010). Recent studies discovered that CCM3 plays also a role in exocytosis. Loss of CCM3 or STK24 resulted in increased exocytosis of neutrophils due to a loss of interaction with UNC13 (Zhang et al., 2013b). In *Drosophila*, loss of CCM3 or GCKIII kinase resulted in dilated tracheal tubes (Song et al., 2013). These studies imply that defective lumen formation and vascular morphology in CCM pathology is in part caused by abnormal exocytosis.

CCM3-MST4 interaction has also been shown to be important in vascular cell polarity and junctional stability. Lkb1 is a tumor supressor gene and seems to control the subcellular localization of MST4 (ten Klooster et al., 2009), whereas CCM3 might regulate MST4 kinase activity (Ma et al., 2007). Loss of Lkb1 in endothelial cells leads to a marked reduction of vascular smooth muscle cells (vSMCs) and disruption of the vasculature due to a loss of TGFβ signaling in endothelial cells (Londesborough et al., 2008).

There is conflicting data on the function of CCM3: CCM3 promotes cell survival by binding to VEGFR2. Loss of CCM3 led to decreased VEGFR2 protein levels and to endocytosis of VEGFR2 after VEGF stimulation (He et al., 2010). In contrast, the loss of CCM3 increased cell survival and proliferation through increased VEGF signaling, inhibition of Notch signaling, or increased ERK activation (Louvi et al., 2011; You et al., 2013; Zhu et al., 2010). In zebrafish, which has two Ccm3 isoforms, it has been demonstrated that Ccm3-mediated signaling through Ste20-like kinases is involved in cardiovascular development (Zheng et al., 2010), and that CCM3 functions in a distinct manner from CCM1 and CCM2 (Yoruk et al., 2012). Indeed, neuronal-specific deletion of CCM3, but not CCM1 or CCM2, in mouse embryos resulted in vascular defects comparable to endothelial-specific knock-out of CCM1, CCM2, or CCM3 (Boulday et al., 2009; Boulday et al., 2011; Cunningham et al., 2011; Louvi et al., 2011). These results imply a neuronal contribution in the development of CCM lesions.

1.1.2.4 HEG1

Heart-of-glass (HEG1) is a transmembrane protein which is specifically expressed in endothelial and endocardial cells (Kleaveland et al., 2009). It contains an extracellular domain with two EGF-like repeats, a transmembrane region, and a cytoplasmic C-terminal NPXY/F domain within its short intracellular part (Introduction Fig. 6). Its only known binding partner is KRIT1. Since, loss of *heg1* in zebrafish results in the same cardiovascular defects as the loss of *krit1/ccm1* or *ccm2* (Kleaveland et al., 2009; Mably et al., 2003; Mably et al., 2006), it has been proposed that these three genes act in a common pathway. Biochemical analyses demonstrated that HEG1, KRIT1, and CCM2 can bind in a ternary complex (Kleaveland et al., 2009). HEG1-KRIT1 binding

Introduction Figure 6

Structural domains and interaction partners of HEG1. HEG1 carries two extracellular EGF-like repeats and interacts with Krit1 via its C-terminal NPXY/F motif. (adapted from Faurobert and Albiges-Rizo, 2010)

occurs through the interaction of the HEG1 NPXY/F domain and the KRIT1 FERM domain. Structural anaylses also showed that KRIT1 is able to simultaneously bind HEG1 and Rap1 via its FERM domain. Thus, HEG1 could act as an anchor protein that can recruit the Rap1-KRIT1 complex to the plasma membrane (Gingras et al., 2013). Since human patients with CCMs do not have mutations in HEG1, its role in this diesease is largely unknown.

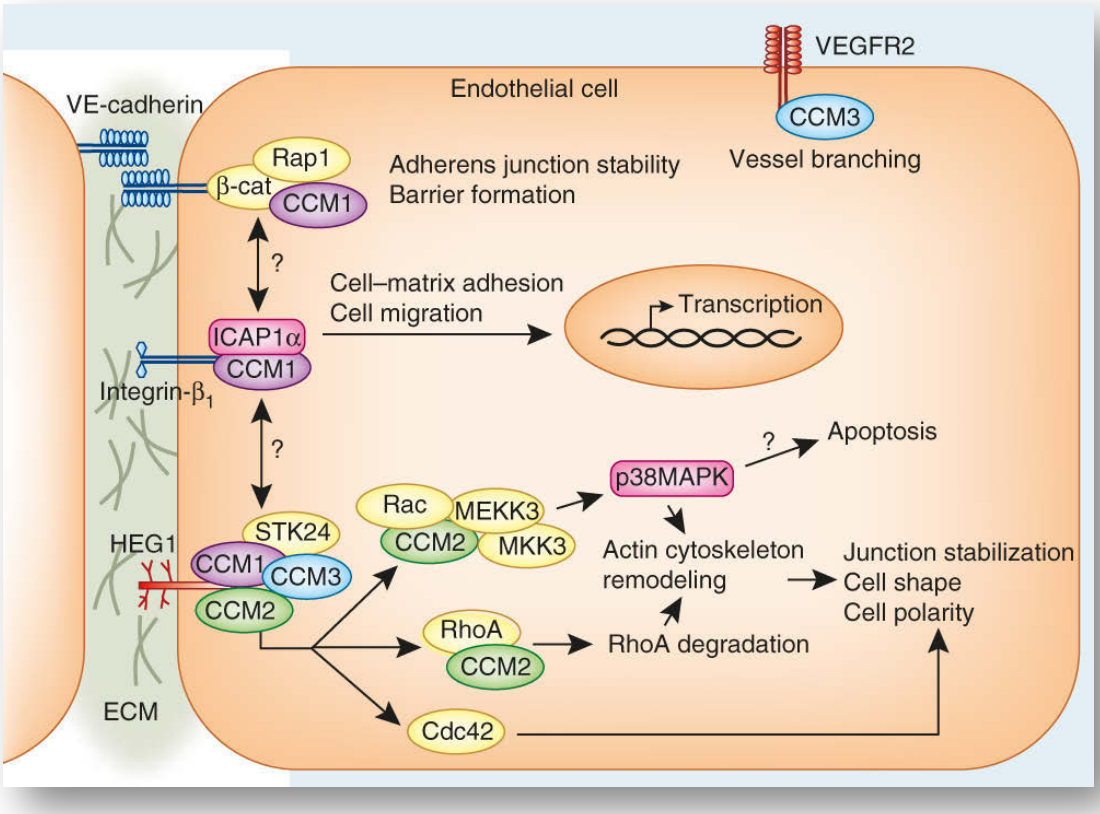

Introduction Figure 7

Molecular pathways of CCM proteins (adapted from Storkebaum et al., 2011)

1.2 Cardiovascular development in the zebrafish *Danio rerio*

1.2.1 Zebrafish as a model for vertebrate cardiovascular development

The zebrafish is an excellent model organism to study cardiovascular development, as the molecular mechanisms are highly similar to those in humans and other higher vertebrates. The eggs are fertilized extrauterinally and have an early stereotyped development. Since zebrafish embryos are optically transparent, organogenesis can be easily monitored during development. In addition, a variety of genetic and cell biological methods are available to manipulate and to investigate cellular processes in real time and to uncover the regulatory mechanisms involved in cardiovascular development.

1.2.2 Heart development in zebrafish

During vertebrate embryonic development, the heart is the first functional organ to form. Although the zebrafish heart has a less complex morphology, with just two heart chambers compared to the four chambered mammalian heart, genes responsible for essential steps of cardiac development are conserved throughout vertebrate evolution. Specification of endocardial and myocardial progenitor cells is the first step in cardiac development. Two pools of myocardial progenitor cells at either side in embryos of the 40% epiboly stage in the lateral marginal zone (Introduction Fig. 8A, Stainier et al., 1993). Ventricular progenitor cells are located more dorsally in the lateral marginal zone compared to atrial progenitor cells (Keegan et al., 2004). Myocardial progenitor cell number is restricted by retinoic acid (RA) signaling and the Hox5b transcription factor (Keegan et al., 2005; Waxman et al., 2008). Fgf signaling has also been shown to act downstream of RA. Retinoic acid signaling restricts the specification of cardiac progenitors by regulating Fgf signaling activity (Lin et al., 2010a; Sirbu et al., 2008). In contrast, endocardial progenitor cells are distributed throughout the marginal zone (Introduction Fig.8A; Keegan et al., 2004). During gastrulation, cardiac progenitor cells involute and are finally located in the anterior lateral plate mesoderm (ALPM) at the beginning of somitogenesis (Stainier et al., 1993; Warga et al., 1990).

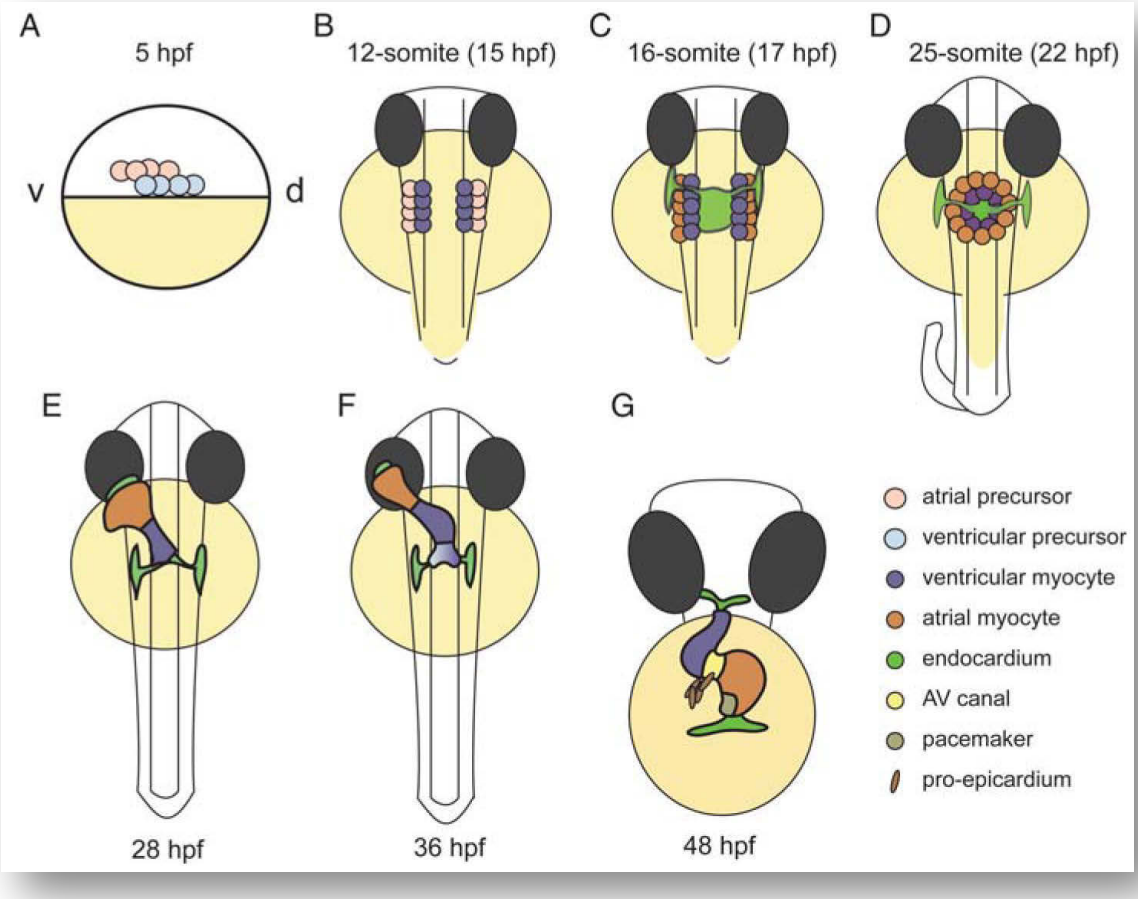

Introduction Figure 8

Heart development in zebrafish Danio rerio (adapted from Bakkers et al., 2011)

Cardiogenic differentiation is initiated at the one- to three-somite stage and requires the expression of the homeobox-containing transcription factor Nkx2.5. *Nkx2.5* expression is induced by bone morphogenic protein (Bmp) and Nodal signaling in the lateral plate mesoderm via the induction of the transcription factor Gata5 (Kishimoto et al., 1997; Reiter et al., 1999).

At the 14-somite stage myocardial cells start to express sarcomeric genes such as *myosin light chain polypeptide 7* (*myl7*) (Introduction Fig. 8B; de Pater et al., 2009; Yelon et al., 1999). At the same time, myocardial cells express chamber-specific genes and are regionalized in a medial to lateral direction in the ALPM. At the 16-somite stage (Introduction Fig. 8C) the bilaterial pools of myocardial cells start to migrate toward the embryonic midline and fuse 1 hour later: ventricular myocardial cells fuse first along the posterior half and then along the anterior half. The resulting structure is called heart cone (Yelon et al., 1999). In contrast to myocardial cells, four-dimensional

confocal microscopy has shown that endocardial cells migrate earlier and reach the midline at the 16-somite stage (Bussmann et al., 2007).

Once the heart cone has formed (Introduction Fig. 8D), myocardial cells from the right cardiac field involute ventrally and move towards the anterior/left with a simultaneous rotation in a clockwise direction (Baker et al., 2008; Bussmann et al., 2007; Rohr et al., 2008; Smith et al., 2008). As a consequence the heart cone is transformed into a tube at 28 hours post fertilization (Introduction Fig. 8E) with its arterial pole at the midline and the venous pole at the left side of the embryo. The endocardial cells are located within the lumen of the cardiac tube (Baker et al., 2008; Bussmann et al., 2007; Rohr et al., 2008). Asymmetric expression of Bmp and Nodal in the ALPM direct asymmetric heart morphogenesis (Baker et al., 2008; Smith et al., 2008; Veerkamp et al., 2013) and myocardial cell polarity and organization are essential for heart tube elongation (Rohr et al., 2008; Rohr et al., 2006; Peterson et al., 2001).

Between 30-48 hours post fertilization (hpf) the linear heart tube bends toward the right side and results in a displacement of the ventricle at the right side of the embryonic midline, whereas the atrium remains at the left side of the embryonic midline (Introduction Fig. 8E-G). Unequal speeds of rotation between the venous pole and arterial pole have been suggested to cause a torsion of the heart tube and to result in cardiac looping (Smith et al., 2008). During ventricular chamber morphogenesis, physical forces generated by blood flow have an impact on myocardial cell shapes and chamber ballooning (Auman et al., 2007; Dietrich et al, 2014).

Blood flow is also required for the formation of cardiac valves between the atrium and the ventricle to prevent blood from flowing back from the ventricle to the atrium. In amniotes, valve formation starts with a local swelling (cardiac cushions) at the atrioventricular canal (AVC). Endocardial cells overlying the local swelling receive a myocardial signal, delaminate and migrate into the space between endocardium and myocardium. The delamination of these endocardial cells occurs via epithelial-to-mesenchymal transition (EMT). In zebrafish, cardiac cushion formation starts at 36 hpf where specialized squamous endocardial cells at the AVC become cuboidal. These cells start to express the cell adhesion molecule Dm-grasp (Beis et al., 2005) and form cellular protrusions that extend into the cardiac jelly. In contrast to epithelial-to-mesenchymal transition in amniote heart valve development (Timmerman et al., 2004),

zebrafish endocardial valves arise by invagination of endocardial cells (Scherz et al., 2008). Although the mechanisms by which heart valves develop differ between zebrafish and amniotes, the underlying molecular pathways are conserved. Several signaling pathways are involved in valve development including Notch, ErbB, TGFb signaling, NFAT, and Wnt-beta-catenin signaling (Beis et al., 2005; Chang et al., 2004; Hurlstone et al., 2003; Scherz et al., 2008; Timmerman et al., 2004). Heart valve remodelling is also dependent on blood flow, since zebrafish *silent heart* mutants, which lack heart contraction, exhibit impaired valve formation (Bartman et al., 2004). Furthermore, expression of the shear stress transcription *klf2a* has been shown to regulate the invagination process of endocardial cells at the AVC by inducing Notch1 (Dietrich et al., 2014; Vermot et al., 2009).

1.2.3 Vascular development in zebrafish

In all vertebrates, endothelial and hematopoietic cells arise in close association with one another during embryonic development. In zebrafish, both cell types develop in the intermediate cell mass of the ventral mesoderm, whereas in birds and mammals, these cells develop in extraembryonic yolk sac blood islands (Detrich et al., 1995; Haar et al., 1971; Moore et al., 1965). Despite the spatially distinct manner across the species, they share the same genetic programs. During early embryonic development endothelial and hematopoietic cells are specified by the expression of *stem cell leukemia* (*scl*) and *fetal liver kinase-1/ vascular endothelial growth factor receptor 2* (*flk1*/ *vegfr2*) (Kabrun et al., 1997). The fact that both cell lineages express the same genes and develop in close association in the primitive lateral mesoderm raised the hypothesis of a common precursor cell referred as the hemangioblast. *In vivo* studies in mice and zebrafish provided evidences for the existence of such a cell (Huber et al., 2004; Vogeli et al., 2006).

During early somitogenesis endothelial precursor cells (angioblasts) begin to express endothelial-specific genes (Fouquet et al., 1997; Kimmel et al., 1990). The expression of transcription factors of the ETS gene family can induce the expression of *vegfr2* and vascular endothelial cadherin (*vecdn*) (Pham et al., 2007; Sumanas et al., 2006; Sumanas et al., 2008). Several studies also demonstrated that the binding of ETS

transcription factors with other factors, including members of the Forkhead (FOX) family of transcrption factors (De Val et al., 2008) and KLF genes (Meadows et al., 2009) plays an important role in the specification of endothelial cells. At the 14 somite stage, after endothelial cells are specified, they start migrate to the embryonic midline above the endoderm. There, the dorsal aorta (DA) and the posterior cardinal vein (PCV), the two major trunk axial vessels (Jin et al., 2005; Lawson et al., 2002b) are formed *de novo* by fusion of endothelial cells called angioblasts (vasculogenesis). It has been proposed that hypochord-derived soluble Vegf acts as a guidance cue for angioblast midline migration (Cleaver et al., 1998; Lawson et al., 2002c) and requires the ventral endodermal layer (Jin et al., 2005).

For a functional circulatory system it is essential that blood vessel acquire a venous or arterial identity. Ephrin B2-EphB4 signaling is crucial in this process. EphB4 is preferentially expressed in veins, whereas its ligand Ephrin B2 is expressed in arterial endothelial cells (Wang et al., 2010c). Additional signaling pathways involved in Ephrin-Eph-mediated arterial-venous specification, including Hedgehog, VEGF, and Notch signaling. Notch ligands and receptors are exclusively expressed in arterial endothelial cells and help to promote arterial differentiation (Lawson et al., 2001; Lawson et al., 2002a; Lawson et al., 2003). Notch signaling restricts arterial-specific *ephrinB2* and venous-specific *ephb4* expression. Alterations in *sonic hedgehog* (*shh*) or *vegf* activity causes the same arterial-venous specification defects like the loss-of-function or gain-of-function of Notch signaling (Lawson et al., 2002c; Lawson et al., 2002a). S*hh* induces the expression of *vegf* in the somites, and that *vegf* then activates Notch signaling in endothelial cells of the developing dorsal aorta, resulting in arterial differentiation.

Following the formation of the lateral dorsal aorta and the posterior cardinal vein by vasculogenesis, new blood vessels are formed by a process called angiogenesis. During angiogenesis, new vessels develop from preexisting vessels. The intersegmental vessels (ISVs) of the trunk are the first angiogenic vessels formed in all vertebrates. They sprout from the dorsal site of the dorsal aorta and migrate dorsally along vertical somite boundaries and interconnect at the dorsal-lateral surface of the neural tube.

The primary cranial vasculature is established by vasculogenesis of mesodermal-derived angioblasts. Subsequently, the craniofacial vascular network develops by

angiogenesis (Lee et al., 2009). At around 20 hours post fertilization (hpf), angioblasts from the lateral plate mesoderm migrate medially as two anterior and posterior cell populations to form the paired lateral dorsal aorta (LDA). These vessels are essential to provide the arterial supply of blood for the entire head (Isogai et al., 2001). Angiogenic growth of the LDA in the caudal direction and the connection with the posterior dorsal aorta results in a Y-shaped junction between these vessels (Isogai et al., 2001; Siekmann et al., 2009). The primordial hindbrain channels (PHBC) provide the sole venous drainage of the head and are also formed by vasculogenesis at the same time as the LDA. The basilar artery (BA), the most important artery in the vertebrate head, is formed between the PHBCs and the bilateral LDA. The central arteries (CtAs) in the hindbrain form later and connect the primordial hindbrain channels and the basilar artery.

Angiogenesis of the cranial vasculature depends on VEGF signaling, as does the ISV formation in the trunk region (Covassin et al., 2006). Furthermore Cxcl12b/ *cxcr4a* chemokine signaling is also involved in cranial vascular development (Siekmann et al., 2009).

Cord or cell hollowing are thought to be the primary mechanisms controlling vascular lumen formation. During this process, lumina form by the creation of fluid-filled spaces between cells or within single cells (Lubarsky et al., 2003). *In vitro* studies demonstrated that lumen formation requires intracellular vacuolation and intercellular fusion of endothelial vacuoles (Bayless et al., 2000; Bayless and Davis, 2002; Kamei et al., 2006). These processes are controlled by integrins, Cdc42, Rac, and cell polarity complexes (Bayless and Davis, 2002; Davis et al., 1996; Koh et al., 2008). In addition, endothelial cells overlap extensively (Blum et al., 2008; Wang et al., 2010b).

1.2.3.1 VEGF-Notch signaling in tip and stalk cell specification during angiogenesis

Blood vessel formation by angiogenesis requires the tight control and coordination of endothelial cell behaviour. The hierarchical organization of sprouting endothelial ´tip cells´(TCs) and trailing ´stalk cells´(SCs) is a key aspect in branching morphogenesis (Introduction Fig. 9). Endothelial tip cells extend long filopodia that sense attractive and/or repulsive signals in their environment and direct vascular growth (De Smet et al.,

2009; Gerhardt et al., 2003). Endothelial stalk cells, that trail TCs are less motile but support the extension of the sprouting vessel by cell proliferation. The regulation of tip cell and stalk cell specification is directed by VEGF and Notch signaling. VEGFR2 activation by binding of its ligand VEGFA leads to an up-regulation of the Notch ligand Delta-like-4 (DLL4) in tip cells and an activation of Notch signaling in adjacent stalk cells, which promotes stalk cell behaviour by lateral inhibition of tip cell fate decision (Hellstrom et al., 2007; Leslie et al., 2007; Lobov et al., 2007; Siekmann et al., 2007; Suchting et al., 2007). Hence, endothelial cells experiencing the highest level of VEGF signaling will be selected as tip cells. Notch activation in stalk cells suppresses VEGFR2 and VEGFR3/FLT4 signaling and proangiogenic fate (Siekmann et al., 2007; Tammela et al., 2008). In zebrafish, *flt4* is normally expressed in tip cells. Loss of Notch signaling results in an expansion of *flt4* expression throughout the stalk cell domain and in an increase of endothelial cells showing tip cell behaviours, including the hyper-sprouting phenotype.

Besides a direct regulation of VEGF signaling, the DLL4-Notch pathway may indirectly influence local guidance of sprouting vessels. It has been shown that Notch

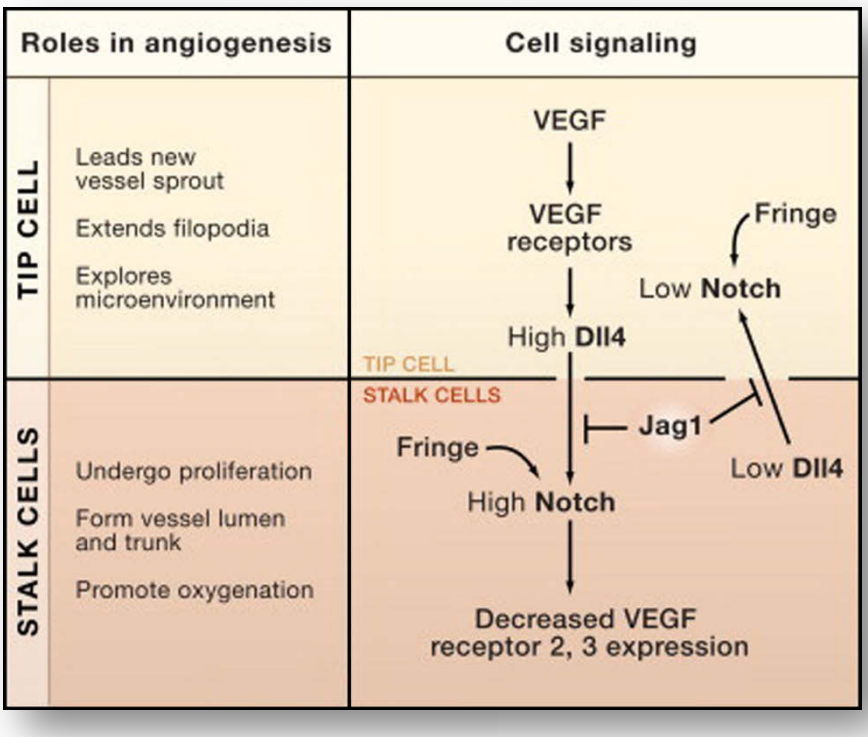

Introduction Figure 9

Delta-Notch signaling in tip/stalk cell specification (modified after Suchting et al., 2009)

signaling can positively regulate *FLT1* expression (Funahashi et al., 2010). FLT1 in stalk cells act as decoy receptor for VEGFA to further prevent VEGFA-mediated tip cell specification. Hence, knock-down of *flt1* in zebrafish promotes increased tip cell formation (Krueger et al., 2011). Tip cell specification is also promoted by the stalk cell-restricted expression of Jagged 1, another Notch ligand (Benedito et al., 2009). Glycosylation of Notch receptors by Fringe family glycosyltransferases enhances Notch signaling via DLL4 but represses signaling via Jagged 1. Stalk cell-restricted Jagged 1 competes with DLL4 for Notch binding and suppresses Notch signaling in tip cells. Thus, endothelial-specific Jagged1 knock-out mice exhibit retinal vessels with disrupted tip cell formation and vascular sprouting, whereas tip cell formation is enhanced upon endothelial Jagged 1 gain-of-function.

1.2.3.2 Integrin signaling in angiogenesis

Communication between endothelial cells and their environment plays an important role in angiogenesis and cancer progression, Thereby angiogenesis is regulated by integrins. Integrins belong to a family of receptors for ECM proteins and immunoglobulin superfamily molecules. They form heterodimers of non-covalent single-pass type I transmembrane α and β subunits (Humphries et al., 2006; Hynes et al., 2002). Integrins can bind to ECM proteins or receptors of adjacent cells with their extracellular domain to mediate cell adhesion and binding their cytoplamic tails to the intracellular cytoskeleton (Calderwood et al., 2000; Evans et al., 2007). Besides cell adhesion, integrins mediate outside-in or inside-out signaling. These signals determine cellular responses such as migration, survival, motility, and differentiation (Calderwood et al., 2004; Hynes et al., 2002; Miranti et al., 2002). Integrin activation requires conformational changes of the heterodimer (Introduction Fig. 10) and can be modulated by the expression of different integrin genes or by growth factor or chemokine receptor signaling. Integrin signaling can be activated by binding of different intracellular proteins including talin and kindlin. Binding of the PTB domain of talin to the conserved WxxxNP(I/L)Y motif of the β integrin cytoplasmic tail results in integrin activation (Wegener et al., 2007). Talin also binds to the actin cytoskeleton and various signaling proteins, thereby directly connecting activated integrins with the cytoskeletal

network (Critchley et al., 2008). In addition, it has been shown that proteins of the kindlin family can bind to the integrin NPxY motif via their FERM domain, and inhibition of talin suppresses integrin activation (Kloeker et al., 2004; Ma et al., 2008; Montanez et al., 2008; Moser et al., 2008). Activated integrins then assemble a

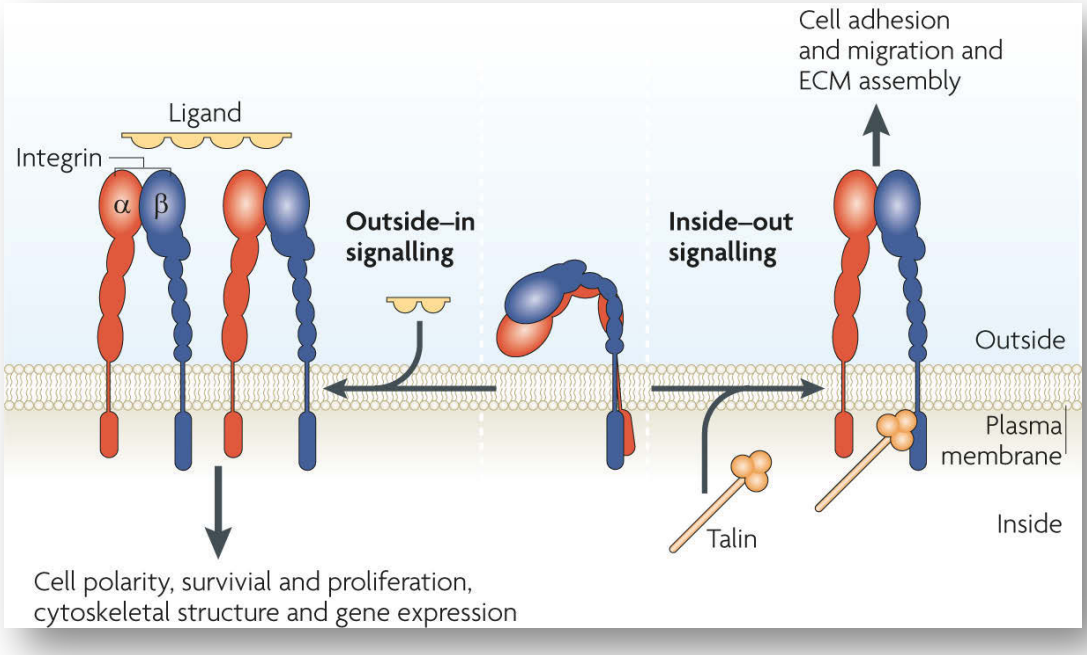

Introduction Figure 10

Integrin activation by outside-in or inside-out signaling (adapted from Shattil et al., 2010)

multiprotein complex at their cytoplasmic tail, which includes focal adhesion kinase (FAK), Src-family kinases, integrin-linked kinase, vinculin, or paxilin and is responsible for outside-in signaling (Deakin et al., 2008; Giannone et al., 2006; Ginsberg et al., 2005; Legate et al., 2006; Mitra et al., 2005; Ziegler et al., 2006).

The role of $\alpha_v\beta3$ in angiogenesis suggests that some pathological conditions might depend on $\alpha_v\beta3$ signaling. Expression analyses of cerebral cavernous malformations (CCM) from human brain tissue revealed that $\alpha_v\beta3$ is strongly expressed in CCM endothelium (Seker et al., 2006). Knock-out of β3 integrin in mice leads to embryonic lethality of 50% due to intrauterine bleeding or defective placental development (Hodivala-Dilke et al., 1999). Intriguingly, only postnatal mice lacking β3 integrin exhibit coronary capillaries of irregular endothelial thickness, with endothelial protrusions into the lumen, and expanded cytoplasmic vacuoles caused by enhanced

VEGF signaling (Weis et al., 2007). Further studies in mice suggested that integrins of glial cell play an important role in maintaining the blood-brain barrier, since neuronal-specific integrin α_v knock-out mice exhibit enlarged, disrupted blood vessels, with defective apposition of endothelial or glial cells (McCarty et al., 2002).

Besides β3 integrin signaling, fibronectin-mediated β1 integrin activation has a crucial role in vascular development. Fibronectin, a component of the ECM, is produced and secreted by endothelial cells during normal and tumor angiogenesis (Clark et al., 1982; Kim et al., 2000; Liao et al., 2002). Endothelial-specific deletion of β1 integrin in mice leads to severe vascular defects. Furthermore, endothelial cell proliferation and vessels branching is impaired, arguing for a essential role of β1 integrin in angiogenesis (Bloch et al., 1997). Integrin $\alpha_5\beta1$ is poorly expressed by quiecent endothelial cells, but is up-regulated during tumor angiogenesis (Kim et al., 2000); their expression is regulated by the homeobox family transcription factor HOXD3 (Boudreau et al., 2004).

Integrin α4β1 is expressed on neovessels of tumors in response to VEGF, IL1β, bFGF, and TNFα signaling . Binding of VCAM1, expressed by smooth muscle cells (VSMCs), to endothelial cells promote adhesion between these two cell types. Loss of integrin α4β1 causes cell death of both endothelial cells and pericytes (Garmy-Susini et al., 2005).

1.2.3.3 The role of EGFL7 in vascular development

Epidermal growth factor-like domain 7 (EGFL7) is a secreted angiogenic signaling molecule, predominantly expressed by endothelial cells (Fitch et al., 2004). It consists of a N-terminal signal peptide domain, an EMI-like domain, and two centrally located EGF-like domains. During embryogenesis and pathological angiogenesis *Egfl7* is mostly expressed by proliferating endothelial cells (Campagnolo et al., 2005; Fitch et al., 2004; Parker et al., 2004; Soncin et al., 2003). In the developing retinal vascular plexus, *Egfl7* expression is restricted to sprouting vessels with a basal localization in stalk cells and a patchy expression in tip cells (Schmidt et al., 2007). *EGFL7*-depleted cultured human umbilical vein endothelial cells (HUVECs) fail to proliferate. Additionaly, depletion of *EGFL7* supresses endothelial cell migration and inhibits

capillary sprouting (Nichol et al., 2010). It has been suggested that EGFL7 promotes these processes by modulating ECM rigidity. EGFL7 inhibits the deposition of mature elastic fibers by repressing lysil oxidase (LOX)-mediated conversion of tropoelastin into elastin (Lelievre et al., 2008).

In vivo studies in zebrafish demonstrated that knock-down of Egfl7 causes pericardial edema, hemorrhaging, and circulatory loop defects due to impaired tubulogenesis of the developing vessels. Furthermore, endothelial cell membranes exhibit disrupted tight, adherens and gap junctions (De Maziere et al., 2008; Parker et al., 2004). The study of the role of *Egfl7* in vascular development has been complicated by the presence of the pro-angiogenic microRNA miR-126 within the *EGFL7* gene (Kuhnert et al., 2008; Nicoli et al., 2010; Wang et al., 2008). *Egfl7* loss-of-function mouse models exhibit partial embryonic lethality and vascular abnormalities (Schmidt et al., 2007). Later experiments showed that these vascular defects can be attributed to a loss of miR-126 rather than a loss-of-function of *Egfl7* (Kuhnert et al., 2008). In addition, endothelial-specific miR-126 knock-out mice exhibit vascular defects similar to those of *Egfl7* loss-of-function mice (Kuhnert et al., 2008; Wang et al., 2008).

Overexpression of *Egfl7* in murine endothelial cells without affecting miR-126 levels resulted in a decrease in cranial blood vessels, collapsed arterial vessels, and abnormal endothelial cell aggregates (Nichol et al., 2010). These phenotypes are mediated, at least in part, by modulation of Notch signaling: EGFL7, as an endothelial secreted ECM protein may interact with Notch receptors in a paracrine or autocrine manner. Depletion of *EGFL7* in HUVECs inhibited endothelial cell proliferation, sprout formation, and migration (Nichol et al., 2010), which could be also obeserved upon Notch signaling activation (Henderson et al., 2001; Noseda et al., 2004; Sainson et al., 2005; Taylor et al., 2002). It has also been shown that EGFL7 interacts with the Notch receptors Notch1 and Notch4 and with their ligand, DLL4 (Introduction Fig. 11A) (Nichol et al., 2010; Schmidt et al., 2009). Thus, EGFL7 could modulate Notch signaling by binding to the Notch receptors or its ligands. Studies in HUVECs suggested that, in contrast to the postnatal retina, EGFL7 enhances Notch signaling in the presence of DLL4 during embryogenesis (Introduction Fig. 11B). This finding is suggested to involve the binding of EGFL7 to Jagged1, an antagonist of Notch signaling. Then, EGFL7-Jagged1 binding

prevents the interaction between the Notch receptor and Jagged1, and in turn promotes DLL4/Notch signaling activation.

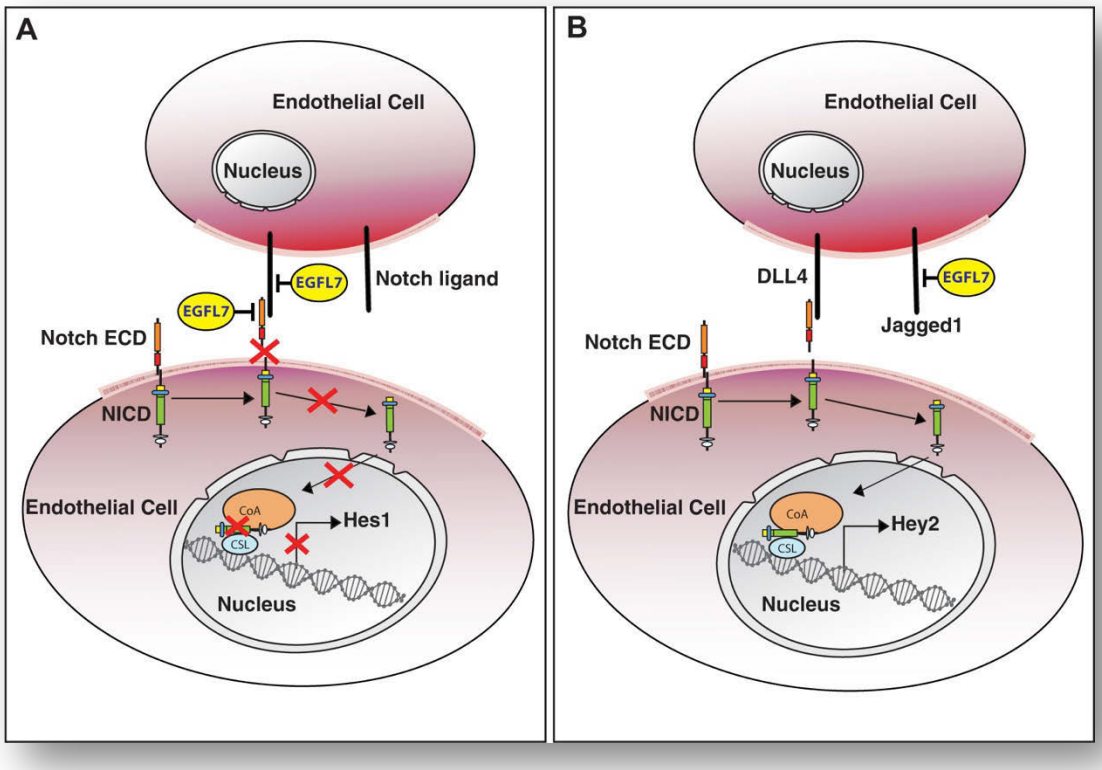

Introduction Figure 11

Regulation of Notch signaling by EGFL7 during (A) postnatal and (B) embryonic development. (A) ln the postnatal retina, EGFL7 antagonizes Notch/ligand interaction and inhibits target gene expression. (B) During embryonic development, EGFL7 indirectly enhances DLL4/Notch signaling by binding to the Notch antagonist Jagged1. ECD: extracellular domain of Notch, NICD: intracellular domain of Notch. (adapted from Nichol et al., 2012)

The findings that EGFL7 is strongly expressed in several tumors and cancer cell lines (Diaz et al., 2008; Huang et al., 2010; Wu et al., 2009), and its possible role in tumor angiogenesis make EGFL7 a potential target for antiangiogenesis therapy.

1.3 The transcription factor KLF2 in cardiovascular development

Blood flow and shear stress have an impact on endothelial cytoskeleton remodeling and therefore influence their cell morphology (Davies et al., 1997; Kim et al., 1989). The

transduction of physical forces between the endothelium and the surrounding tissue is important for maintaining vascular homeostasis and function. Mechanical forces exerted by blood flow act on the apical surface of endothelial cells and are translated into molecular signals for vascular function. These forces can act parallel to the direction of flow and result in shear stress, or perpendicular to the vessel wall and tensile stress (White et al., 2007). Accordingly, different downstream signaling cascades may be activated and regulate endothelial cell behaviour and morphology. One of the best characterized genes is the zinc-finger transcription factor KLF2. The zebrafish genome habours two *KLF2* paralogues, *klf2a* and *klf2b* due to genome duplication. Zebrafish Klf2a is considered to be the ortholog of the human and murine *KLF2*. In adult human tissue samples, KLF2 mRNA was detected in the heart, skeletal muscle, pancreas, lungs, placenta, and vascular tissues (Wani et al., 1999). In the vasculature, KLF2 expression levels within the endothelium correlates with local shear stress patterns (Introduction Fig. 12). Decreased *KLF2* expression is generally seen in areas of lower shear stress levels and disturbed flow patterns (Dekker et al., 2002; Dekker et al., 2005; Parmar et al., 2006). In HUVECs, it has been demonstrated that *KLF2* overexpression results in stretched shaped endothelial cells with actin stress fiber formation even in the absence of blood flow. In contrast, the shear stress induced alignment of endothelial cells in flow direction is abolished after siRNA-mediated KLF2 silencing (Boon et al., 2010). Further studies demonstrated that *KLF2* is not only expressed in large blood vessels, but also in the duodenal, hepatic, or the glomerular microvasculature (Gracia-Sancho et al., 2011; Kobus et al., 2012; Slater et al., 2012).

In zebrafish, *klf2* expression starts at 70% epiboly in the ventral, animal portion of the epiblast (Oates et al., 2001). At 24 hours post fertilisation (hpf), *klf2a* is expressed in head vessels, the heart, clusters of cells lateral to the most posterior notochord, and in the anus. At 36 hpf *klf2* mRNA expression can be detected in the trunk vasculature, and after two days in endocardial cells of the developing heart valves. Concomitant with human and mice, *klf2* expression in the zebrafish vasculature is blood flow dependent (Parmar et al., 2006; Stainier et al., 1996; Wang et al., 2011).

Shear stress-induced expression of *KLF2* requires a single consensus myocyte enhancer factor 2 (MEF2)-binding site up-stream of the transcription start of the Klf2 gene (Introduction Fig. 12) (Kumar et al., 2005). Phosphorylation of MEF2 by the

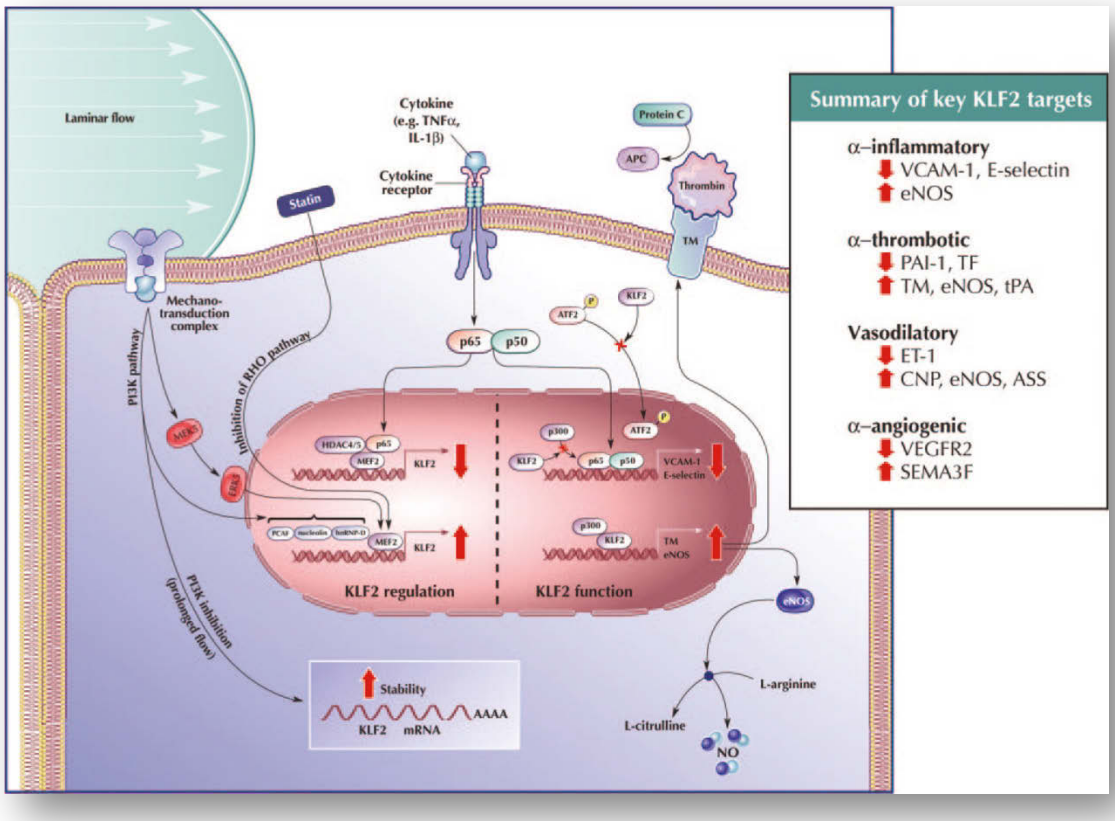

Introduction Figure 12

Regulation and function of KLF2 in endothelial cells (adapted from Atkins et al., 2007)

MEK5/ERK5 pathway is critical for the expression of *KLF2* under shear stress (Parmar et al., 2006; Young et al., 2009). Epigenetic modification of MEF2 is another mechanism for the regulation of KLF2 expression. Under low blood flow conditions, histone deacetylase 5 (HDAC5) binds to MEF2 and inhibits its transcriptional activity. Phosphorylation of HDAC5 in a Ca^{2+}/ calmodulin-dependent manner under high laminar shear stress results in dissociation of HDCA5 from MEF2 and transcription of *KLF2* (Wang et al., 2010a). Blood-flow dependent expression of *KLF2* can be also regulated by the endothelial thioredoxin-interacting protein (*TXNIP*). Under disturbed flow conditions *TXNIP* is up-regulated and binds as a part of a transcriptional repressor complex to the shear responsive region of *KLF2* promoter and inhibits KLF2 expression

(Wang et al., 2012). Recent data demonstrated a contribution of microRNAs in blood flow-mediated regulation of *KLF2*: Under laminar flow, *miR-92a* is down-regulated which results in higher levels of *KLF2* expression. Overexpression of *miR-92a* decreases *KLF2* expression by binding to a *miR-92a*-binding site at the *KLF2* 3´-UTR region (Bonauer et al., 2009).

Besides the flow-dependent regulation of KLF2, many drugs have been found to induce KLF2 expression independently of flow. One of the best studied group of are statins. Statins are inhibitors of 3-hydroxy-3-methylglutaryl-coenzyme A (HMG-CoA) reductase, a enzyme in cholesterol synthesis and are used in clinical practice. In addition, a combination of prolonged shear stress and statins have been shown to have a additive effect on KLF2-mediated expression of eNOS and thrombomodulin, because shear stress stabilizes *KLF2* mRNA via inhibition of PI3K and results in higher *KLF2* mRNA levels (Introduction Fig. 12) (van Thienen et al., 2006). Concomitant with these findings, it has been shown that rapamycin increases *KLF2* expression in HUVECs by inhibition of mTOR, a component of the PI3K/AKT/mTOR pathway (Hay et al., 2004; Ma et al., 2012).

Blood-flow mediated gene expression plays a important role in vascular homeostasis, endothelial barrier function, vasodilation, angiogenesis, and inflammation. KLF2 regulates the expression of about 70% of shear-stress induced endothelial genes together with nuclear factor erythroid2-related factor 2 (Nrf2) (Fledderus et al., 2008).

1.3.1 KLF2 in angiogenesis and valvulogenesis

Several studies have shown that VEGF signaling is a key regulator of physiologic and pathologic angiogenesis by promoting EC cell migration, vascular permeabilty, inflammation, and endothelial cell survival (Ferrara et al., 2003; Kim et al., 2001; Leung et al., 1989; Maharaj et al., 2007; Senger et al., 1983). During zebrafish development, blood flow-mediated expression of *klf2a* has a pro-angiogenic role in aortic arch development (Introduction Fig. 13). Klf2a induces the expression of the endothelial-specific mircroRNA *miR-126* which inhibits *spred-1* a negativ regulator of VEGF signaling. Loss of *klf2a* down-regulates *miR-126* and inhibits pro-angiogenic VEGF signaling by the up-regulation of *spred-1* (Nicoli et al., 2010).

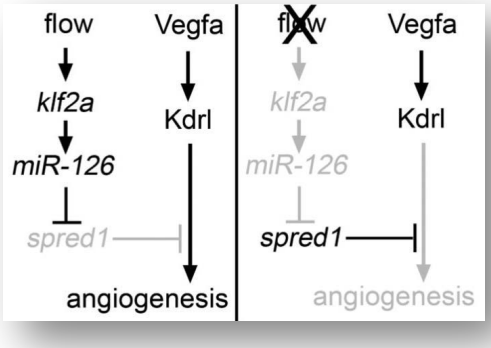

Introduction Figure 13.
Pathway for blood flow-mediated angiogenesis via Klf2a during aortic arch development (adapted from Nicoli et al., 2010)

In Xenopus, Klf2 regulates Flk1 expression by binding, together with the ETS transcription factor ERG to the enancer of the *Flk1* gene. Knock-down of *Klf2* leads to severe vascular defects due to a significant decrease of Flk1 (Meadows et al., 2009). Together, these studies indicate that Klf2 has pro-angiogenic role during embryonic development. Conversely, studies in mice demonstrated an opposite effect of *Klf2* overexpression on VEGF-mediated angiogenesis. Moreover, KLF2 competes with Sp1 for a binding site in the *VEGFR2* promoter and overexpression of *KLF2* in HUVECs inhibits VEGFR2 expression (Bhattacharya et al., 2005). Additionaly, angiogenesis can also be induced under hypoxic conditions by the activation of the hypoxic-inducible factor 1 (*HIF-1*). *KLF2* knock-down in HUVECs increases the expression of HIF-1 target genes including VEGF, whereas *KLF2* overexpression inhibits their expression and also results in a failure endothelial tube formation (Kawanami et al., 2009).

In adult, endothelial progenitor cells (EPCs) participate in neovascularization (Asahara et al., 1997). EPCs are bone marrow-derived cells and circulate in the blood stream. Recent studies have shown that *KLF2* overexpression in human EPCs increases their cell number and improves neovascularization capacity in an ischemic hind limb model (Egorova et al., 2012).

Cardiac valve formation in vertebrates is essential for a functional circulatory system. Cardiac cushions at the atrioventricular canal (AVC) are remodeled and become functional valves (Armstrong et al., 2004). In zebrafish, it has been shown that *klf2a* plays a major role cardiac valve development. Klf2a expression is up-regulated by retrogade flow at the AVC and knock-down of *klf2a* and its target genes *bmp4*, *notch1b*, *edn1*, and *nrg1* results in valvular defects (Introduction Fig. 14) (Vermot et al., 2009). Studies in murine endothelial cells indicate that shear stress at the AVC activates

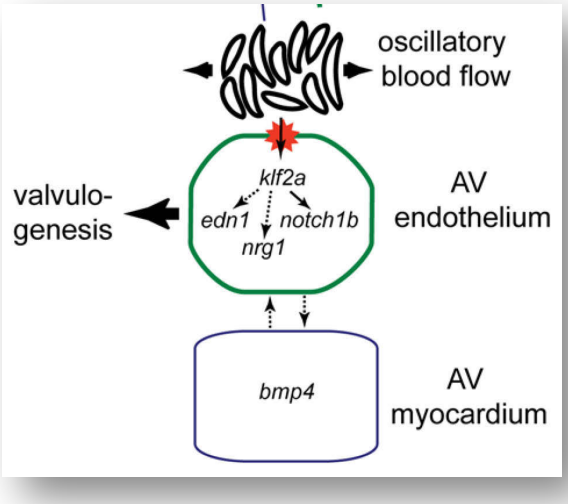

Introdction Figure 14.
Klf2 function during heart valve formation in zebrafish. (adapted from Vermot et al., 2009)

Tgfβ/Alk5 signaling. Then, Alk5 activates the MEK5/ERK5/MEF2 pathway and induces *Klf2* expression (Egorova et al., 2011). Analyses of the zebrafish mutant *bungee* (*bng*^{jh177}) revealed the important role of *klf2a* in valve development. In these mutants, the phosphorylation of Hdac5 is impaired. Consequently, Hdac5 remains in its active state to the *klf2a* promoter and inhibits the expression of *klf2a* which results in cardiac valve defects (Just et al., 2011).

1.3.2 KLF2 in vascular tone regulation

Vascular tone is controlled by various factors produced in endothelial cells. Among these factors, eNOS, C-natriuretic peptide (CNP), and adrenomodulin act as a vasodilator, whereas endothelin-1 (ET1) and angiotensin-converting enzyme (ACE) have a vasoconstrictiv function (Chauhan et al., 2003; Drexler et al., 1999; Malek et al., 1993). KLF2 binds to the eNOS promoter and induces its expression. Moreover, KLF2 also induces *CNP* and inhibits *ET1* and *ACE* expression (Dekker et al., 2005; SenBanerjee et al., 2004).

2 Aims of this study

The cerebral cavernous malformation (CCM) protein complex is crucial for normal blood vessel development and vascular integrity. Patients with cerebral cavernous malformations (CCMs) frequently suffer from hemorrhages and/or cavernoma leading to strokes or even death due to a loss of any of the three genes, KRIT1/CCM1, CCM2/OSM, or CCM3/PDCD10. However, the roles of CCM proteins during cardiovascular development remain largely unknown.

In this study, microarray expression analyses yield a first hint for potential candidate genes. Furthermore, knock-down experiments of candidate genes or pharmacological inhibition of different signaling pathways shed light on the molecular relationships between the CCM complex proteins and vascular signaling cascades during zebrafish embryonic cardiovascular development.

3 Material and Methods

3.1 *In vivo* experiments

3.1.1 Fish maintenance and stocks

Zebrafish embryos were kept in egg water (60µg/ml Instant Ocean Sea Salts, Aquarium Systems Inc., USA; 1µg/ml Methylene blue) at 28,5°C. To prevent pigmentation, embryos were kept in egg water supplied with 0,003% (w/v) PTU (1-Phenyl-2-thiourea, Sigma-Aldrich, USA). Embryos were staged according to morphological criterias (Kimmel et al., 1995). Adult zebrafish were maintained under standard conditions at 28,5°C (Westerfield et al., 1997).
The following fish lines were used:

Transgenic lines:
Tg(*myl7:GFP*)^{twu34} (Huang et al., 2003)
Tg(*kdrl:GFP*)^{s843} (Jin et al., 2005)

Mutant lines:
heg^{m552} (Mably et al., 2003)
krit1^{ty219c} (Mably et al., 2006)
ccm2^{m201} (Mably et al., 2006)
tnnt2a^{b109} (Chen et al., 1996)

3.1.2 Embryo injections

Glass injection needles (Drummond Scientific, USA) were pulled in a P-97 Flaming/Brown Micropipette puller Sutten Instruments). For injections, needles were fixed onto a micromanipulator (MM33 Micromanipulator, Maerzhaeuser, Germany) and connected to a microinjector (MPPI-2 Pressure Injector, BP15 back pressure unit,

Applied Scientific Instrumentation). Embryos were injected the stereomicroscope at 1-cell stage.

3.1.3 Morpholino and expression construct injections

Morpholino antisense oligonucleotides were purchased from GeneTools, LLC, USA. Morpholinos (MO)s were diluted with ddH_2O to 1mM stock solution and stored at -20°C. For experiments, MOs were further diluted in Danieau´s. Morpholinos were injected into one-cell stage embryos in the following amounts:

Morpholino name	**Morpholino sequence**	**Amount /embryo**
klf2a ATG (Nicoli et al., 2010)	5‘-GGACCTGTCCAGTTCATCCTTCCAC-3‘	12ng
klf2b ATG (Renz et al., 2015)	5‘-AAAGGCAAGGTAAAGCCATGTCCAC-3‘	12ng
	5ng *klf2a*MO + 5ng *klf2b*MO	
egfl7 ATG (Parker et al., 2004)	5‘-CAGGTGTGTCTGACAGCAGAAAGAG-3‘	650pg
	2,5ng *klf2a*MO + 2,5ng *klf2b*MO + 0,3ng *egfl7*MO	
tnnt2a ATG (Sehnert et al., 2002)	5‘-CATGTTTGCTCTGATCTGACACGCA-3‘	2ng
itgb1b splice (Ablooglu et al., 2010)	5‘-GCCAGTTTGAGTGAATAACTCACCT-3‘	6,3ng
icap-1 ATG	5‘-TCGAAACATCCTTCACCATGACGCC-3‘	8,3ng

The plasmids *hsp70l:klf2a_IRES_GFP* or *hsp70l:klf2b_IRES_GFP* (Renz et al., 2015) were injected into one-cell stage embryos together with the tol2 transposase capped mRNA synthetized using the SP6 polymerase (mMessage Machine, Ambion, USA). For efficient genomic integration, a concentration of 12,5ng/µl plasmid DNA and

25ng/µl mRNA (diluted in Danieau´s) was used. Injected embryos were raised under standard conditions (see fish maintainance and stocks). Based on their strong EGFP expression, 1 transgenic fishline Tg(*hsp70l:KLF2a_IRES_EGFP*)^{md8} and 2 transgenic fishlines Tg(*hsp70l:KLF2b_IRES_EGFP*)^{md9,11} were further analyzed.

3.1.4 Heat-shock experiments

Prior to the heat-shock, up to 50 embryos were collected in 50ml tubes and pre-heated egg water was added. The heat-shock was performed at 37°C in a waterbath for 40 minutes. Time-points for the following experiments are detailed within the results section.

3.1.5 Pharmacological treatment

Dechorionated embryos were kept in E3 medium and treated with 12,5µM PTK787 (ChemieTek, USA, Lot# VT-ETJN-2A), a Vegf inhibitor at 28,5°C (Renz et al., 2015). Control embryos were treated with 0.01% DMSO (Dimethylsulfoxide, Sigma-Aldrich), at 28,5°C. Briefly, embryos were treated in a 1% agar-coated petridish to prevent sticking to it. After treatment, embryos were washed several times with E3 medium and then transferred to a new petridish. Treatment protocols for the different experiments are detailed within the results section.

3.1.6 Embedding of embryos for live imaging

Embryos were anesthetised with 0,03% Tricaine (3-amino benzoic acid ethylester, Sigma-Aldrich, USA) in E3 medium for 2 minutes and then embedded in 1% Low Melting Agarose (Lonza, Switzerland, cat# 50081)/0,03% tricaine solution on a Petridish. Embryos were covered with 0,03% tricaine solution to prevent dehydration of the agarose during imaging. Multiple z-stacks were recorded at the Zeiss confocal microscope LSM700 with 20x/dry objective. Between each timepoint, embryos were

removed from the agarose and incubated in petridishes in E3 medium without Tricaine at 28,5°C.

3.2 Molecular biology methods

3.2.1 Total RNA extraction and cDNA synthesis

20-30 live embryos were collected in a 2ml Eppendorf tube (Eppendorf, Germany) and 1ml Trizol (Invitrogen, USA, cat#15596-026) was added. Total RNA was extracted according to manufacturer´s protocol. The RNA pellet was dissolved in 25µl RNAse-free ddH_2O.

cDNA was generated from total RNA by using the Sensiscript Reverse Transcription Kit (Qiagen, Germany, cat#205211) according manufacturer´s protocols.

3.2.2 *In vitro* transcription of DIG-labelled antisense RNA

The templates for the *in situ* hybridization probes for *klf2a* and *klf2b* were generated by PCR amplification using 24hpf WT cDNA. The amplicons were cloned into the pSC-B vector with the StrataClone Blunt PCR Cloning Kit (Stratagene, cat#240207). Antisense RNA was generated by *in vitro* transcription using the DIG RNA Labeling Kit (Roche Diagnostics, Zwitzerland, cat#11175025910) in collaboration with Jana Richter.

PCR-Primer :

Primer name	Primer sequence
Klf2a_fwd	5‘-GCAAGAGTCCAGAAACATGTACAACCCG-3‘
Klf2a_rev	5‘-GCGTTTAGTCCACATTTTCCAGAGTCCG-3‘
Klf2b_fwd	5‘-GGAGTTTCCTGAAATCAAAGTGGAGCCG-3‘
Klf2b_rev	5‘-TAACAGTCTCCGGATTGGACACCGATTC-3‘

3.2.3 Extraction of cardiac tissue

Whole hearts were extracted manually with collaborative support of Franziska Rudolph (MDC, Berlin) and Jana Richter (MDC, Berlin) (Lombardo et al., 2015). For heart extraction, a modified protocol after Burns (Burns et al. 2006) was used. 50-100 of wild-type or *ccm2*^{m201} mutant embryos in the transgenic line Tg(*myl7:GFP*)^{twu34} background were collected in a 1,5 ml Eppendorf tube and washed twice with 10% fetal bovine serum (FBS, Sigma-Aldrich, USA) in L-15 (Gibco, cat#11415-049). Embryos were ruptured by repeated uptake into a loading pipette and filtered on a 100µM nylon mesh (BD Bioscience, cat#BD352360). Subsequently the flow-through was filtered again on a 30µM mesh (Miltenyi Biotec., cat#130-098-458) which retained the hearts. Hearts were then washed out onto an agar-coated plate containing 10%FBS/L-15, collected under a stereomicroscope (Leica MZFLIII) and transferred into RNAlater (Ambion, USA, cat#AM7020) for RNA stabilization. This procedure was repeated several times to obtain sufficient heart tissue for RNA extraction.

3.2.4 RNA extraction and processing

Total RNA was extracted with the RNeasy Micro Kit (Qiagen, Germany, cat#74004). RNA was quantified on a ND-1000 spectrophotometer (Nanodrop Technologies). For quality analysis, the 2100 Bioanalyzer RNA 6000 Nano chip (Agilent Technologies) was used. RNA processing and chip hybridization was done by imaGenes GmbH (Berlin, Germany). Briefly, for each sample, 200ng of intact (RIN>8) total RNA was subjected to a single amplification step and Cy3 labeling reaction. 1,5 mg of labeled cRNA were hybridized to Zebrafish (V2) Gene Expression Microarrays (G2519F-019161, 4x44K) and spot intensities recorded on a G2565BA scanner (Agilent Technologies). Microarrays were performed in duplicates for WT and *CCM2* samples. Raw expression values were adjusted in R (www.r-project.org) using variance stability normalization (Huber et al., 2002). Significance p-values for differentially expressed probes were calculated with the limma R package (G Smyth 2005) and associated false discovery tresholds determined according to the Benjamini and Hochberg FDR method (Benjamini et al., 1995).

3.2.5 Gateway cloning

The open reading frame of zebrafish *klf2a* (NM_131856, (Vermot et al., 2009) was amplified by PCR using the Phusion polymerase (Finnzymes, Finland) and cloned via BP Gateway (Kwan et al., 2007 ; Villefranc et al., 2002) recombination into the pDONR 221 vector (Invitrogen, USA) to generate a middle entry vector referred to as pME-*klf2a*. To generate an injection construct, a LR Gateway recombination reaction with pDestTol2, p5E-*hsp70l*, pME-*klf2a* and p3E-*IRES_EGFP* was performed to generate pTol2-*hsp70l:KLF2a_IRES_EGFP*. Similarly, the open reading frame of zebrafish *klf2b* (NM_131857) was amplified and cloned via BP Gateway (Kwan et al., 2007; Villefranc et al., 2007) recombination with pDONR 221 to generate the middle entry vector pME-*klf2b.* To generate an injection construct, a LR Gateway recombination reaction with pDestTol2, p5E-*hsp70l*, pME-*klf2b* and p3E-*IRES_EGFP* was performed to generate pTol2-*hsp70l:KLF2b_IRES_EGFP*. All Gateway plasmids were kindly provided by Nathan Lawson´s and Shu Chien´s lab.

Primer name	Primer sequence
attB1_klf2a	5`-GGGGACAAGTTTGTACAAAAAAGCAGGCTTAATGCATCT CAGCTGCATAGCTGACCTAT-3`
attB2_klf2a	5´-GGGGACAAGTTTGTACAAGAAAGCTGGGTACTATCACAG GTGTCTCTTCATGTGCAGC-3
attB1_klf2b	5´-GGGGACAAGTTTGTACAAAAAAGCAGGCTTAATGGCTTT ACCTTGCCTTTTGCCT-3
attB2_klf2b	5´-GGGGACAAGTTTGTACAAGAAAGCTGGGTACTATCACAG GTGTCTCTTCATGTGCAGC-3

3.2.6 Quantitative RT-qPCR

The RT-qPCR was performed in collaboration with Dr. Cécile Otten (MDC, Berlin) as described (Renz et al., 2015) using 6ng total cDNA. Quantitative real-time PCR was performed with iTaqTM Universal SYBR Green Supermix (Bio-Rad) in a 20 µl reaction on a ABI Prism 7900 sequence detection system (Applied Biosystems). Product sizes were controlled by DNA gel electrophoresis and the melt curves were

evaluated using the SDS 2.4 software (Applied Biosystems). Ct-values were determined with the same software. The following primers were used for RT-qPCR:

	Primer name	Primer sequence	UniGene identifier
zebrafish	Klf2aDr_fwd Klf2aDr_rev	5‘-CTGGGAGAACAGGTGGAAGGA-3‘ 5‘-CCAGTATAAACTCCAGATCCAGG-3‘	Dr.29173
	Klf2bDr_fwd Klf2bDr_rev	5‘-GGATAGATGGAAGATTGAGGAGCA-3‘ 5‘-CTCCAGGTCTAAATAATTGCTGAG-3‘	Dr.9976
	Egfl7_fwd Egfl7_rev	5‘-TTTACCCAGAATGCTGTCCG-3‘ 5‘-AAAACTGCCCAGCGTATTCA-3‘	Dr.89996
	Eif1bDr_fwd Eif1bDr_rev	5‘-CAGAACCTCCAGTCCTTTGATC-3‘ 5‘-GCAGGCAAATTTCTTTTTGAAGGC-3‘	Dr.162048

3.3 Histology

3.3.1 Immunohistochemistry

Embryos were fixed in 4% paraformaldehyde (PFA) in PBS (see 3.7) for 1 hr at RT on a shaker. Embryos were then washed four times in PBT for 5 min each at RT and subsequently 5 min in ddH_2O. Then embryos were briefly rinsed in PBDT. Embryos were incubated at least 2hrs at RT in PBDT/5% NGS (normal goat serum, Invitrogen, USA) solution for blocking. Embryos were incubated with the primary antibody Zn8/Alcam (1:100 Developmental Studies Hybridoma Bank) with PBDT/1%NGS overnight at 4°C on a shaker. Next, embryos were extensively washed several times with PBDT/1% NGS for at least 3 hrs and incubated with the secondary antibody Cy5-conjucated goat-anti-mouse (1:250; Jackson ImmunoResearch Laboratories, cat#968229) in PBDT/1%NGS overnight at 4°C. For actin staining, Rhodamine Phalloidine (1:100; Sigma-Aldrich, USA, cat#658740) was added together with the secondary antibody. After overnight incubation, embryos were washed several times extensively with PBDT/1% NGS for a total of 3hrs and then embedded for confocal imaging.

3.3.2 Zebrafish embedding

Hearts were dissected from whole embryos under a stereomicroscope (Leica MZFLIII, Germany) using forcep and needle, placed into a drop of 6µl Slow Fade Gold antifade reagent (Invitrogen, USA, cat#536938) on a slide (superfrost, 76x26mm, Menzel, Germany) in a ring of vaseline to prevent damages by the coverslip (18x18mm #1, Roth, Germany). For whole mount imaging, the embryos were embedded in 1% Low Melting Agarose (Lonza, USA)/ PBS.

3.3.3 Whole mount *in situ* hybridization

Whole mount *in situ* hybridizations were performed with the help of Dr. Cécile Otten (MDC, Berlin). For the solutions, see 3,7. Embryos were fixed with 4% PFA overnight at 4°C, washed several times in 100% methanol and stored at -20°C for dehydration. For *in situ* hybridization, embryos were rehydrated at RT with:

- 75% Methanol/ 25% PBT (5 min)
- 50% Methanol/ 50% PBT (5 min)
- 25% Methanol/ 75% PBT (5 min)
- 100% PBT (4x5 min)

Embryos were then permeabilized with Proteinase K (10µg/ml in PBT) for 15 minutes at RT and briefly washed in PBDT. After fixation with 4% PFA for 20 minutes, embryos were washed 5 times for 5 minutes with PBT. Embryos were incubated for at least 2 hrs in prehybridization buffer at 67°C. After prehybridization embryos were incubated overnight at 67°C in 5µg/ml of DIG-labeled RNA probe in pre-heated hybridization buffer. After overnight incubation, embryos were washed in different pre-heated (67°C) solutions:

- Hyb buffer (20 min)
- 50% SSCT (2x)/ 50% Formamide (3x20 min)

- 75% SSCT (2x)/ 25% Formamide (20 min)
- SSCT (2x) (2x 20 min)
- SSCT (0,2x) (4x30 min)
- PBT (5 min)

Embryos were incubated in blocking solution for at least 2hrs on a shaker at RT, and subsequently incubated with 200µl anti-DIG antiserum (1:4000 in PBT + 2mg/ml BSA) overnight at 4°C. Embryos were washed several times (6-8 times over 3hrs) with PBT on a shaker at RT. Then embryos were washed 3 times (5 min each) in freshly prepared NTMT solution. During this step, the embryos were transfered into a 24 well plate. Then, embryos were incubated in staining solution at RT. The staining was stopped by washing the embryos three times in PBT. Embryos were transferred into 1,5ml Eppendorf tubes and cleared with benzyl-benzoate (2:1, Sigma-Aldrich, USA). For imaging, embryos were mounted in permount (Fisher Scientific, USA). Stained embryos were imaged at the Axioplan2 microscope (Zeiss, Germany) using a SPOT digital camera (Diagnostic Instruments Inc, USA) and the Metamorph software (Molecular Devices).

3.4 Microscopy

3.4.1 Confocal imaging

Immunostained embryos were scanned at the Zeiss confocal microscope LSM700 with 20x/dry or 40x/oil objectives. Images were analyzed with the LSM image browser 4.2 (Zeis, Germany) or Volocity 5.3 (Perkin Elmer, USA), and Adobe Photoshop CS5 (Adobe).

3.5 Data analysis

3.5.1 Statistical analysis of endocardial and lateral dorsal aorta cell numbers

In Figure 9, 12 and Figure 16, nuclei were visualized by Tg(*kdrl:GFP*)^{s843} expression and were counted within the heart (for endocardium), or in both lateral dorsal aortae in an area defined between the branching point from the dorsal aorta and the branching point of the first aortic arch. Cell numbers are shown as means with S.E.M. Prism 5 (GraphPad) was used to perform unpaired t-tests and Bonferroni´s multiple comparisons test. Means are statistically significantly different when $P < 0.05$ (for detailed information see appendix)

3.5.2 Statistical analysis of the subintestinal vein (SIV) branchpoints and sprouts

In Figure 13, SIVs were visualized at 72 hpf by Tg(*kdrl:GFP*)^{s843} expression and branchpoints and sprouts were counted. Branchpoint and sprout numbers are shown as means with S.E.M. Prism 5 (GraphPad) was used to perform 1-way ANOVA tests. Means are statistically significantly different when $P < 0.05$ (for detailed information see appendix).

3.5.3 RT-qPCR data analyses

Results were analyzed using the comparative threshold cycle (Ct) method ($2^{-\Delta\Delta Ct}$) to compare gene expression levels between samples as previously described (Livak and Schmittgen, 2001). As internal reference genes, zebrafish *eif1b* was used, yielding comparable results (Veerkamp et al., 2013). The results of the RT-qPCR experiments shown in Figure 24B and 20F,G are representative of more than 3 experiments. The mRNA expression levels of *klf2a, klf2b, egfl7* (zebrafish) are shown as relative mean values with S.E.M. The statistical analysis was done with Prism 5 (GraphPad) using the following algorithm: unpaired t-test, 1-way ANOVA tests followed by Sidak´s Multiple Comparisons Tests, or 1-way ANOVA tests with Dunnett's Multiple Comparison Test.

Means are statistically significantly different if $P < 0.05$ (for detailed informations see appendix).

3.6 Software

- LSM browser 4.2 (Zeiss, Germany)
- Adobe Photoshop CS5 (Adobe Systems Inc, USA)
- Adobe Illustrator CS5 (Adobe Systems Inc, USA)
- Volocity 5.3 (Perkin Elmer, USA)
- ImageJ 1.48
- Metamorph (Molecular Devices, USA)
- MacVector (MacVector Inc, USA)
- Bookends 12.2.4 (Sonny Software, USA)
- GraphPadPrism5
- SDS 2.4 (Applied Biosystems)

3.7 Solutions

Solution	Composition
anti-DIG antiserum	Anti-Digoxigenin-AP (Roche Diagnostics, Switzerland)
blocking solution	5% sheep serum (Dianova, Germany), 10mg/ml BSA (Sigma-Aldrich, USA) in PBT
Danieau´s	58mM NaCl; 0,7mM KCl; 0,4mM $MgSO_4$; 0,6mM $Ca(NO_3)_2$; 5mM HEPES; pH 7,2
DMSO	Dimethylsulfoxide (Sigma-Aldrich, USA)
E3 medium	5mM NaCl; 0,17mM KCl; 0,33mM $CaCl_2$; 0,33mM $MgSO_4$

hybridization buffer	5x SSC (20x); 0,1% Tween; 9mM citric acid; 50% formamide; 0,5mg/ml Torula yeast RNA (Sigma-Aldrich, USA); 50µg/ml heparin (Sigma-Aldrich, USA); pH 6-6,5
NTMT	100mM Tris HCl; 50mM $MgCl_2$; 100mM NaCl; 0,1% Tween 20; pH9,5
PBDT	PBT; 1% DMSO
PBS	2,7mM KCl; 80,9mM $NaHPO_4$; 1,5mM KH_2PO_4 in ddH_2O; pH 7,4
PBT	PBS; 0,1% Tween (Sigma-Aldrich, USA)
4% PFA	4% paraformaldehyde in PBS
pre-hybridization buffer	5x SSC (20x); 0,1% Tween; 9mM citric acid; 50% formamide
Proteinase K	10µg/ml (Roche Diagnostics, Switzerland) in PBT
SSC (20x)	3M NaCl; 300mM citric acid in ddH_2O; pH 7,0
SSCT (0,2x)	SSC (20x); 0,1% Tween in ddH_2O, pH 7,0
SSCT (2x)	SSC (20x); 0,1% Tween in ddH_2O, pH 7,0
staining solution	NBT/BCIP (Roche Diagnostics, Switzerland)

4 Results

4.1 Loss of Ccm2 influences endocardial and myocardial morphogenesis

Previous studies have shown, that *krit1*, *ccm2*, and *heg* are expressed in endothelial and endocardial cells in zebrafish (Kleaveland et al., 2009; Mably et al., 2003; Mably et al., 2006). The role of Ccm complex proteins in endocardial morphogenesis is largely unknown. To analyze the role of Ccm proteins in endocardial development, I used a stable transgenic reporter line Tg(*kdrl*:GFP)^{s843}, which expresses a green fluorescent protein (GFP) in endocardial and endothelial cells. In WT embryos, the heart is looped and the atrium and the ventricle are connected by the atrioventricular canal (AVC) at 48 hours post fertilization. In Ccm2-deficient zebrafish, I observed a dilation of cardiac chambers, heart looping defects, and an enlargement of the inflow tract region (Fig. 1 C). To visualize cardiac cushions, I performed an antibody counter staining with an

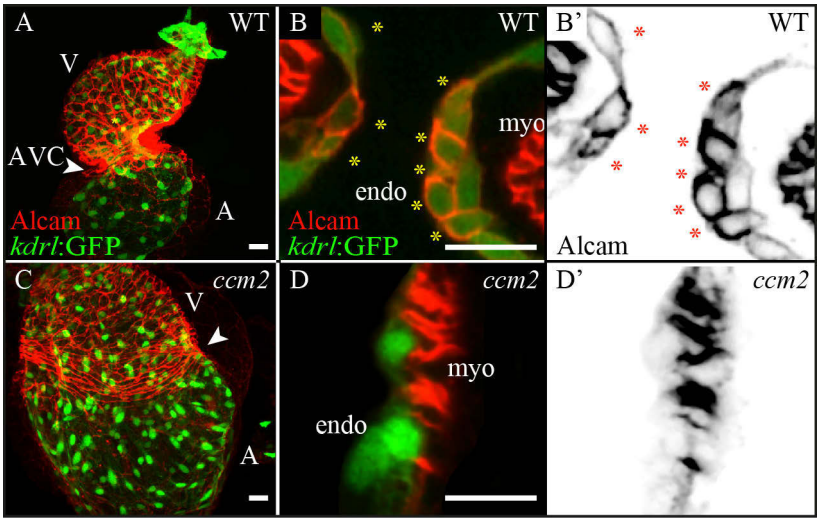

Fig. 1 Cardiac cushion phenotype in *ccm2*^{m201} mutants. (A-D) Shown are hearts of different genotypes marked by the endocardial reporter line Tg(*kdrl:GFP*)^{s843} (green) and Alcam (red) at 48 hpf. (B-D) Details showing single confocal z-stacks of the atrioventricular canal (AVC). Endocardial cushion cells are marked by Tg(*kdrl:GFP*)^{s843} and Alcam (B-D, yellow asterisks) or by Alcam alone (B´-D´, inverted image, red asterisks). V, ventricle; A, Atrium; endo, endocardium; myo, myocardium. Scale bars, 25µm.

anti-ALCAM antibody (Activated Leukocyte Cell Adhesion Molecule), a specific marker of the AVC cushions. In WT embryos the cushions consist of compact, cuboidal endocardial cells, whereas in *ccm2*^{m201} mutants the AVC completely lacks cardiac cushions. As previously mentioned, the heart chambers are dilated in *ccm2*^{m201} zebrafish mutants compared to wild-type embryos. The dilation of cardiac chambers suggested an increased endocardial cell number. Cell counts of 2 dpf (days post fertilization) hearts showed that in comparison to wild-type embryos (n=3 embryos; average cell number=144,7; S.E.M. 1,202) endocardial cell numbers in *heg*^{m552} (n=2 embryos; average cell number=219,5; S.E.M. 3,5) and *ccm2*^{m201} (n=3 embryos; average cell number=205,3; S.E.M. 6,692) mutant embryos was massively increased.

During zebrafish heart development, the myocardial layer grows by addition of new cardiomyocytes and in a concentric thickness of the myocardium (Mably et al., 2003; Mably et al., 2006). A loss-of-function of Ccm complex proteins has been associated with concentric growth defects of the myocardium (Mably et al., 2003; Mably et al., 2006). Nevertheless, a detailed characterization of cardiac defects in zebrafish *ccm* mutants was missing. To analyze the role of Ccm proteins in myocardial morphogenesis, I used an anti-ALCAM antibody, which marks myocardial cell membranes. Analyses of myocardial cell shapes showed that the loss of Ccm2 had a massive effect on myocardial cell morphology: in particular, ventricular myocardial cells were elongated and squamous in *ccm2*^{m201} mutant embryos (Fig. 2 B) causing a

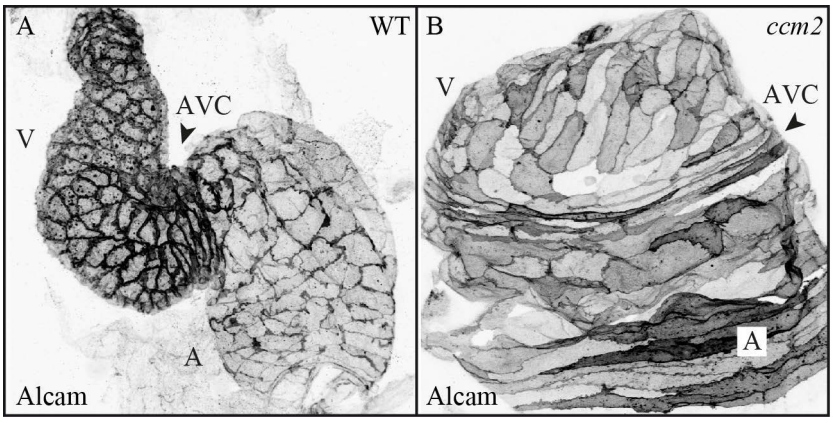

Fig. 2. Cardiac phenotype in *ccm2*^{m201} mutants. Comparison of myocardial cell morphology in wild-type (A) *and ccm2*^{m201} mutants (B) at 48 hpf using an anti-ALCAM antibody, which marks myocardial cell membranes. V, ventricle; A, Atrium; AVC , atrioventricular canal.

thinning of the ventricular chamber (Fig. 3 F), in contrast to WT ventricular myocardial cells which are typically cuboidal (Fig. 3D). Furthermore, the dense myofibrilar network present in WT was less dense in *ccm2*^{m201} mutants Fig. 3 A, B).

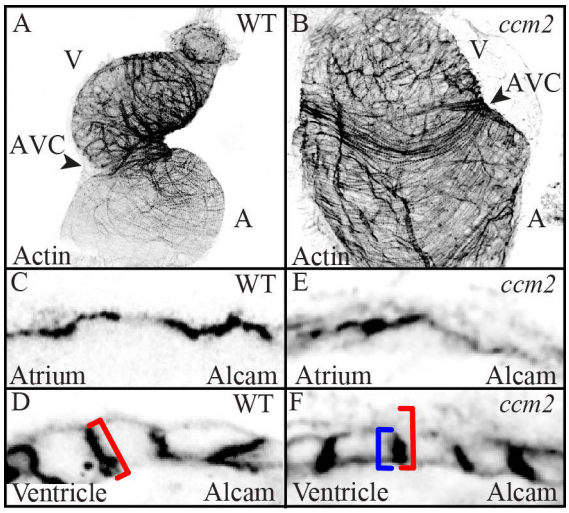

Fig. 3. Loss of Ccm2 causes thinning of the ventricular chamber. (A,B) Myocardial chamber organization is visualized by myofibrillar Actin staining in different genotypes at 48 hpf. The dense myofibrillar Actin-rich network present in WT is less dense in *ccm2*^{m201} mutants. (C-F) Anti-Alcam staining indicates that WT ventricular myocardial cells are thicker (D) than in *ccm2*^{m201} mutants (F). For comparison, red brackets in (D) and (F) have same length. V, ventricle; A, Atrium; AVC , atrioventricular canal.

Taken together, my results showed that the loss of Ccm complex proteins has a major effect on endocardial and myocardial morphogenesis. Loss of Ccm2 affects myocardial cell shapes and prevents cardiac looping. Moreover, the Ccm complex is required to restrict endocardial cell number and is required for cardiac cushion formation.

4.2 Endocardial atrioventricular canal markers are misexpressed in zebrafish *ccm* mutants

To elucidate the molecular changes associated with the loss of cardiac cushions in zebrafish *ccm* mutants, a whole mount *in situ* hybridization (WISH) assay was performed. In collaboration with Dr. Cécile Otten, I assessed the expression of genes required for the establishment of the atrioventricular canal (AVC), including *tbx2b*, *bmp4*, and *notch1b* in *ccm* mutants. Tbx2b is a myocardially expressed transcription factor, which marks the AVC region at 48 hpf (Fig. 4 A). Since it is correctly expressed in *ccm2*^{m201} mutant hearts (Fig. 4 A), the atrioventricular canal is molecularly defined. A molecular signaling cascade, which involves the endocardial gene *notch1b* and the myocardial gene *bmp4*, triggers cardiac cushion formation (MacGrogan et al., 2011; Timmerman et al., 2004). Bmp4 is prominently expressed within the myocardial AVC region and the inflow-tract (IFT) (Fig. 4 B). Consistent with the expression of *tbx2b*, *bmp4* was correctly expressed in *ccm2*^{m201}, *krit1*^{ty219c}, and *heg*^{m552} mutant hearts (Fig. 4

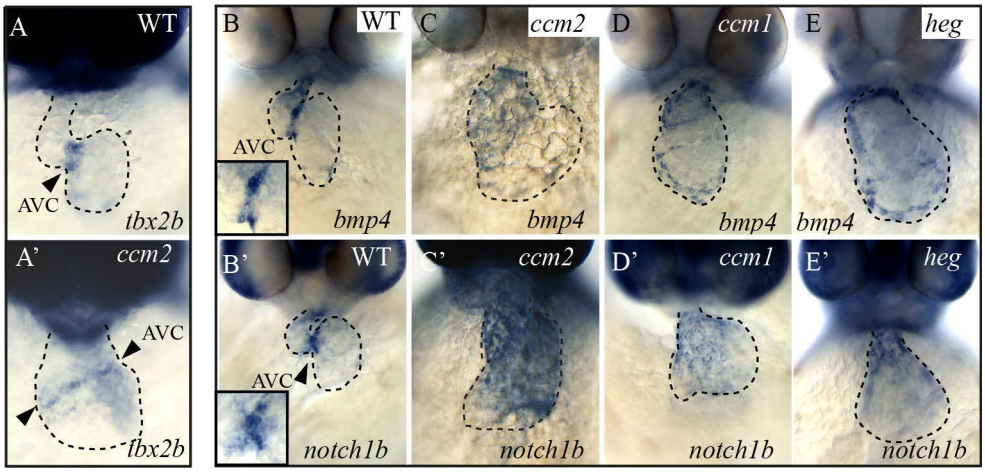

Fig. 4. Expression patterns of atrioventricular canal markers in *ccm* mutants. Shown are whole mount *in situ* hybridizations in different genotypes at 48 hpf. The AVC region is correctly marked by the expression of *tbx2b* in *ccm2*^{m201} mutants (A, A´). (B-E) Expression of *bmp4*, a myocardial marker expressed at the AVC is similar in *ccm2*^{m201}, *heg*^{m552}, or *krit1*^{ty219c} mutants. (B´-E´) Expression of *notch1b*, an endocardial AVC marker, is altered within the entire heart in *heg*^{m552}, *ccm1*^{ty219}, and *ccm2*^{m201} mutants. Arrowheads indicate the AVC. Insets are enlarged views of the AVC region. The dotted lines indicate the outline of the heart. AVC, antrioventricular canal

C-E). However, contrary to the expression of myocardially expressed genes, I found that the expression of endocardial *notch1b* was impaired in *ccm2*^{m201}, *krit1*^{ty219c}, and *heg*^{m552} mutants (Fig. 4 C`-E`). In contrast to the AVC specific expression in wild-type embryos, *notch1b* was expressed thoughout the entire endocardium in all *ccm* mutants.

Several lines of evidence suggest that AVC restricted expression of *notch1b* is crucial for normal cardiac cushion development, since both a loss- and gain-of-function of Notch signaling results in defects in AVC formation (Timmerman et al., 2004; Watanabe et al., 2006). Vermot et al. demonstrated that *notch1b* expression at the AVC was induced by blood flow. Zebrafish *silent heart* (*tnnt2a*) mutants, which lack cardiac contractility due to a mutation in the gene encoding cardiac Troponin t2a (Tnnt2a), do not express *notch1b* at the AVC. Furthermore, these mutants also lack cardiac cushions, arguing for an impact of blood flow, or of cardiac contraction, in cushion development (Chen et al., 1996). Although *ccm2*^{m201}, *krit1*^{ty219c}, or *heg*^{m552} mutants have heart contractions, these mutants lack blood flow within the major blood vessels. To examine the role of heart contraction in the misregulation of *notch1b*, I used a previously

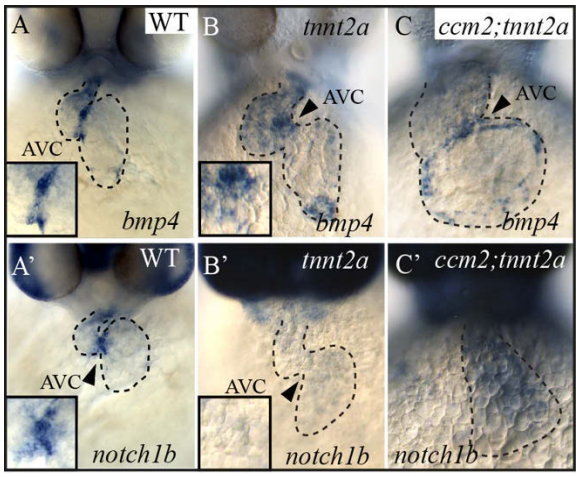

Fig. 5. Expression patterns of *bmp4* and *notch1b* under no-flow conditions. Shown are whole mount *in situ* hybridizations in different genotypes at 48 hpf. (A-C) Expression of *bmp4* at the AVC and the IFT in *ccm2*^{m201} mutant; *tnnt2a* morphant, and *tnnt2a* morphant is similar to WT. (B`) Expression of *notch1b* is abolished in *tnnt2a* morphants, whereas *notch1b* is still expressed within the entire endocardium in *ccm2*^{m201}mutant; *tnnt2a* morphants (C´) compared WT (A´). Arrowheads indicate the AVC. Insets are enlarged views of the AVC region. The dotted lines indicate the outline of the heart. AVC, antrioventricular canal

validated anti-sense oligonucleotide morpholino (MO) against Troponin t2a (Tnnt2a) (Sehnert et al., 2002), which prevents cardiac contraction. The *bmp4* expression pattern was unchanged in *tnnt2a* morphants (Fig.5 B) and *ccm2*^{m201} mutants; *tnnt2a* morphants (Fig.5 C) compared to WT. In contrast, *tnnt2a* morphants lacked *notch1b* expression within the heart (Fig.5 B´). Intriguingly, in *ccm2*^{m201} mutants; *tnnta2a* morphants, *notch1b* was still broadly expressed within the heart (Fig.5 C´).

Together, these data demonstrated that the loss of Ccm proteins prevents cardiac cushion formation, although the atrioventricular canal is molecularly defined. Furthermore, in contrast to wild-type embryos, the misexpression of *notch1b* in zebrafish *ccm* mutants is independent of blood flow.

4.3 Loss of Ccm proteins leads to elevated cardiac *klf2* expression levels

To gain a deeper insight into the molecular changes responsible for cardiac defects in *ccm2*^{m201} mutants, I performed, in collaboration with Franziska Rudolph and Jana Richter, a comparative transcriptome microarray analysis using highly purified cardiac tissue from 72 hpf *ccm2*^{m201} mutant and WT embryos. Analysis of transcriptional changes confirmed that the loss-of-function of Ccm2 affects both endocardial and myocardial gene expression, including genes involved in TGFβ signaling, angiogenesis, blood vessel development, and cardiac muscle development (data not shown). Since Krit1, Ccm2, and Heg are expressed within the endocardium but not the myocardium (Kleaveland et al. 2009 Mably et al., 2003; Mably et al., 2006), the altered expression of genes with a function in blood vessel development might be a direct consequence, whereas changes in myocardial gene expression might be an indirect consequence of the loss-of-function of Ccm proteins.

Among several endocardial genes misregulated in *ccm2*^{m201} mutants, the up-regulation of the zinc-finger transcription factors Klf2a and Klf2b was of particular interest. In zebrafish, *klf2a* plays a crucial role during endocardial cushion formation (Vermot et al., 2009). During cushion development, *klf2a* is induced by pulsatile blood flow at the AV boundary and regulates the expression of *notch1b*, *neuregulin1*, and

endothelin1 (Introduction Figure 14). The role of the *klf2b* gene during zebrafish cardiovascular development has not been elucidated so far. The fact that zebrafish *ccm* mutants lack blood flow, raised the hypothesis that the Ccm complex might regulate Klf2 expression within the heart independently of blood flow.

RT-qPCR for *klf2a* and *klf2b* was performed and confirmed the microarray results (Fig. 6). Of note, the microarray was done on heart tissue of 72 hpf old embryos,

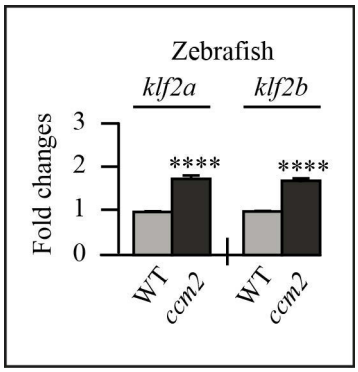

Fig. 6. Klf2 overexpression in *ccm2*^{m201} mutants. RT-qPCR analyses reveal that loss of Ccm2 causes elevated *klf2a/b* mRNA levels in zebrafish. Statistical data are means and S.E.M.; ns, not significant; *, p<0.05; **, p<0.01; ***, p<0.001; ****, p<0.0001. (for details see appendix).

whereas the RT-qPCR analyses were done on 48 hpf old whole embryonic tissue. Furthermore, whole mount *in situ* hybridizations showed that *klf2a* and *klf2b* mRNA is misexpressed in *ccm* mutants. Endocardial *klf2a* and *klf2b* expression is restricted to the cardiac cushions at the AVC at 48 hpf in wild-type embryos (Fig. 7 A, A´). In contrast,

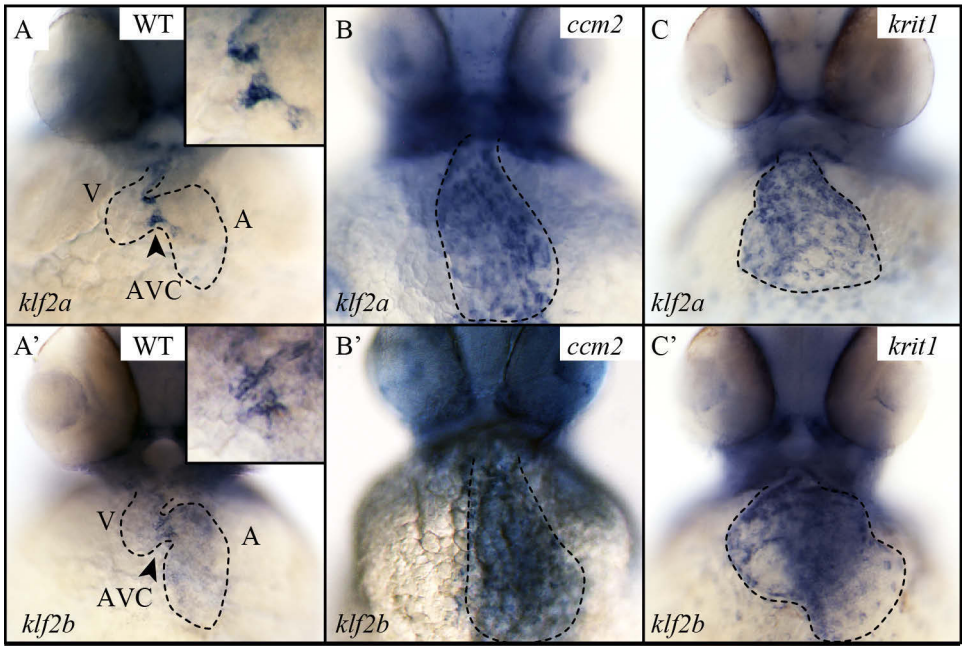

(legend on the next page)

Fig. 7. Expression of *klf2a* and *klf2b* in *ccm* mutants. Whole mount *in situ* hybridization of *klf2a* and *klf2b* mRNA in different genotypes at 48 hpf. (A, A´) *klf2a* and *klf2b* expression is restricted to the AVC in WT. (B, B´, C, C´) Both factors are expressed within the entire endocardium in *ccm2*^{m201} and *krit1*^{ty219c} mutants. V, ventricle; A, atrium; AVC, atrioventricular canal.

both factors are expressed within the entire endocardium in *ccm2*^{m201} (Fig. 7 B, B´) and *krit1*^{ty219c} (Fig. 7 C, C´) mutants.

Taken together, these results showed that the loss of CCM proteins causes an up-regulation of the blood flow sensitive transcription factor KLF2 in zebrafish hearts.

4.4 Elevated *klf2* expression levels induce cardiovascular defects similar to the phenotype resulting from loss of Ccm proteins in zebrafish

4.4.1 The knock-down of *klf2a/b* rescues the *ccm* mutant cardiac phenotype

To functionally test whether the up-regulation of *klf2a* and *klf2b* contribute to the cardiac phenotype in *ccm* mutants, I injected anti-sense oligonucleotide morpholinos (MOs) into *ccm2*^{m201} mutant embryos to partially reduce Klf2a and Klf2b protein levels. Since *klf2a* and *klf2b* are normally expressed in wild-type zebrafish embryos, a complete knock-down of Klf2 might have a phenotype on its own, but a partial reduction might restore normal Klf2 protein levels in *ccm* mutants. To visualize cardiac cushion cells, I used an anti-ALCAM antibody. High dose injection of either *klf2a* (12ng) or *klf2b* (12ng) morpholino only partially rescued endocardial cushion formation in *ccm2*^{m201} mutants at 48 hpf: The AVC exihibited only few cushion cells in *ccm2*^{m201}mutant; *klf2a* morphants or in *ccm2*^{m201} mutant; *klf2b* morphants (Fig. 8 E-H). Remarkably, a combinatorial injection of only 5ng of each MO could rescue the cardiac phenotype in *ccm2*^{m201} mutants (no *ccm2*^{m201} phenotype among n>100 injected embryos; Fig. 8 I, J). The hearts were looped and cardiac cushion cells at the AVC were cuboidal, similarly to wild-type hearts. As the cardiac rescue was complete, *ccm2*^{m201} mutant; *klf2a*/*b* morphants had to be genotyped to confirm that these were indeed *ccm2*^{m201} mutant embryos (n=8/16 mutants identified by genotyping).

As *ccm2*^{m201} and *heg*^{m552} mutants exhibited more endocardial cells than wild-type hearts, next I elucidated whether endocardial cell number could be restored when Klf2a/b protein levels were decreased in *ccm2*^{m201} and *heg*^{m552} mutants. Indeed, endocardial cell counts showed that endocardial cell numbers in *ccm2*^{m201} mutant/ *klf2a*/*b* morphant embryos were comparable to wild-type embryos (Fig. 9; wt, n=3 embryos; average cell number=144,7; S.E.M. 1,202; *ccm2*^{m201}, n=3 embryos; average cell number=205,3; S.E.M. 6,692; *ccm2*^{m201} mutant/ *klf2a*/*b* morphant, n=3 embryos; average cell number=131; S.E.M. 2,082).

Intriguingly, not only the endocardial mutant phenotype was rescued by a reduction of Klf2a and Klf2b protein levels, but also myocardial defects. The ventricular actin network of *ccm2*^{m201} mutant; *klf2a*/*b* morphants was more dense than that of *ccm2*^{m201} mutants and morphologically indistinguishable from wild-type. Even the heart looping and the dilation of the heart chambers was rescued. Together, these results suggest that the myocardial morphogenesis defects in *ccm2*^{m201} mutants were caused by an up-regulation of Klf2 in the endocardium.

To test whether the knock-down of *klf2a* and *klf2b* has a similar effect on cardiac morphogenesis of *heg*^{m552} and *krit1*^{ty219c} mutants, I injected *klf2a*/*b* morpholinos in these mutants. Indeed, knock-down of *klf2a/b* (5ng of each morpholino) also rescued cardiac cushion formation, dilation of the atrial and ventricular chambers, and the myofibrils of the ventricular myocardium in *heg*^{m552} (n=10/27 mutants identified by genotyping; Fig. 8 K,L) and *krit1*^{ty219c} (n=11/32 mutants identified by genotyping; Fig. 8 M,N).

Together, these results showed that the shear-stress transcription factors Klf2a and Klf2b act together downstream of Ccm proteins and that overexpression of both contributes to cardiac defects in *ccm* mutants.

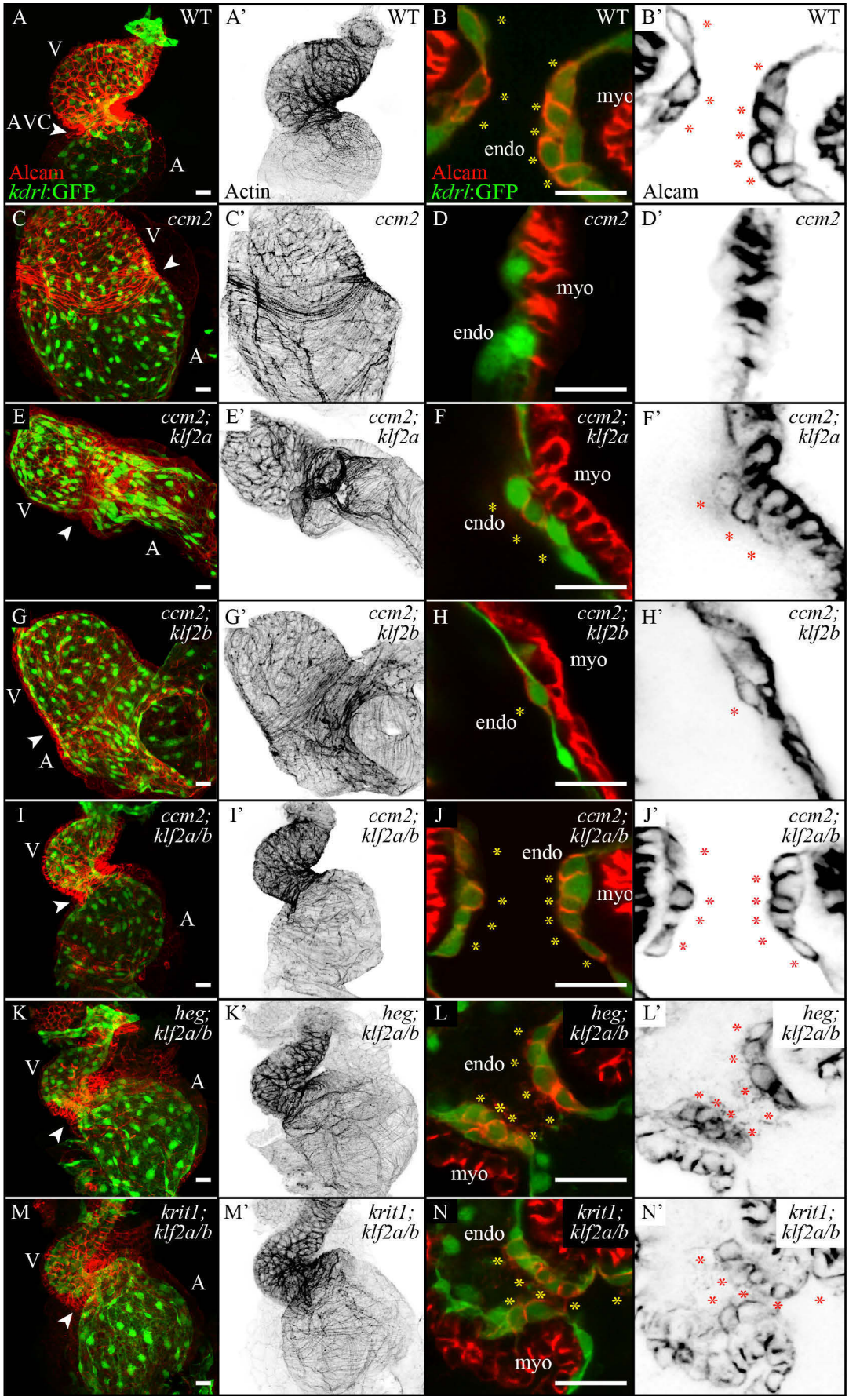

(legend on the next page)

Fig. 8. Rescue of cardiac cushions in *ccm2*^{m201}, *krit1*^{ty219}, and *heg*^{m552} mutants by knock-down of *klf2a* and *klf2b*. (A-M) Shown are hearts of different genotypes marked by the endocardial reporter line Tg(*kdrl:GFP*)^{s843} (green) and Alcam (red) or Actin staining alone (A´-M´) at 48 hpf. Details showing single confocal z-stacks of the atrioventricular canal (AVC). Endocardial cushion cells are marked by Tg(*kdrl:GFP*)^{s843} and Alcam (B-N, yellow asterisks) or by Alcam alone (B´-N´, inverted image, red asterisks). (E-H) Neither knock-down of *klf2a* (E-F) nor of *klf2b* (G-H) rescues cardiac morphogenesis and results in few cardiac cushion cells in *ccm2*^{m201} mutants. Double knock-down of *klf2a*/*b* recovers cardiac chamber differentiation and cardiac cushion formation in *ccm2*^{m201}, *krit1*^{ty219}, and *heg*^{m552} mutants (I-N). V, ventricle; A, Atrium; endo, endocardium; myo, myocardium. Scale bars, 25µm.

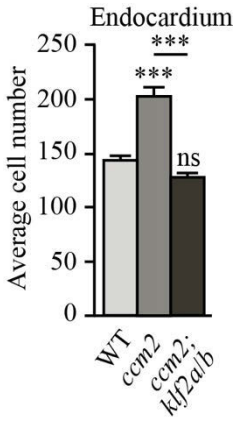

Fig. 9. Increased endocardial cell number in *ccm2*^{m201} mutants. Knock-down of *klf2a*/*b* in *ccm2*^{m201} mutants rescues endocardial cell number. Statistical data are means and S.E.M. ns, not significant; **, p<0.01; ***, p<0.001; ****, p<0.0001. (for details see appendix).

4.4.2 Klf2a and Klf2b expression is flow-independent in *ccm* mutants

Expression of Klf2 is induced by pulsatile shear stress during cardiac cushion formation (Chiplunkar et al., 2013; Dekker et al., 2002; Vermot et al., 2009). As zebrafish *ccm* mutants lack blood flow but still have a contractile heart, I was interested whether oscillatory flow within the heart chambers is causative for the elevated *klf2a* and *klf2b* expression levels and the *ccm* mutant heart phenotype. To asses the role of oscillatory flow in the regulation of Klf2 expression, I injected an antisense oligonucleotide morpholino (MO) against *tnnt2a* into *ccm2*^{m201} mutant embryos to block heart contraction.

Whole mount *in situ* hybridization against *klf2a*/*b* mRNA showed that *klf2a* and *klf2b* are expressed at the AVC in wild-type embryos at 48 hpf (Fig. 10 A, A´), whereas a lack of blood flow in *tnnt2a* morphants abolishes the expression of both genes (Fig. 10 C, C´). Contrary, in *ccm2*^{m201} mutants which lack heart contraction and blood flow, *klf2a* and *klf2b* were misexpressed within the entire endocardium (Fig. 10 D, D). RT-qPCR on whole embryonic tissue was performed and support the finding that Klf2 expression levels are still elevated in *ccm2*^{m201} mutant; *tnnt2a* morphants (Fig. 10 E).

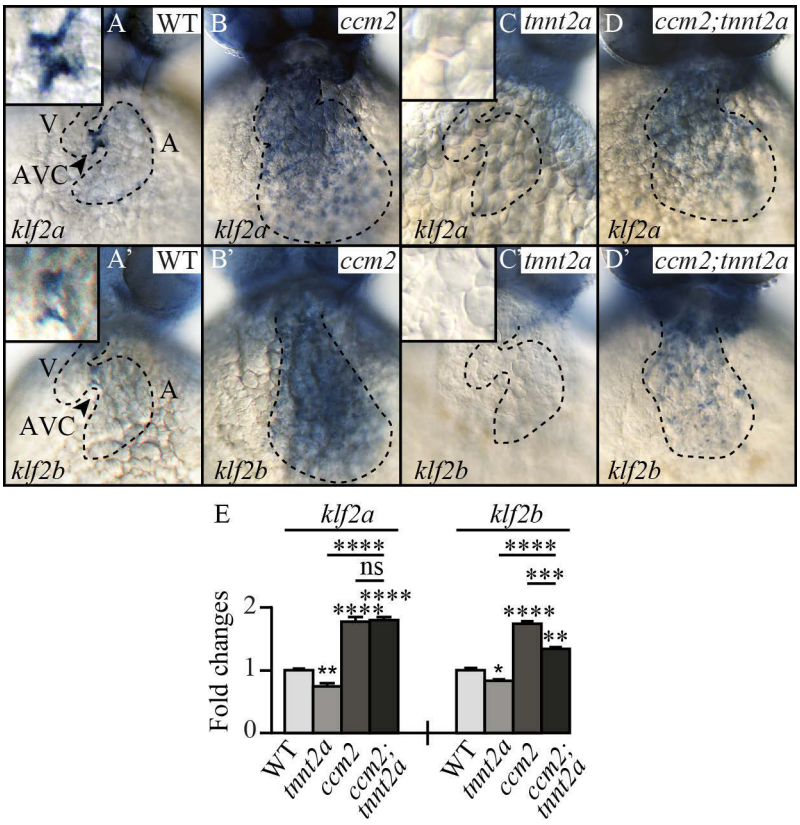

Fig. 10. Klf2 expression is independent of blood flow in the heart of *ccm2*^{m201} mutants. (A-D) Whole mount *in situ* hybridization against *klf2a*/*b* mRNA in different genotypes at 48 hpf. Loss of heart contraction abolishes *klf2* expression at the AVC in *tnnt2a* morphants (C-C´). (D-D´) *Klf2a* and *klf2b* are misexpressed within the entire endocardium in *ccm2*^{m201}mutant; *tnnt2a* morphants. (E) RT-qPCR demonstrates flow-independent overexpression of *klf2a*/*b* mRNA in whole embryos. V, ventricle; A, atrium; AVC, atrioventricular canal. Statistical data are means and S.E.M.; ns, not significant; *, p<0.05; **, p<0.01; ***, p<0.001; ****, p<0.0001. (for details see appendix).

Taken together, these results indicated a previously unappreciated role of Ccm proteins in cardiac development in limiting the expression levels of the transcription factors Klf2a and Klf2b in a flow-independent manner.

4.4.3 Vascular defects are due to increased Klf2 expression in *ccm* mutants

So far, I could show that the loss-of function of Ccm proteins in the endocardium cause an up-regulation of the transcription factor Klf2. This raised the question of whether Klf2 expression is also affected in endothelial cells in *ccm* mutants. Whole mount *in situ* hybridization analyses showed that *klf2a* is expressed in endothelial cells, e.g. the intersomitic vessels (red arrowheads) and the vascular plexus (red arrow) in wild-type embryos (Fig. 11 A). In contrast, in *ccm2*^{m201} mutants *klf2a* was up-regulated in most endothelial cells including the caudal artery (CA, black arrowhead) and the posterior cardinal vein (PCV, white arrowhead) (Fig. 11 B). Since *klf2a* was strongly up-regulated within veins and arteries in zebrafish *ccm2*^{m201} mutants, I investigated whether the up-regulation of Klf2 affects different blood vessels in addition to the endocardium and directly causes the *ccm* mutant phenotype.

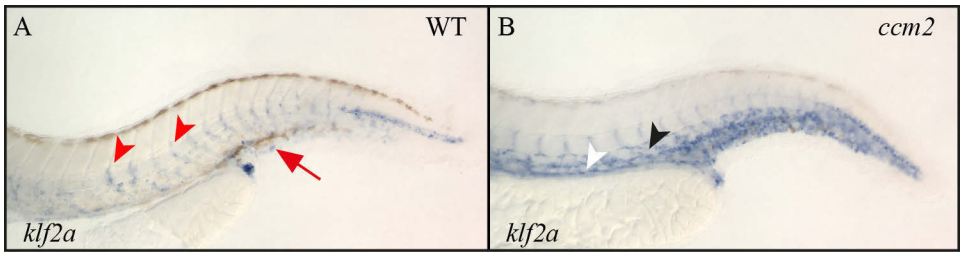

Fig.11 Loss of Ccm2 increases *klf2a* expression in the vasculature. (A, B) Whole mount *in situ* hybridization for *klf2a* in different genotypes at 48 hpf. (A) Expression of *klf2a* in endothelial cells (intersomitic vessels, red arrowheads; vascular plexus, red arrow) (B) Elevated *klf2a* mRNA levels within most endothelial cells upon loss of Ccm2 (caudal artery, black arrowhead; posterior cardinal vein, white arrowhead).

Using the stable transgenic reporter line Tg(*kdrl*:GFP)^{s843}, I could observe an expansion of the lateral dorsal aorta (LDA) in *ccm2*^{m201} mutants (Fig. 12 B). Endothelial cells counts showed, that similar to endocardium, the expansion of the LDA is due to an

increase in endothelial cell numbers (wt; n=3 embryos; average cell number=57,6; S.E.M. 1,45; *ccm2*^{m201}, n=3 embryos; average cell number=83; S.E.M 1,53). In addition to the lateral dorsal aorta, the subintestinal vein (SIV, Fig. 13, arrowhead) of *ccm2*^{m201} mutants exhibit increased numbers of sprouts compared to wild-type (wt, n=10 embryos; average number of sprouts=0,6; S.E.M. 0,339; *ccm2*^{m201}, n=10 embryos; average number of sprouts=7,3; S.E.M. 0,495) and vessel branch points (wt, n=10 embryos; average number of branchpoints=9,6; S.E.M. 0,371; *ccm2*^{m201}, n=10 embryos; average number of branchpoints=12,3; S.E.M. 0.882) at 72 hpf (Fig. 13 B, D). Vascular oversprouting and branchpoint defects are both hallmarks for increased angiogenesis (Ghajar et al. 2013, Yu et al., 2010; Avraham-Davidi et al., 2011). To asses whether these phenotypes were due to the up-regulation of *klf2a*/*b*, I injected a combination of *klf2a*/*b* MOs (5ng of each morpholino) into *ccm2*^{m201} mutants. Knock-down of *klf2a*/*b* rescued the endothelial cell number and the dilation defects of the LDA (Fig. 12 C, D; n=2 embryos; average cell number=56,5; S.E.M. 3,5). Furthermore, knock-down of *klf2a* and *klf2b* also restored the sprouting- and branchpoint defects of the SIV (n=5 embryos; average number of branchpoints=8,2; S.E.M. 0,583; average number of sprouts=2,6; S.E.M. 0,678) (Fig. 13 C, D).

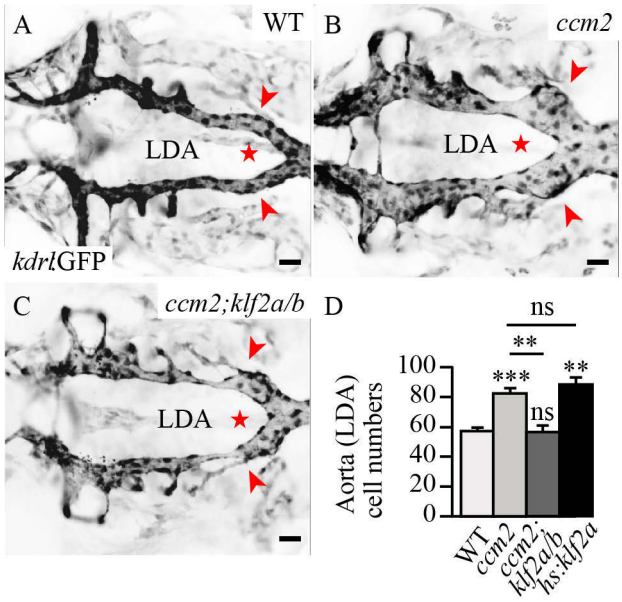

Fig. 12. Elevated *klf2* mRNA levels causes expansion and increased cell number of the lateral dorsal aorta. (A-C) Dorsal views of the lateral dorsal aorta (LDA, red arrowheads) in different genotypes marked by Tg(*kdrl:GFP*)^{s843} at 48 hpf. (B) Expansion and overproliferation in *ccm2*^{m201} mutants is rescued by knock-down of *klf2a*/*b* mRNA levels (C-D). LDA, lateral dorsal aorta; red star, branchpoint of the LDA; Statistical data are means and S.E.M. ns, not significant; **, p<0.01; ***, p<0.001; ****, p<0.0001. (for details see appendix). Scale bars, 25µm.

For functional studies, I generated a Tg(*hsp70l:klf2a*)^{md8} transgenic zebrafish line for heat-shock-inducible *klf2a* overexpression in the entire embryo. Consecutive heat-shock

induction of this transgene at 15, 30, and again 38 hpf resulted in increased LDA cell numbers at 48 hpf (*hsp70l:klf2a*; n=2 embryos; average cell number=88,8; S.E.M. 4,5), which is comparable to *ccm2*^{m201} mutants (Fig. 12 D).

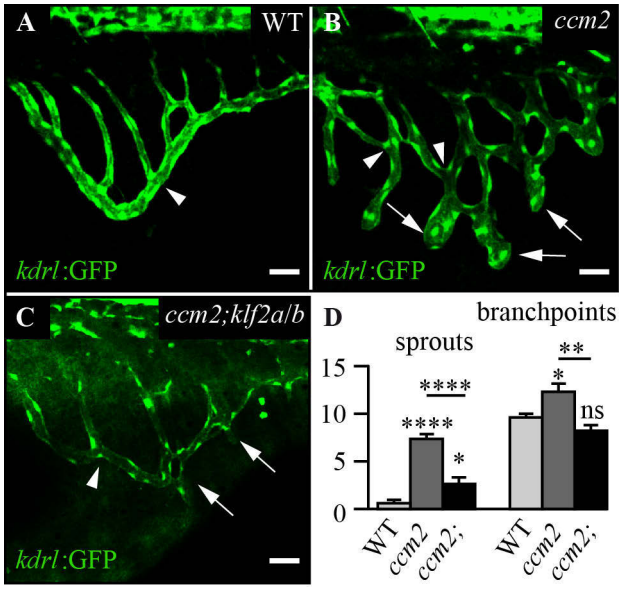

Fig. 13. Oversprouting and vascular branch point defects in *ccm2*^{m201} mutant rescued by knock-down of *klf2*. (A-C) Shown are subintestinal veins (SIV) of different genotypes marked by the endothelial reporter line Tg(*kdrl:GFP*)^{s843} at 72 hpf. (B-D) SIVs (arrowhead) exhibit ectopic sprouts (arrow) in *ccm2*^{m201} mutans. (C-D) Knock-down of *klf2a*/*b* rescues branchpoints and sprouting phenotypes. Statistical data are means and S.E.M. ns, not significant; **, p<0.01; ***, p<0.001; ****, p<0.0001. (for details see appendix). Scale bars. 25µm.

Together, these results supported the role of Klf2 as a pro-angiogenic factor in endothelial cells.

4.4.4 Lack of blood flow mediates cerebral vascular sprout growth in *ccm* mutants

Vascular malformations in *iCCM2* knockout mice and in human patients occur predominantly in the cerebral vasculature (Boulday et al., 2009; Boulday et al., 2011). Therefore, I was particurlarly interested, whether these vessels were also affected in *ccm* mutant zebrafish embryos. Here, I describe for the first time the consequences of loss-of-function of the Ccm complex proteins on cerebral blood vessel development in zebrafish. The cerebral blood vessel are dilated and well perfused under normal conditions. Furthermore, endothelial cells exhibit a smooth surface in wild-type embryos (Fig. 14A´). In contrast, within the cerebral vasculature of *ccm2*^{m201}, *krit1*^{ty219c}, and *heg*^{m552} mutants, several blood vessels including the middle and the posterior mesencephalic central arteries (pmCtA) are characterized by ectopic sprouts and a lack of vascular lumen at 48 hpf (Fig. 14 B´, C´, D´). Remarkably, ectopic sprouting in the

cerebral vasculature of *ccm2*^{m201} mutants was suppressed by the simultaneous knock-down of *klf2a* and *klf2b* (Fig. 14 E-E´). Vascular lumen and blood flow could also be observed in some embryos. Since *ccm* mutants lack a functional circulatory system, I hypothesized that the observed phenotype might be due to hypoxia. To test this, I analyzed cerebral blood vessel development in zebrafish no-flow *tnnt2a*^{b109} mutants.

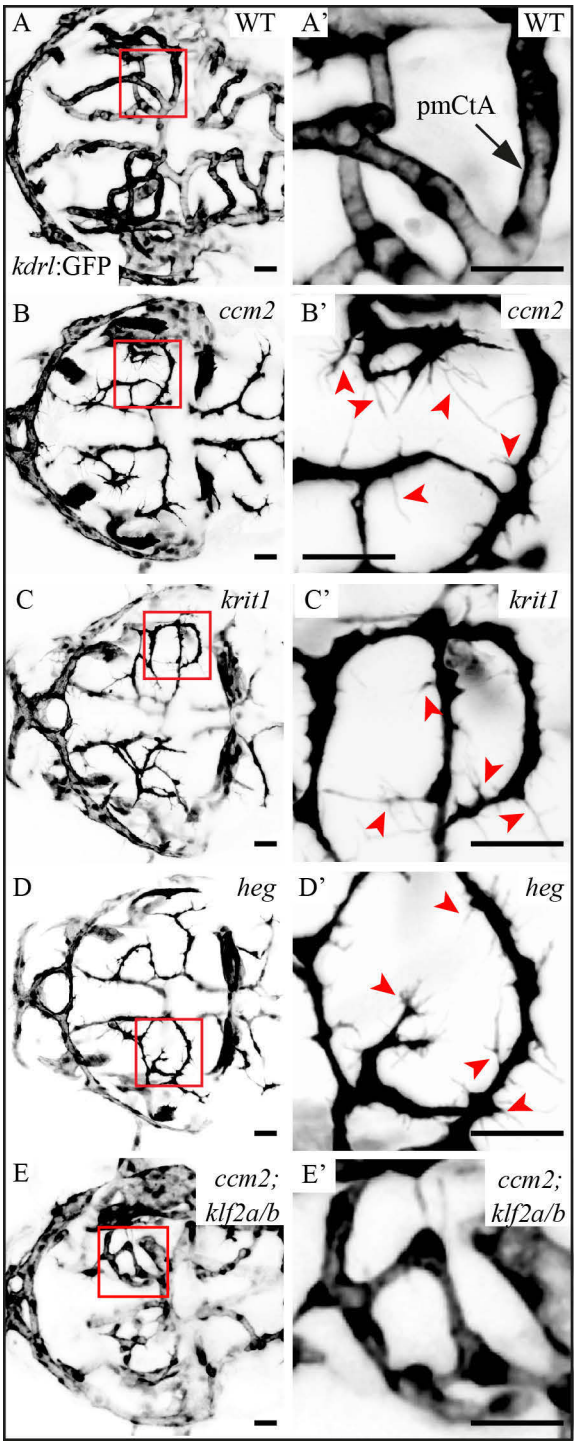

Fig. 14. Cerebral blood vessel defects in different *ccm* mutants. (A,E) Dorsal views of the cerebral blood vessels in different genotypes marked by Tg(*kdrl:GFP*)^{s843} at 48 hpf. (B-D) Vascular oversprouting in *ccm2*^{m201}, *krit1*^{ty219}, and *heg*^{m552} mutants (red arrowheads). (E) Rescue of sprouting and lumenization defects in *ccm2*^{m201} mutants by knock-down of *klf2a/b*. pmCtA, posterior mesencephalic central artery. Scale bars, 25μm

Similar to *heg*^{m552}, *krit1*^{ty219c}, and *ccm2*^{m201}, *tnnt2a*^{b109} mutant cerebral blood vessels exhibit extensive vascular sprouts and vascular lumenization defects (Fig. 15 B-B´, n=5/5 embryos).

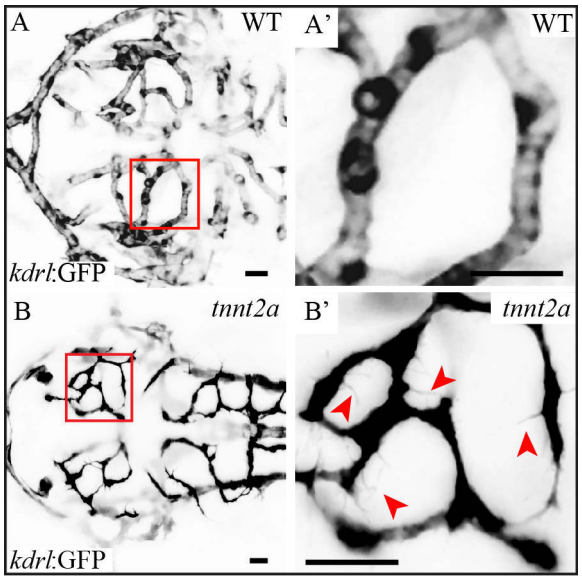

Fig. 15. Cerebral blood vessel defects in *tnnt2a*^{b109} mutants. (A,B) Dorsal views of the cerebral blood vessels marked by Tg(*kdrl:GFP*)^{s843} at 48 hpf. (B´) Vascular oversprouting in *tnnt2a*^{b109} mutants (red arrowheads). Scale bars, 25µm

Taken together, knock-down of *klf2a* and *klf2b* not only rescued increased endocardial cell number but also ectopic sprouting of the cerebral blood vessels in zebrafish *ccm* mutants, possibly in part by re-establishment of blood flow, and therefore vascular lumen formation.

4.5 An anti-angiogenic activity of Ccm proteins contributes to normal cardiovascular development in zebrafish

4.5.1 A loss of Ccm proteins triggers a VEGF-dependent angiogenic activity in endocardial cells

Angiogenesis is the formation of new blood vessels from pre-existing vessels. Proliferation and sprout formation of endothelial cells drive this process. Studies in EC culture have shown that angiogenesis signaling activity is increased upon loss of Ccm proteins (Wustehube et al., 2010; Zhu et al., 2010). In human patients, cerebral cavernous malformation lesion growth was found to correlate with increased circulating

concentrations of VEGF, a prowth factor required for angiogenesis (Jung et al., 2003). Since the cardiovascular defects and microarray data suggested ongoing, active angiogenesis in *ccm* mutants, I investigated whether elevated angiogenesis signaling

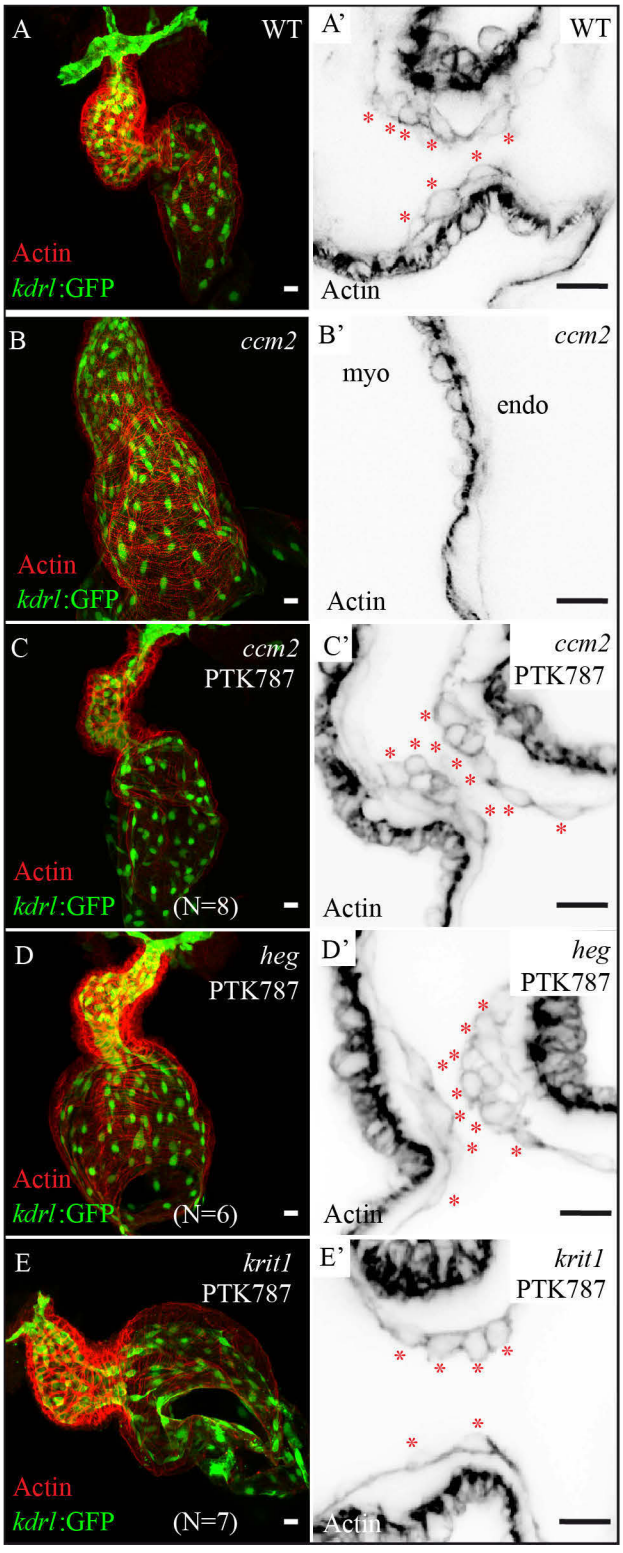

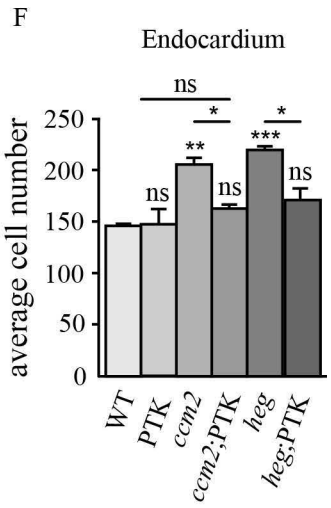

Fig. 16. Increased VEGF signaling is involved in *ccm* mutant phenotypes. (A-E) Shown are hearts of different genotypes marked by the endocardial reporter line Tg(*kdrl:GFP*)^{s843} (green) and Actin (red) at 48 hpf. (A´-E´) Details showing single confocal z-stacks of the atrioventricular canal (AVC). Endocardial cushion cells are marked by Actin (inverted image, red asterisks). (F) Endocardial cell numbers are significantly reduced in PTK787 treated *ccm2*^{m201} and *heg*^{m552} mutants compared to untreated mutants. Statistical data are means and S.E.M. ns, not significant; *, p<0.05; **, p<0.01; ***, p<0.001; ****, p<0.0001. (for details see appendix). Scale bars, 25µm.

was involved in the *ccm2* mutant phenotype. Using a pharmacological approach, I inhibited the VEGF signaling pathway using the compound PTK787 (Chan et al., 2002). Pharmacological inhibition of VEGF signaling during different developmental periods helped to determine a critical time window between 15-17 hpf during which the inhibition of VEGF signaling could rescue the cardiac phenotypes of *heg*^{m552} (n=6/8 mutants identified by genotyping), *krit1*^{ty219c} (n=7/8 mutants identified by genotyping), or *ccm2*^{m201} (n=8/8 mutants identified by genotyping) mutants at 48hpf (Fig. 16). Similar to the knock-down of *klf2a*/*b*, PTK787-treated mutant embryos developed normal cardiac cushions consisting of compact, cuboidal endocardial cells. Additionally, cardiac looping occured normally, and the ventricular myocardium exhibited a compact actin-rich myofibrilar network (Fig. 16 C-E). Furthermore, cell counts revealed a reduction of endocardial cell numbers comparable to wild-type embryos in *heg*^{m552} and *ccm2*^{m201} mutants treated with PTK787 (wt, n=3 embryos; average cell number=144,7; S.E.M. 1,202; *heg*^{m552}, n= 2 embryos; average cell number=219,5; S.E.M. 3,5; *ccm2*^{m201}, n=3 embryos; average cell number=205,3; S.E.M. 6,692; *heg*^{m552} + PTK787, n=3 embryos; average cell number=170,3; S.E.M. 12; *ccm2*^{m201} + PTK787, n=4 embryos; average cell number=162,5; S.E.M. 3,797). Due to the complete cardiac rescue, including blood flow in *ccm* mutants, it was nescessary to genotype these embryos. Moreover, I could show that VEGF signaling was dispensable for normal endocardial proliferation, since the inhibition with PTK787 had no impact on endocardial cell numbers at 48 hpf (wt, n=3 embryos; average cell number=144,7; S.E.M. 1,202; wt + PTK787, n=3 embryos; average cell number=146,7; S.E.M. 14,52) (Fig. 16 F) (Dietrich et al., 2014). Intriguingly, at 15-17 hpf the zebrafish heart is not yet formed and endocardial and myocardial progenitor cells are located as bilateral populations in the anterior lateral plate mesoderm (ALPM). Nevertheless, *heg*^{m552}, *krit1*^{ty219c}, or *ccm2*^{m201} mutant hearts were rescued as a consequence of the early PTK787 treatment.

Taken together, these data showed that there is excessive VEGF-dependent angiogenesis in *ccm* mutants. Therefore, one function of Ccm proteins is to control angiogenesis in endocardial progenitor cells at 15-17hpf.

4.5.2 Vascular defects are due to elevated VEGF-dependent angiogenesis in *ccm* mutants

To examine whether increased angiogenesis signaling was responsible for the vascular phenotype in *ccm* mutants, I treated *ccm2*^{m201} mutant embryos between 24-48 hpf with PTK787 (12,5µM). Analysis of the lateral dorsal aorta (LDA) showed that the increased endothelial cell number of this vessel was rescued upon inhibition of VEGF signaling (Fig. 17, wt, n=3 embryos; average cell number=57,6; S.E.M. 1,45*;* *ccm2*^{m201}, n=3 embryos; average cell number=83; S.E.M. 1,53; *ccm2*^{m201} + PTK787, n=3 embryos; average cell number=62; S.E.M. 1,53).

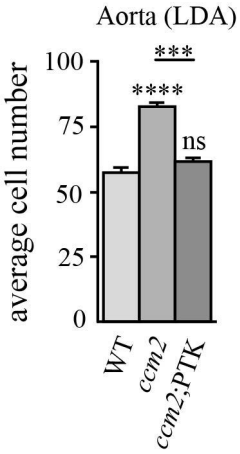

Fig. 17. VEGF inhibition rescues the vascular phenotype in *ccm2*^{m201} mutants. Treatment of *ccm2*^{m201} mutants with PTK787 between 24-48 hpf rescues the increased cell number of the lateral dorsal aorta**.** Statistical data are means and S.E.M. ns, not significant; **, p<0.01; ***, p<0.001; ****, p<0.0001. (for details see appendix).

Cerebral blood vessel are highly sensitive to VEGF signaling. To avoid that an early inhibition of VEGF signaling may affect proper cerebral vascular development, I treated WT and *ccm2*^{m201} mutant embryos at 48 hpf, a timepoint at which the head vasculature is already established. Treatment with PTK787 between 48-49 hpf had no obvious effect on cerebral blood vessels in wild-type embryos (Fig. 18 A-A´´´), whereas the short inhibition was sufficient to inhibit ectopic vascular sprout formation in *ccm2*^{m201} mutants (Fig. 18 B´´). Intriguingly, ECs of the cerebral vessels started sprouting upon the removal of the VEGF inhibitor PTK787 within 1 hour (Fig. 18 B´´´). In summary, I found that Ccm complex proteins prevent aberrant pro-angiogenic VEGF signaling in endocardial and endothelial cells.

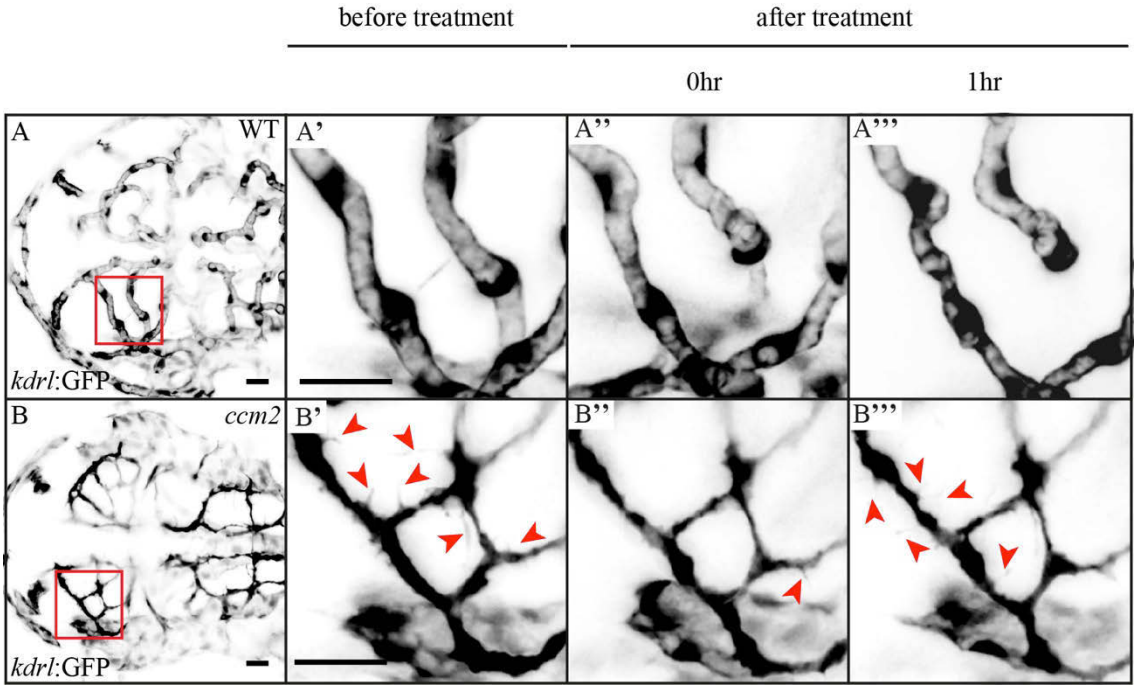

Fig. 18. Elevated VEGF signaling causes ectopic sprout formation in the cerebral vasculature of *ccm2*^{m201} mutants. (A,B) Dorsal views onto cerebral blood vessels in wild-type and *ccm2*^{m201} mutants marked by Tg(*kdrl:GFP*)^{s843} between 48-50 hpf. (A-A´´´) Treatment with PTK787 between 48-49 hpf has no effect on blood vessels in WT. In *ccm2*^{m201} mutants, blood vessels exhibit extensive sprout formation (B´, red arrowheads). Treatment with PTK787 significantly reduced the oversprouting phenotype (B´´). (B´´´) Reoccurence of ectopic sprouts within 1hr after removal of the inhibitor (red arrowheads). Timeseries between 48-50 hpf. Scale bars, 25µm.

4.5.3 Klf2 up-regulation is independent of the VEGF signaling pathway in *ccm2* mutants

Because either *klf2a*/*b* knock-down or inhibition of VEGF signaling rescued the cardiovascular phenotype of *ccm* mutants, I next tested whether Klf2 expression is regulated by VEGF signaling (or vice versa). *Klf2a*/*b* mRNA levels were measured in PTK787- treated WT and *ccm2*^{m201} mutant embryos. RT-qPCR analyses showed that inhibition of the VEGF signaling pathway did not affect *klf2a*/*b* mRNA expression in either WT or *ccm2*^{m201} mutants (Fig. 19). Thus, Klf2 is not regulated by VEGF but seems rather to act upstream or in parallel of VEGF signaling.

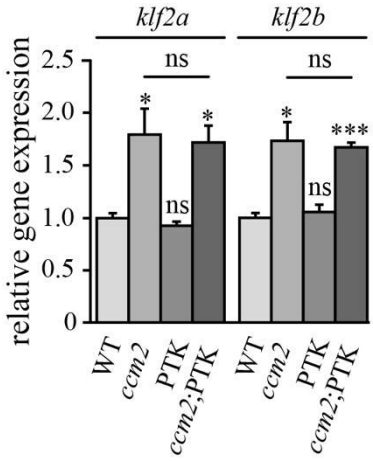

Fig. 19. Klf2 up-regulation is independent of VEGF signaling in *ccm2* mutants. PTK787 treatment between 15-48 hpf does not affect the elevated expression levels of *klf2a* and *klf2b* mRNA in *ccm2*^{m201} mutants as validated by RT-qPCR. Statistical data are means and S.E.M. ns, not significant; *, p<0.05; **, p<0.01; ***, p<0.001; ****, p<0.0001. (for details see appendix).

4.6 Klf2 up-regulation in endothelial cells involves aberrant β1 integrin signaling

Given that neither VEGF signaling nor blood flow regulates Klf2 expression in *ccm* mutants suggested that other mechanisms might be involved in the induction of *klf2a*/*b* mRNA expression. Previous studies showed that CCM proteins play an important role in the regulation of β1 integrin signaling (Faurobert et al., 2013) by interacting with and stabilizing the negative regulator integrin cytoplasmic domain-associated protein-1 (ICAP-1) (Faurobert et al., 2013; Hilder et al., 2007; Zawistowski et al., 2005; Zhang et al., 2001). Therefore, we tested whether Klf2 levels are changed upon knock-down of β1 integrin. Loss of CCM proteins in HUVECs resulted in elevated KLF2 expression levels, which could be suppressed by simultaneous depletion of ITGB1 (Renz et al., 2015).

To verify the role of β1 integrin signaling in *ccm* pathology in an animal model, I injected a morpholino against β1 integrin (*itgb1b*; 6,3ng) in zebrafish *ccm2*^{m201} mutants (Ablooglu et al., 2010). Similar to the knock-down of *klf2a*/*b*, the loss of Itgb1b rescued the cardiac phenotypes of *ccm2*^{m201} mutants including cushion formation and chamber morphogenesis (n=5/5 *ccm2*^{m201} mutants identified by genotyping; Fig. 20 C-C`) at 48 hpf.

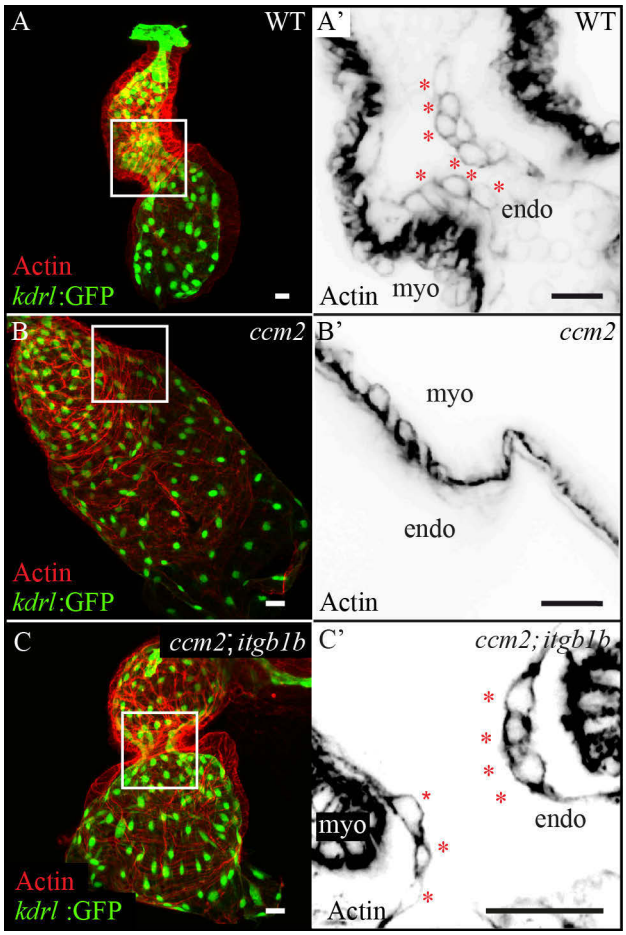

Fig. 20. Knock-down of *itgb1b* rescues cardiac phenotypes in *ccm2*^{m201} mutants. (A-C) Shown are hearts of different genotypes marked by the endocardial reporter line Tg(*kdrl:GFP*)^{s843} (green) and Actin (red) at 48 hpf. Details showing single confocal z-stacks of the atrioventricular canal (AVC). Endocardial cushion cells are marked by Actin (A´-E´, inverted image, red asterisks). (C-C´) Reduction of *itgb1b* mRNA levels rescues cardiac defects including chamber differentiation and cardiac cushion formation in *ccm2*^{m201} mutants. Scale bars, 25µm

In a complementary approach, I injected a morpholino against the negative regulator ICAP-1 (*icap-1*; 8,3ng) in wild-type embryos to test whether increased β1 integrin signaling is responsible for the cardiovascular phenotype in *ccm2*^{m201} mutants. Indeed,

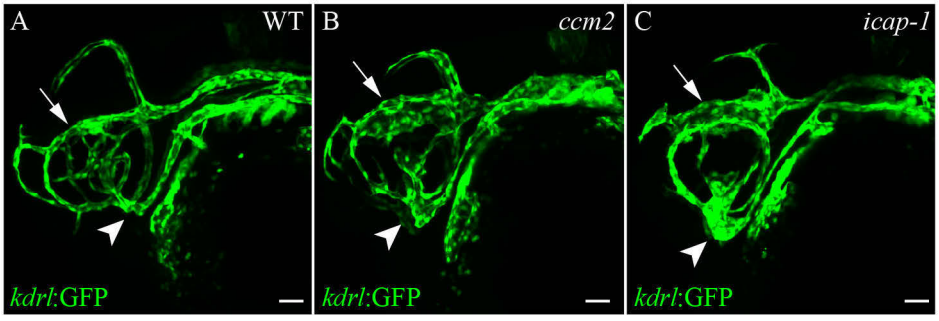

Fig. 21. Loss of ICAP1 causes phenotypes similar to *ccm2*^{m201} in cranial blood vessel at 30 hpf. (A-C) Lateral views of different genotypes marked by Tg(*kdrl:GFP*)^{s843}. (B) Dilation of the primordial midbrain channel (PMBC, arrow) and of the primitiv internal carotid artery (PICA, arrowhead) in *ccm2*^{m201} mutants. (C) Knock-down of ICAP1 phenocopies the *ccm2*^{m201} mutant phenotype. Scale bars, 50µm

knock-down of ICAP-1 caused a dilation of the primordial midbrain channel (PMBC, arrow) and of the primitiv internal carotid artery (PICA, arrowhead) (Fig. 21 C) at 30 hpf similar to the phenotype observed in *ccm2*^{m201} mutants (Fig. 21 B).

Taken together, these results suggested that aberrant β1 integrin signaling has a role in *ccm* mutants upon loss of the ICAP1-CCM complex.

4.7 Epidermal growth factor-like domain 7 (EGFL7) as a mediator of pro-angiogenic Klf2 activity in endocardial and endothelial cells

4.7.1 Klf2 mediates increased VEGF-dependent angiogenesis via Egfl7 in *ccm2*^{m201} mutants

The finding that *egfl7* has a putative binding site for Klf2 in its promoter region (Harris et al., 2010) and is involved in angiogenesis by binding to various receptors in the extracellular matrix (ECM), e.g. integrins (Nikolic et al., 2013) or the Notch pathway (Nichol and Stuhlmann, 2012; Schmidt et al., 2009), raised the hypothesis that elevated Klf2 levels may result in an overexpression of *egfl7* that might contribute to the *ccm* phenotype.

In zebrafish, cardiac microarray analysis and RT-qPCR experiments of whole embryonic tissue, done in collaboration with Dr. Cécile Otten, revealed significantly increased *egfl7* mRNA levels in *ccm2*^{m201} mutants compared to wild-type embryos, which can be reduced by the injection of *klf2a*/*b* MOs (Fig. 22 A). Conversely, the overexpression of either *klf2a* [Tg(*hsp70l:klf2a_IRES_GFP*)^{md8}] or of *klf2b* [Tg(*hsp70l_klf2b_IRES_GFP*)^{md9}] was sufficient to increase *egfl7* mRNA expression levels, validated by RT-qPCR analysis (Fig.22 A). To further investigate the role of *egfl7* in *ccm2*^{m201} mutant cardiovascular malformations, I knocked-down Egfl7, which rescued the *ccm2*^{m201} mutant cardiac cushion and dilation defects (n=15/24 mutants identified by genotyping; Fig. 22 D-D´). Moreover, the cerebral ectopic sprouts were suppressed in *ccm2*^{m201} mutants (n=5/5 mutants identified by genotyping; Fig. 23 C-C´), even in the absence of blood flow due to a failure of cardiac recovery in some *ccm2*^{m201} mutant embryos (n=3/3; Fig. 23 D-D´). This finding is intriguing, since *tnnt2a*^{b109}

mutants which also lack blood flow, exhibit ectopic sprouts of the cerebral vasculature (Fig. 15 B´). Together, these results suggested that Klf2 mediates increased VEGF-dependent angiogenesis via Egfl7 independent of blood flow in *ccm2*^{m201} mutants.

.

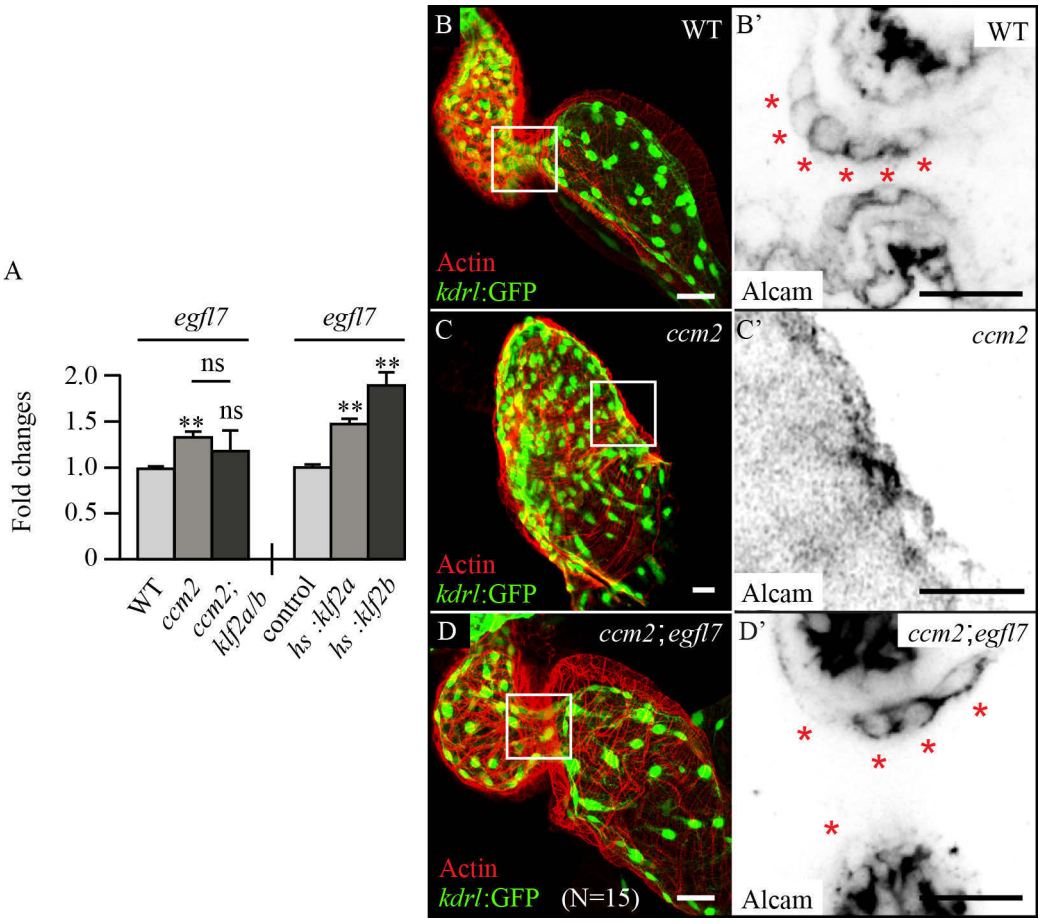

Fig. 22. Misregulation of the angiogenic signaling factor Egfl7 is involved in the zebrafish *ccm2* mutant phenotype. (A) Loss of Ccm2 or overexpression of *klf2a/b* in Tg(*hsp70l:klf2a_IRES_GFP*)^{md8} or Tg(*hsp70l:klf2b_IRES_GFP*)^{md9} transgenic embryos increased *egfl7* mRNA levels as validated by RT-qPCR. (B-D) Shown are hearts of different genotypes marked by the endocardial reporter line Tg(*kdrl:GFP*)^{s843} (green) and Actin (red) at 48 hpf. (B´-D´) Details showing single confocal z-stacks of the atrioventricular canal (AVC). Endocardial cushion cells are marked by Alcam (inverted image, red asterisks). Knock-down of *egfl7* rescues cardiac cushion development and chamber morphogenesis in *ccm2*^{m201} mutants. Statistical data are means and S.E.M. ns, not significant; *, p<0.05; **, p<0.01; ***, p<0.001; ****, p<0.0001. (for details see appendix). Scale bars, 25µm.

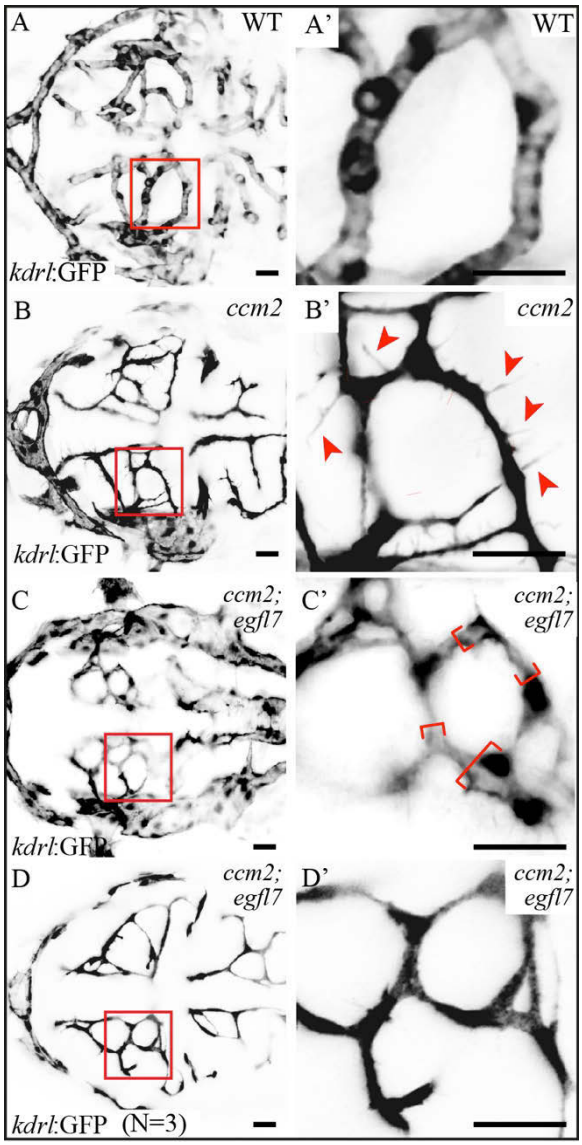

Fig. 23. Rescue of extensive sprout growth and vascular lumen formation in *ccm2*^{m201} mutants by knock-down of *egfl7*. (A,D) Dorsal views of the cerebral blood vessels in different genotypes marked by Tg(*kdrl:GFP*)^{s843} at 48 hpf. (A´-D´) Details of the cerebral vasculature. (C-C`) Knock-down of *egfl7* with cardiac rescue (lumen formation, red bracktes). (D-D´) Knock-down of *egfl7* without cardiac rescue in *ccm2*^{m201} mutants. Scale bars, 25µm.

4.7.2 Klf2a/b and Egfl7 genetically interact to promote cardiovascular malformation defects in *ccm2*^{m201} mutants

To test whether *klf2a*/*b* and *egfl7* genetically interact in a common pathway in *ccm* mutants, I injected low doses of either *klf2a*/*b* MOs (2,5ng each) or *egfl7*MO (0,3ng) into *ccm2*^{m201} mutants. Whereas single injections did not rescue the lumenization defects of the intersegmental vessels (ISVs) of *ccm2*^{m201} mutants (no rescue among n>50 *ccm2*^{m201} mutants tested for each MO; Fig. 24 C,D), a combination of *klf2a*/*b* MOs and *egfl7* MO re-established proper intersegmental vessel lumen formation (n=19/21 mutants identified by genotyping; Fig. 24 E).

In a complemetary effort, I injected *egfl7* MO into wild-type and *ccm2*^{m201} mutants and Dr. Cécile Otten measured *klf2a*/*b* mRNA levels by RT-qPCR to examine whether *egfl7* activity affects *klf2a*/*b* expression. Indeed, analysis of *egfl7* morphants and *ccm2*^{m201} mutant; *egfl7* morphants showed a reduction of *klf2a* and *klf2b* mRNA levels in both WT and *ccm2*^{m201} mutants upon knock-down of *egfl7* (Fig. 24 E). Thus, Klf2 may not only regulate Egfl7, but in turn Egfl7 may affect *klf2* mRNA expression.

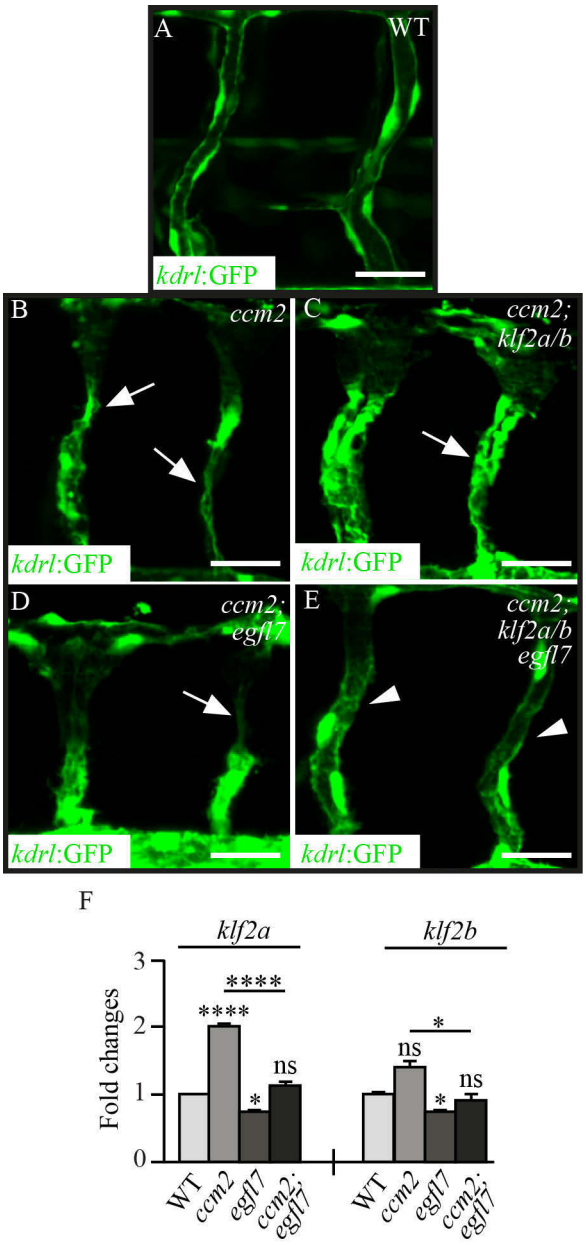

Fig. 24. Klf2a/b and Egfl7 genetically interact to regulate vascular lumen formation of the intersegmental blood vessels. (A-E) Shown are intersegmental blood vessels marked by Tg(*kdrl:GFP*)^{s843} at 48 hpf. (B) Lack of intersegmental vessels in *ccm2*^{m201} mutants (arrow). (C-D) Low doses of *klf2a*/*b* MOs or *egfl7* MO do not rescue the lumenization defects (arrows). (E) Triple-injection of *klf2a*/*b* MOs and *egfl7* MO completely rescues lumenization defects (arrowheads). (F) Knock-down of *egfl7* affects *klf2a* and *klf2b* mRNA levels in WT and *ccm2*^{m201} mutants as detected by RT-qPCR. Statistical data are means and S.E.M. ns, not significant; *, $p<0.05$; **, $p<0.01$; ***, $p<0.001$. (for details see appendix). Scale bars, 25μm.

Taken together, these results showed that Klf2 and Egfl7 act together in the regulation of VEGF-dependent angiogenesis during cardiovascular development in zebrafish.

5 Discussion

In my study, I showed that the cardiovascular defects in zebrafish *ccm* mutants are caused by a β1 Integrin-Klf2-dependent up-regulation of VEGF angiogenesis signaling in endothelial and endocardial cells. Furthermore, I showed that the pro-angiogenic activity of Klf2 is mediated by the stimulation of *egfl7* expression and that *klf2* expression in CCM-deficient cells is independent of blood flow (Fig. 25).

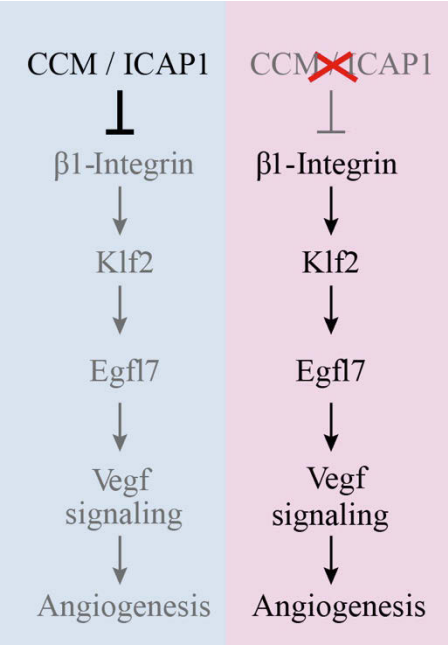

Fig. 25. Model for CCM/ICAP1–dependent pro-angiogenic activity via β1 integrin, Klf2, and Egfl7. (A) The CCM/ICAP-1 complex prevents pro-angiogenic β1 integrin signaling in endothelial/endocardial cells. (B) The loss of the CCM/ICAP-1 complex causes elevated β1 integrin activity, resulting in increased angiogenesis via Klf2 and Egfl7.

5.1 The CCM protein complex prevents extensive pro-angiogenic Klf2 activity in endocardial and endothelial cells

During vascular development, the CCM complex plays a major role in regulating vascular lumen formation, vascular integrity, and junctional stability (Hogan et al., 2008; Kleaveland et al., 2009; Lampugnani et al., 2010; Stockton et al., 2010; Whitehead et al., 2009). However, these findings could not explain why only small capillary veins are affected by cavernoma formation in patients and in mice. Compared to arteries, veins have a wider inner diameter and decreased blood pressure. Furthermore, arteries and veins differ from each other by their genetic program. This

genetic program may, in part, be regulated by CCM proteins and blood flow. Genes which are normally suppressed in venous tissue, are expressed upon loss of the CCM complex and may result in the formation of CCMs. Among several blood flow-regulated genes, the zinc-finger transcription factor KLF2 plays an important role in blood vessel biology. In endothelial cells, Klf2 activity is involved in vascular tone regulation (Dekker et al., 2005; Parmar et al., 2006; SenBanerjee et al., 2004), inflammation (Boon et al., 2007; Egorova et al., 2011; Fledderus et al., 2007; Helbing et al., 2011), thrombosis (Allen et al., 2011; Lin et al., 2005), oxidative stress (Dekker et al., 2006; Fledderus et al., 2008; Lee et al., 2012), endothelial barrier function (Lin et al., 2010b; Shi et al., 2013), and endothelial morphology (Boon et al., 2010; Dekker et al., 2006). Previous studies have shown that KLF2 has a vasoprotective function in the vasculature, dependent on blood flow patterns (Dekker et al., 2005; Huddleson et al., 2005; Parmar et al., 2006). Klf2 activity can be modulated at different levels, including at the transcriptional (Wu et al., 2011) and posttranscriptional level (Wu et al., 2011), or by posttranslational modifications (Wang et al., 2010a; Young et al., 2009). In contrast, several lines of evidence suggest a pro-angiogenic function of Klf2 in vascular biology. During zebrafish aortic arch blood vessel development, Klf2 regulates a signaling cascade involved in the expression of the endothelial-specific *miR126*, which promotes VEGF-dependent angiogenesis (Nicoli et al., 2010)

Based on the results obtained from the zebrafish cardiac microarray, I found that the shear-stress sensitive transcription factors *klf2a* and *klf2b* are up-regulated in zebrafish upon loss of Ccm2. These results were confirmed independently by collaborators working with CCM2-depleted HUVECs and i*CCM2* knock-out mice (Renz et al., 2015), which demonstrates that this mechanism is conserved in higher vertebrates. This finding is intriguing since zebrafish *ccm* mutants fail to generate a functional circulatory system due to vascular lumen defects. Klf2 expression in *ccm* mutants should be blocked as in *silent heart* (*tnnt2a*) mutants. Furthermore, I could show that the up-regulation of *klf2a* and *klf2b* is necessary for causing CCM-dependent cardiovascular defects in zebrafish.

Whereas loss of VEGF signaling activity has no effect on endocardial cell number in WT embryos (Dietrich et al., 2014), elevated Vegf-dependent angiogenesis signaling in endocardial cells resulted in the endocardial overproliferation phenotype in *ccm*

mutants. Since Heg, Krit1, and Ccm2 may act together in a complex, a lack of either one of these proteins may cause a break-down of the entire Ccm complex. This hypothesis is supported by the fact, that these mutants have similar cardiovascular phenotypes. Endocardial and endothelial overproliferation in zebrafish *heg*^{m552}, *krit1*^{ty219c}, and *ccm2*^{m201} mutants were either rescued by Klf2 knock-down or by inhibition of VEGF signaling, arguing for a pro-angiogenic activity of Klf2. Furthermore, unchanged expression levels of *klf2* upon pharmacological inhibition of VEGF signaling showed that Klf2 acts upstream of the VEGF signaling pathway. In addition, blocking VEGF signaling prior to heart tube formation and the onset of blood flow was sufficient to rescue the myocardial and endocardial defects in *ccm* mutants which shows that Klf2 regulates Vegf signaling in endocardial progenitor cells. In sum, the CCM protein complex regulates VEGF-dependent angiogenesis via the shear-stress responsive transcription factor Klf2 in a manner that is independent of flow in endocardial and endothelial cells.

CCMs are characterized by thin-walled, dilated blood vessels that resemble the primordial midbrain channel (PMBC), primitiv internal carotid artery (PICA), and the lateral dorsal aorta (LDA) phenotype of zebrafish *ccm* mutants. Additionally, endothelial cells of cavernoma lack associated vascular smooth muscle cells (VSMCs) in patients (Shenkar et al., 2008b; Shenkar et al., 2008a) and in mice (Cunningham et al., 2011). This finding is reminiscent of the observation that KLF2-overexpressing or shear-stress stimulated HUVECs secrete extracellular vesicles containing miR143/145 to control gene expression in neighbouring smooth muscle cells (Hergenreider et al., 2012). Therefore, overexpression of KLF2 in endothelial cells may explain the lack of vascular smooth muscle cells in patients. For cardiac development, it will be important to investigate whether this mechanism is also involved in endocardial-myocardial interaction.

Furthermore, it has been shown that cavernoma in human patients exhibit areas with proliferative activity of endothelial cells (Notelet et al., 1997). However, the correlation between elevated KLF2 expression levels and CCM formation in human patients remains to be elucidated. A possible explanation for the venous-specific defects in mice and in patients may come from the role of KLF2 in the endothelium. Klf2 is highly expressed in regions of high shear-stress, e.g. the carotid artery, where it has a

vasoprotective function. Therefore, elevated KLF2 activity would not enhance vasoprotection in these vessels. In contrast, in low-flow blood vessels, like venous capillaries, Klf2 is not expressed. An up-reguation of Klf2 due to a loss of CCM proteins may induce signaling cascades including VEGF signaling that lead to cerebral cavernous malformation defects.

In addition to VEGF signaling, a recent study demonstrated that postnatal endothelial-specific deletion of the CCM1 gene in mice induced a TGFβ-dependent endothelial-to-mesenchymal transition (EndMT), which contributes to the development of vascular malformations (Maddaluno et al., 2013). Intriguingly, Klf2 and TGFβ signaling act together during embryonic cardiac, and adult vascular development (Boon et al., 2007; Egorova et al., 2011). In this context, it will be important to investigate the role of Klf2 in TGFβ-mediated vascular malformations.

5.2 The instructive role of β1 integrin signaling in Klf2-dependent cardiovascular defects

Integrins are transmembrane cell adhesion receptors that allow the communication between the extracellular matrix (ECM) and intracellular signaling pathways (Hynes et al., 2002) involved in actin cytoskeleton organization (Shibue et al., 2013), cell adhesion (Papusheva et al., 2010), ECM deposition (Schwarzbauer et al., 2011), and cell polarity (Cox et al., 2001; Etienne-Manneville et al., 2001). Previous studies indicated that β1 integrin signaling is involved in CCM-related vascular defects by interacting with the negative regulator ICAP-1 through KRIT1 (Hilder et al., 2007; Zawistowski et al., 2005; Zhang et al., 2008). KRIT1 binds to and stabilizes ICAP-1 to prevent talin-mediated activation of the β1 integrin signaling pathway. Furthermore, *in vitro* and *in vivo* studies showed that a loss of either ICAP-1, KRIT1, or CCM2 destabilizes the entire ICAP-1-CCM complex and results in increased β1 integrin activation and actin stress fiber formation, while simulatenous depletion of β1 integrin in HUVECS abolishes actin stress fiber formation (Faurobert et al., 2013).

The flow-inpendent up-regulation of *KLF2* in *ICAP-1*-, *KRIT1*-, or *CCM2*-depleted HUVECS is mediated by elevated β1 integrin signaling (Renz et al., 2015).

Additionally, the cardiovascular defects in zebrafish *ccm2* mutants were rescued by knock-down of β1 integrin implying a conserved mechanism in the regulation of Klf2 by β1 integrin signaling. Complementary to these effects, the knock-down of *icap-1* in zebrafish recapitulate the early vascular *ccm2* phenotype. However, the dilation of the heart chambers could not be observed in these *icap-1* morphant embryos.

β1 integrin signaling induces RhoA-dependent stress fiber formation by a crosstalk with Scr-family kinases and Rho-family GTPases (Huveneers et al., 2009). The CCM proteins have been shown to regulate RhoA activation and ROCK activity (Borikova et al., 2010; Chan et al., 2010; Stockton et al., 2010; Whitehead et al., 2009). In brain endothelial cells, CCM2 binding to the Smad ubiquitin regulatory factor-1 (Smurf1) increases Smurf1-mediated degradation of RhoA (Crose et al., 2009). Remarkably, Smurf1 is also required for the ubiquitination and degradation of KLF2 in human lung cancer H1299 cells (Xie et al., 2011), suggesting a potential role of the CCM complex, at least of CCM2, in regulating KLF2 protein levels by Smurf1-mediated degradation. Intriguingly, shear-stress induced overexpression of KLF2 in HUVECs also results in actin stress fiber formation (Boon et al., 2010). These actin stress fibers are assembled in the direction of flow and result in an elongation of endothelial cells along the flow in a Rho kinase-independent mechanism (Boon et al., 2010). Thus, the CCM complex may play a previously unappreciated role in the onset of CCM-dependent cardiovascular defects by the regulation β1 integrin-dependent induction of KLF2 via ICAP-1. Furthermore, CCM2 may regulate KLF2 protein levels by Smurf1-mediated degradation. However, whether CCM2 interacts with Smurf1 in this context remains to be elucidated.

So far, the molecular mechanism by which β1 integrin regulates Klf2 expression are unknown and need further investigation. Moreover, it is not known whether other integrins besides β1 integrin are also involved in KLF2 regulation at different developmental stages or in specific blood vessels.

5.3 Klf2 mediates pro-angiogenic activity via Egfl7

During vascular development, the VEGF signaling pathway can be regulated by pro-angiogenic miR-126 activity or by inhibition of the Notch signaling pathway. The role of the transcription factors Klf2a and Klf2b in this context is largely unknown.

Knock-out experiments in mice showed that a loss of EGFL7 caused severe vascular defects (Schmidt et al., 2007). These phenotypes were similar to the loss of miR-126. Endothelial-specific deletion of EGFL7, without affecting miR-126 expression, showed that knock-out mice were phenotypically normal, whereas the knock-out of miR-126 recapitulated the previously described *Egfl7* vascular defects (Kuhnert et al., 2008). Thus, the vascular defects were attributed to the loss of miRNA-126 rather than to loss of *EGFL7*. In zebrafish, Klf2 regulates VEGF-dependent angiogenesis during aortic arches development by miRNA-126a (Nicoli et al., 2010). However, qRT-PCR analyses done by David Hassel´s lab showed that neither *miR-126a* nor *miR-126b* were up-regulated in zebrafish *ccm2*^{m201} mutants compared to wild-type embryos (Renz et al., 2015).

Together, here I showed that Klf2 positively regulates the expression of the endothelial-specific gene *egfl7*, the host gene of miR-126, and that overexpression of this factor causes the VEGF-dependent cardiovascular defects in zebrafish *ccm* mutants independently of *miR-126*.

Several lines of evidence suggest an antagonistic role of Egfl7 in VEGF-dependent angiogenesis via the negative regulation of the Notch signaling pathway (Nichol et al., 2010). Endothelial overexpression of EGFL7 in mice caused partial lethality, hemorrhaging, cardiac morphogenesis defects, and a reduced number of major cranial blood vessels, findings which are similar to the cardiovascular phenotypes in zebrafish *ccm* mutants. Since the vascular defects in patients and in mice occur in mature venous blood vessels, venous-specific expression of Egfl7 and arterial-specific expression of components of the Notch signaling pathway argue against a Egfl7-Notch-mediated regulation of the VEGF signaling pathway in veins (Bambino et al., 2014; Poissonnier et al., 2014; Villa et al., 2001). Furthermore, the inhibition of Notch signaling in zebrafish by morpholino injection against RbpSuH (a transcriptional co-activator) did not recapitulate the Ccm cardiovascular defects (Siekmann et al., 2007). In follow-up

experiments, analyses of zebrafish *heg*^{m552}, *krit1*^{ty219c}, and *ccm2*^{m201} mutant using different transgenic reporter lines for components of the Notch signaling pathway will be necessary to exclude or to validate whether angiogenesis defects upon loss of Ccm are Notch-dependent processes.

Besides the regulation of the VEGF signaling pathway by *miR-126* or by inhibition of the Notch signaling pathway, Egfl7 may also affect angiogenesis by activating the β3 integrin signaling pathway (Nikolic et al., 2013; Takeuchi et al., 2014). In HUVECs, EGFL7 binds specifically to $\alpha_v\beta3$ integrin via its RGD motif and positively affects blood vessel formation (Nikolic et al., 2013). Furthermore, Takeuchi et al. demonstrated that VEGF-induced up-regulation of phospho-Akt and phospho-Erk(1/2) was suppressed by knock-down of EGFL7. Hence, Egfl7 may regulate VEGF-dependent angiogenesis by activating β3 integrin signaling (Takeuchi et al., 2014).

Transferred to a pathological condition, a loss of Ccm complex proteins could induce abberant β1 integrin activity, leading to increased Klf2 expression, and subsequently elevated Egfl7 expression. Egfl7 overexpression in turn may activate β3 integrin signaling resulting in enhanced VEGF-dependent angiogenesis signaling.

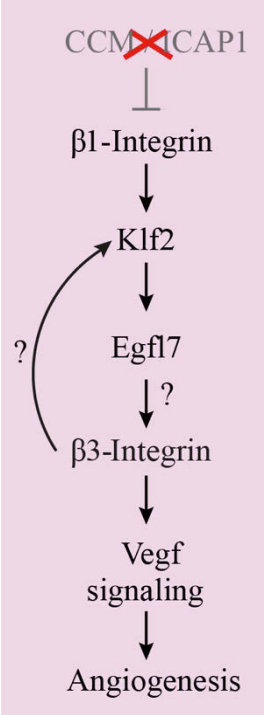

Fig. 26. Proposed model for Egfl7-dependent regulation of Klf2 via β3 integrin. The loss of the CCM/ICAP-1 complex induces β1 integrin-dependent up-regulation of Egfl7 via Klf2. In turn, Egfl7 may bind to β3 integrin and trigger Klf2 expression via a positive feedback-loop. Hence, knock-down of Egfl7 may decrease β3 integrin-dependent expression of Klf2.

The finding that *egfl7* knock-down in zebrafish significantly decreased *klf2a*/*b* expression levels (Results Fig.24E) implies that Klf2 may also be regulated, in part, by a Egfl7/β3 integrin-dependent mechanism. Double knock-down of *klf2a*/*b* and *egfl7* by low-dose morpholino injection into *ccm* mutants support the idea that these factors act together in VEGF-dependent angiogenesis. Knock-down of β3 integrin in zebrafish may be the first step in assessing its potential role in the regulation of Klf2 (Fig. 26).

5.4 Ectopic cerebral sprouts and vascular lumen formation in zebrafish *ccm* mutants

Investigations of primary defects in *ccm*-deficient cerebral blood vessels are complicated since *ccm* mutants lack a functional circulatory system. Blood flow is nescessary to supply organs with nutrients and oxygen for proper function. Hypoxia, an undersupply with oxygen, induces neoangiogenesis from quiescent blood vessels by activating the HIF-1 signaling pathway (Forsythe et al., 1996; Goldberg et al., 1994; Liu et al., 1995; Shweiki et al., 1992). In zebrafish *silent heart* (*tnnt2a*) mutants, which lack blood flow, I noticed ectopic sprout formation of cerebral blood vessels similar to the vascular phenotype in heg^{m552}, $krit1^{ty219c}$, and $ccm2^{m201}$ mutants. Thus, this ectopic sprouting phenotype may be a secondary effect due to a lack of blood flow and hypoxia-induced angiogenesis signaling. Strikingly, sprout formation was suppressed by knocking-down either *klf2a*/*b*, *itgb1b*, or *egfl7* in *ccm* mutants. For instance, in $ccm2^{m201}$ mutant; *egfl7* morphants, vascular sprout formation was suppressed (n=3/3 embryos) even in the absence of blood flow, indicating that hypoxia-induced angiogenesis may also be affected by the β1 integrin-Klf2-Egfl7 signaling cascade. It will be interesting to test whether the oversprouting phenotype in *tnnt2a* mutants can also be rescued by knock-down of either of these factors.

As blood vessels in zebrafish *tnnt2a* mutants fail to form a vascular lumen, the partial rescue of the lumenization defects in *ccm* mutants injected with *klf2a/b* or *egfl7* morpholino may be attributed to a recovery of the heart, and therefore circulation of fluid within blood vessels rather than a rescue of the endothelial cells themself. In addition, $ccm2^{m201}$ mutants injected with a combination of *klf2a*/*b* and *egfl7* morpholino

exhibited cardiac rescue and circulating blood cells within the entire vascular network resulting in vascular lumen formation of intersegmental vessels. Hence, vascular lumenization defects in zebrafish *ccm* mutants may be a consequence of a failure in blood circulation rather than a loss of Ccm proteins in endothelial cells.

5.5 Outlook

Further research is necessary to understand the biology of cerebral cavernous malformations. Pharmacological compound screens of known drugs may be a first step to identify new targets involved in Ccm-dependent diseases. The zebrafish, as an ideal model organism, allows to test many drugs in a short period of time. Subsequently, potential canditates can be tested in more disease relevant organisms, such as mice or rat.

In addition, clonal studies of *ccm*-deficient endothelial cells in wild-type background are necessary to get a better understanding of how these cells behave under normal physiological conditions and whether they recapitulate the vascular defects observed in mice and human with respect to bleeding or cavernoma development.

Genetic and molecular evidence from inheritable forms of aneurysms points to an involvement of aberrant TGF-β signaling in vascular pathologies (Pardali et al., 2010; Lindsay and Dietz, 2011). Since murine *KLF2* knockout animals frequently present with aortic aneuryms (Kuo et al., 1997) and aberrant TGF-β signaling is involved in cerebral cavernous malformations (Maddaluno et al., 2013), future research should reveal whether the signaling pathway elucidated in this study, is relevant for other pathologies of the human vasculature as well.

6 Appendix

6.1 Statistical analysis of endocardial and lateral dorsal aorta cell numbers

	Unpaired t-tests	P value
Fig. 9, endocardium	wt vs *ccm2*	*** P=0,0009
	wt vs *ccm2*;*klf2ab*MO	** P=0,0047
	ccm2 vs *ccm2*;*klf2ab*MO	*** P=0,0004

	1-way ANOVA test	P value
Fig. 15F, endocardium	wt vs *ccm2*	** P=0,002
	wt vs wt + PTK787	n.s. P>0,999
	wt vs *ccm2* + PTK787	n.s. P=0,971
	ccm2 vs *ccm2* + PTK787	* P=0,0174
	wt vs *heg* + PTK787	n.s. P=0,3781
	wt vs *heg*	*** P=0,0009
	heg vs *heg* + PTK787	* P=0,0229

	Unpaired t-tests	P value
Fig.12D, LDA	wt vs *ccm2*	*** P=0,0003
	wt vs *ccm2*;*klf2ab*MO	n.s. P=0,74
	wt vs *hsp70l:klf2a*	** P=0,004
	ccm2 vs *hsp70l:klf2a*	n.s. P=0,252
	ccm2 vs *ccm2*;*klf2ab*MO	** P=0,004

	Unpaired t-tests	P value
Fig.17, LDA	wt vs *ccm2*	*** P=0,0003
	wt vs *ccm2* + PTK787	n.s. P=0,109
	ccm2 vs *ccm2* + PTK787	*** P=0,0006

6.2 Statistical analysis of SIV branchpoints and sprouts

	1-way ANOVA test	P value
Fig. 13D (branchpoints)	wt vs *ccm2* wt vs *ccm2*;*klf2ab*MO *ccm2* vs *ccm2*;*klf2ab*MO	* P=0,0198 n.s. P=0,5214 ** P=0,0036

	1-way ANOVA test	P value
Fig. 13D (sprouts)	wt vs *ccm2* wt vs *ccm2*;*klf2ab*MO *ccm2* vs *ccm2*;*klf2ab*MO	**** P<0.0001 * P=0,0108 **** P<0,0001

6.3 RT-qPCR data analysis

		n=	*klf2a*		*klf2b*	
			Mean	SEM	Mean	SEM
Fig. 6	wt	4	1,002	0,033	1,004	0,052
	ccm2	5	1,779	0,073	1,740	0,046

	Unpaired t-tests	P value	
		klf2a	*klf2b*
Fig. 6	wt vs *ccm2*	**** P<0,0001	**** P<0,0001

		n=	*klf2a*		*klf2b*	
			Mean	SEM	Mean	SEM
Fig. 10H	wt	4	1,002	0,033	1,004	0,052
	*tnnt2a*MO	5	0,740	0,046	0,831	0,040
	ccm2	5	1,779	0,073	1,740	0,046
	ccm2 + *tnnt2a*MO	4	1,804	0,051	1,343	0,023

	1-way ANOVA test	P value	
		klf2a	***klf2b***
Fig. 10H	wt vs *tnnt2a*MO	* P=0,0257	n.s. P=0,0628
	wt vs *ccm2*	**** P<0,0001	**** P<0,0001
	wt vs *ccm2*;*tnnt2a*MO	**** P<0,0001	*** P=0,0006
	*tnnt2a*MO vs *ccm2*;*tnnt2a*MO	**** P<0,0001	**** P<0,0001
	ccm2 vs *ccm2*;*tnnt2a*MO	n.s. P=0,990	**** P<0,0001

		n=	***klf2a***		***klf2b***	
			Mean	**SEM**	**Mean**	**SEM**
Fig. 19	wt	3	1,001	0,029	1,002	0,043
	ccm2	3	1,796	0,248	1,725	0,173
	wt + PTK787	3	0,925	0,030	1,054	0,062
	ccm2 + PTK787	3	1,713	0,163	1,666	0,039

	1-way ANOVA test	P value	
		klf2a	***klf2b***
Fig. 19	wt vs *ccm2*	* P=0,0225	** P=0,0029
	wt vs wt + PTK787	n.s. P=0,9946	n.s. P=0,9933
	wt vs *ccm2* + PTK787	* P=0,0395	** P=0,0050
	ccm2 vs *ccm2* + PTK787	n.s. P=0,9925	n.s. P=0,9893

		n=	***egfl7***	
			Mean	**SEM**
Fig. 23A	Heat-shock control	3	1,001	0,034
	hsp70l:klf2a_IRES_GFP	3	1,477	0,058
	hsp70l:kfl2b_IRES_GFP	3	1,9	0,14

	1-way ANOVA test	P value
		egfl7
Fig. 23A	ctrl vs *hsp70l:klf2a_IRES_GFP*	* P=0,0170
	ctrl vs *hsp70l:klf2b_IRES_GFP*	*** P=0,0007

		n=	*egfl7*	
			Mean	**SEM**
Fig. 22A	wt	3	1	0,017
	ccm2	3	1,335	0,070
	ccm2 + *klf2ab*MO	3	1,188	0,221

	Unpaired t-tests	**P value**
		egfl7
Fig. 22A	wt vs *ccm2*	** P=0,01
	wt vs *ccm2;klf2ab*MO	n.s. P=0,446
	ccm2 vs *ccm2;klf2ab*MO	n.s. P=0,561

		n=	*klf2a*		*klf2b*	
			Mean	**SEM**	**Mean**	**SEM**
Fig. 24E	wt	3	1,000	0,002	1,000	0,021
	*egfl7*MO	3	0,742	0,003	0,724	0,037
	ccm2	3	2,033	0,046	1,406	0,113
	ccm2 + *egfl7*MO	3	1,160	0,073	0,921	0,067

	1-way ANOVA test	**P value**	
		klf2a	***klf2b***
Fig. 24E	wt vs *ccm2*	**** P<0,0001	n.s. P=0,0691
	wt vs *egfl7*MO	* P=0,0455	* P=0,0122
	wt vs *ccm2* + *egfl7*MO	n.s. P=0,2633	n.s. P=0,4358
	ccm2 vs *ccm2* + *egfl7*MO	**** P<0,0001	* P=0,0208

References

Ablooglu, A. J., Tkachenko, E., Kang, J. *et al.* (2010). Integrin alphaV is necessary for gastrulation movements that regulate vertebrate body asymmetry. *Development*, *137*(20), 3449-3458.

Akers, A. L., Johnson, E., Steinberg, G. K. *et al.* (2009). Biallelic somatic and germline mutations in cerebral cavernous malformations (CCMs): evidence for a two-hit mechanism of CCM pathogenesis. *Hum Mol Genet*, *18*(5), 919-930.

Allen, K. L., Hamik, A., Jain, M. K. *et al.* (2011). Endothelial cell activation by antiphospholipid antibodies is modulated by Kruppel-like transcription factors. *Blood*, *117*(23), 6383-6391.

Armstrong, E. J., & Bischoff, J. (2004). Heart valve development: endothelial cell signaling and differentiation. *Circ Res*, *95*(5), 459-470.

Asahara, T., Murohara, T., Sullivan, A. *et al.* (1997). Isolation of putative progenitor endothelial cells for angiogenesis. *Science*, *275*(5302), 964-967.

Atkins, G. B., & Jain, M. K. (2007). Role of Kruppel-like transcription factors in endothelial biology. *Circ Res*, *100*(12), 1686-1695.

Auman, H. J., Coleman, H., Riley, H. E. *et al.* (2007). Functional modulation of cardiac form through regionally confined cell shape changes. *PLoS Biol*, *5*(3), e53.

Baker, K., Holtzman, N. G., & Burdine, R. D. (2008). Direct and indirect roles for Nodal signaling in two axis conversions during asymmetric morphogenesis of the zebrafish heart. *Proc Natl Acad Sci U S A*, *105*(37), 13924-13929.

Bakkers, J. (2011). Zebrafish as a model to study cardiac development and human cardiac disease. *Cardiovasc Res*, *91*(2), 279-288.

Bambino, K., Lacko, L. A., Hajjar, K. A. *et al.* (2014). Epidermal growth factor-like domain 7 is a marker of the endothelial lineage and active angiogenesis. *Genesis*, *52*(7), 657-670.

Bartman, T., Walsh, E. C., Wen, K. K. *et al.* (2004). Early myocardial function affects endocardial cushion development in zebrafish. *PLoS Biol*, *2*(5), E129.

Bayless, K. J., & Davis, G. E. (2002). The Cdc42 and Rac1 GTPases are required for capillary lumen formation in three-dimensional extracellular matrices. *J Cell Sci*, *115*(Pt 6), 1123-1136.

Bayless, K. J., Salazar, R., & Davis, G. E. (2000). RGD-dependent vacuolation and lumen formation observed during endothelial cell morphogenesis in three-dimensional fibrin matrices involves the alpha(v)beta(3) and alpha(5)beta(1) integrins. *Am J Pathol*, *156*(5), 1673-1683.

Beis, D., Bartman, T., Jin, S. W. *et al.* (2005). Genetic and cellular analyses of zebrafish atrioventricular cushion and valve development. *Development*, *132*(18), 4193-4204.

Benedito, R., Roca, C., Sorensen, I. *et al.* (2009). The notch ligands Dll4 and Jagged1 have opposing effects on angiogenesis. *Cell*, *137*(6), 1124-1135.

Benjamini, Y. & Hochberg, Y. (1995). Controlling the false discovery rate: a practical and powerful approach to multiple testing. *J.R. Statist. Soc. B, 57(1), 289-300.*

Beraud-Dufour, S., Gautier, R., Albiges-Rizo, C. *et al.* (2007). Krit 1 interactions with microtubules and membranes are regulated by Rap1 and integrin cytoplasmic domain associated protein-1. *FEBS J*, *274*(21), 5518-5532.

Bergametti, F., Denier, C., Labauge, P. *et al.* (2005). Mutations within the programmed cell death 10 gene cause cerebral cavernous malformations. *Am J Hum Genet*, *76*(1), 42-51.

Bhattacharya, R., Senbanerjee, S., Lin, Z. *et al.* (2005). Inhibition of vascular permeability factor/vascular endothelial growth factor-mediated angiogenesis by the Kruppel-like factor KLF2. *J Biol Chem*, *280*(32), 28848-28851.

Bloch, W., Forsberg, E., Lentini, S. *et al.* (1997). Beta 1 integrin is essential for teratoma growth and angiogenesis. *J Cell Biol*, *139*(1), 265-278.

Blum, Y., Belting, H. G., Ellertsdottir, E. *et al.* (2008). Complex cell rearrangements during intersegmental vessel sprouting and vessel fusion in the zebrafish embryo. *Dev Biol*, *316*(2), 312-322.

Bonauer, A., Carmona, G., Iwasaki, M. *et al.* (2009). MicroRNA-92a controls angiogenesis and functional recovery of ischemic tissues in mice. *Science*, *324*(5935), 1710-1713.

Boon, R. A., Fledderus, J. O., Volger, O. L. *et al.* (2007). KLF2 suppresses TGF-beta signaling in endothelium through induction of Smad7 and inhibition of AP-1. *Arterioscler Thromb Vasc Biol*, *27*(3), 532-539.

Boon, R. A., Leyen, T. A., Fontijn, R. D. *et al.* (2010). KLF2-induced actin shear fibers control both alignment to flow and JNK signaling in vascular endothelium. *Blood*, *115*(12), 2533-2542.

Borikova, A. L., Dibble, C. F., Sciaky, N. *et al.* (2010). Rho kinase inhibition rescues the endothelial cell cerebral cavernous malformation phenotype. *J Biol Chem*, *285*(16), 11760-11764.

Boudreau, N. J., & Varner, J. A. (2004). The homeobox transcription factor Hox D3 promotes integrin alpha5beta1 expression and function during angiogenesis. *J Biol Chem*, *279*(6), 4862-4868.

Boulday, G., Blecon, A., Petit, N. *et al.* (2009). Tissue-specific conditional CCM2 knockout mice establish the essential role of endothelial CCM2 in angiogenesis: implications for human cerebral cavernous malformations. *Dis Model Mech*, *2*(3-4), 168-177.

Boulday, G., Rudini, N., Maddaluno, L. *et al.* (2011). Developmental timing of CCM2 loss influences cerebral cavernous malformations in mice. *J Exp Med*, *208*(9), 1835-1847.

Bussmann, J., Bakkers, J., & Schulte-Merker, S. (2007). Early endocardial morphogenesis requires Scl/Tal1. *PLoS Genet*, *3*(8), e140.

Calderwood, D. A. (2004). Integrin activation. *J Cell Sci*, *117*(Pt 5), 657-666.

Calderwood, D. A., Shattil, S. J., & Ginsberg, M. H. (2000). Integrins and actin filaments: reciprocal regulation of cell adhesion and signaling. *J Biol Chem*, *275*(30), 22607-22610.

Campagnolo, L., Leahy, A., Chitnis, S. *et al.* (2005). EGFL7 is a chemoattractant for endothelial cells and is up-regulated in angiogenesis and arterial injury. *Am J Pathol*, *167*(1), 275-284.

Chan, A. C., Li, D. Y., Berg, M. J. *et al.* (2010). Recent insights into cerebral cavernous malformations: animal models of CCM and the human phenotype. *FEBS J*, *277*(5), 1076-1083.

Chan, J., Bayliss, P. E., Wood, J. M. *et al.* (2002). Dissection of angiogenic signaling in zebrafish using a chemical genetic approach. *Cancer Cell*, *1*(3), 257-267.

Chang, C. P., Neilson, J. R., Bayle, J. H. *et al.* (2004). A field of myocardial-

endocardial NFAT signaling underlies heart valve morphogenesis. *Cell*, *118*(5), 649-663.

Chauhan, S. D., Nilsson, H., Ahluwalia, A. *et al.* (2003). Release of C-type natriuretic peptide accounts for the biological activity of endothelium-derived hyperpolarizing factor. *Proc Natl Acad Sci U S A*, *100*(3), 1426-1431.

Chen, J. N., Haffter, P., Odenthal, J. *et al.* (1996). Mutations affecting the cardiovascular system and other internal organs in zebrafish. *Development*, *123*, 293-302.

Chiplunkar, A. R., Lung, T. K., Alhashem, Y. *et al.* (2013). Kruppel-like factor 2 is required for normal mouse cardiac development. *PLoS One*, *8*(2), e54891.

Clark, R. A., DellaPelle, P., Manseau, E. *et al.* (1982). Blood vessel fibronectin increases in conjunction with endothelial cell proliferation and capillary ingrowth during wound healing. *J Invest Dermatol*, *79*(5), 269-276.

Clatterbuck, R. E., Elmaci, I., & Rigamonti, D. (2001). The juxtaposition of a capillary telangiectasia, cavernous malformation, and developmental venous anomaly in the brainstem of a single patient: case report. *Neurosurgery*, *49*(5), 1246-1250.

Cleaver, O., & Krieg, P. A. (1998). VEGF mediates angioblast migration during development of the dorsal aorta in Xenopus. *Development*, *125*(19), 3905-3914.

Cooper, A. D., Campeau, N. G., & Meissner, I. (2008). Susceptibility-weighted imaging in familial cerebral cavernous malformations. *Neurology*, *71*(5), 382.

Costa, B., Kean, M. J., Ast, V. *et al.* (2012). STK25 protein mediates TrkA and CCM2 protein-dependent death in pediatric tumor cells of neural origin. *J Biol Chem*, *287*(35), 29285-29289.

Covassin, L. D., Villefranc, J. A., Kacergis, M. C. *et al.* (2006). Distinct genetic interactions between multiple Vegf receptors are required for development of different blood vessel types in zebrafish. *Proc Natl Acad Sci U S A*, *103*(17), 6554-6559.

Cox, E. A., Sastry, S. K., & Huttenlocher, A. (2001). Integrin-mediated adhesion regulates cell polarity and membrane protrusion through the Rho family of GTPases. *Mol Biol Cell*, *12*(2), 265-277.

Critchley, D. R., & Gingras, A. R. (2008). Talin at a glance. *J Cell Sci*, *121*(Pt 9), 1345-1347.

Crose, L. E., Hilder, T. L., Sciaky, N. *et al.* (2009). Cerebral cavernous malformation 2 protein promotes smad ubiquitin regulatory factor 1-mediated RhoA degradation in endothelial cells. *J Biol Chem*, *284*(20), 13301-13305.

Cunningham, K., Uchida, Y., O'Donnell, E. *et al.* (2011). Conditional deletion of Ccm2 causes hemorrhage in the adult brain: a mouse model of human cerebral cavernous malformations. *Hum Mol Genet*, *20*(16), 3198-3206.

Davies, P. F., Barbee, K. A., Volin, M. V. *et al.* (1997). Spatial relationships in early signaling events of flow-mediated endothelial mechanotransduction. *Annu Rev Physiol*, *59*, 527-549.

Davis, G. E., & Camarillo, C. W. (1996). An alpha 2 beta 1 integrin-dependent pinocytic mechanism involving intracellular vacuole formation and coalescence regulates capillary lumen and tube formation in three-dimensional collagen matrix. *Exp Cell Res*, *224*(1), 39-51.

De Maziere, A., Parker, L., Van Dijk, S. *et al.* (2008). Egfl7 knockdown causes defects in the extension and junctional arrangements of endothelial cells during zebrafish vasculogenesis. *Dev Dyn*, *237*(3), 580-591.

de Pater, E., Clijsters, L., Marques, S. R. *et al.* (2009). Distinct phases of cardiomyocyte differentiation regulate growth of the zebrafish heart. *Development*, *136*(10), 1633-1641.

De Smet, F., Segura, I., De Bock, K. *et al.* (2009). Mechanisms of vessel branching: filopodia on endothelial tip cells lead the way. *Arterioscler Thromb Vasc Biol*, *29*(5), 639-649.

De Val, S., Chi, N. C., Meadows, S. M. *et al.* (2008). Combinatorial regulation of endothelial gene expression by ets and forkhead transcription factors. *Cell*, *135*(6), 1053-1064.

Deakin, N. O., & Turner, C. E. (2008). Paxillin comes of age. *J Cell Sci*, *121*(Pt 15), 2435-2444.

Dekker, R. J., Boon, R. A., Rondaij, M. G. *et al.* (2006). KLF2 provokes a gene expression pattern that establishes functional quiescent differentiation of the endothelium. *Blood*, *107*(11), 4354-4363.

Dekker, R. J., van Soest, S., Fontijn, R. D. *et al.* (2002). Prolonged fluid shear stress induces a distinct set of endothelial cell genes, most specifically lung Kruppel-like factor (KLF2). *Blood*, *100*(5), 1689-1698.

Dekker, R. J., van Thienen, J. V., Rohlena, J. *et al.* (2005). Endothelial KLF2 links local arterial shear stress levels to the expression of vascular tone-regulating genes. *Am J Pathol*, *167*(2), 609-618.

Denier, C., Goutagny, S., Labauge, P. *et al.* (2004). Mutations within the MGC4607 gene cause cerebral cavernous malformations. *Am J Hum Genet*, *74*(2), 326-337.

Detrich, H. W., Kieran, M. W., Chan, F. Y. *et al.* (1995). Intraembryonic hematopoietic cell migration during vertebrate development. *Proc Natl Acad Sci U S A*, *92*(23), 10713-10717.

Diaz, R., Silva, J., Garcia, J. M. *et al.* (2008). Deregulated expression of miR-106a predicts survival in human colon cancer patients. *Genes Chromosomes Cancer*, *47*(9), 794-802.

Dietrich, AC., Lombardo, VA. *et al.* (2014). Blood flow and Bmp signaling control endocardial chamber morphogenesis. *Dev.Cell*, *30*(4), 367-377.

Dobyns, W. B., Michels, V. V., Groover, R. V. *et al.* (1987). Familial cavernous malformations of the central nervous system and retina. *Ann Neurol*, *21*(6), 578-583.

Drexler, H., & Hornig, B. (1999). Endothelial dysfunction in human disease. *J Mol Cell Cardiol*, *31*(1), 51-60.

Eerola, I., Plate, K. H., Spiegel, R. *et al.* (2000). KRIT1 is mutated in hyperkeratotic cutaneous capillary-venous malformation associated with cerebral capillary malformation. *Hum Mol Genet*, *9*(9), 1351-1355.

Egorova, A. D., DeRuiter, M. C., de Boer, H. C. *et al.* (2012). Endothelial colony-forming cells show a mature transcriptional response to shear stress. *In Vitro Cell Dev Biol Anim*, *48*(1), 21-29.

Egorova, A. D., Van der Heiden, K., Van de Pas, S. *et al.* (2011). Tgfbeta/Alk5 signaling is required for shear stress induced klf2 expression in embryonic endothelial cells. *Dev Dyn*, *240*(7), 1670-1680.

Etienne-Manneville, S., & Hall, A. (2001). Integrin-mediated activation of Cdc42 controls cell polarity in migrating astrocytes through PKCzeta. *Cell*, *106*(4), 489-498.

Evans, E. A., & Calderwood, D. A. (2007). Forces and bond dynamics in cell adhesion.

Science, *316*(5828), 1148-1153.

Faurobert, E., Rome, C., Lisowska, J. *et al.* (2013). CCM1-ICAP-1 complex controls beta1 integrin-dependent endothelial contractility and fibronectin remodeling. *J Cell Biol*, *202*(3), 545-561.

Faurobert, E. and Albiges-Rizo, C. (2010). Recent insights into cerebral cavernous malformations: a complex jigsaw puzzle under construction. *FEBS J*, *277(5)*, 1084-96.

Ferrara, N., Gerber, H. P., & LeCouter, J. (2003). The biology of VEGF and its receptors. *Nat Med*, *9*(6), 669-676.

Fidalgo, M., Fraile, M., Pires, A. *et al.* (2010). CCM3/PDCD10 stabilizes GCKIII proteins to promote Golgi assembly and cell orientation. *J Cell Sci*, *123*(Pt 8), 1274-1284.

Fischer, A., Zalvide, J., Faurobert, E. *et al.* (2013). Cerebral cavernous malformations: from CCM genes to endothelial cell homeostasis. *Trends Mol Med*, *19*(5), 302-308.

Fitch, M. J., Campagnolo, L., Kuhnert, F. *et al.* (2004). Egfl7, a novel epidermal growth factor-domain gene expressed in endothelial cells. *Dev Dyn*, *230*(2), 316-324.

Fledderus, J. O., Boon, R. A., Volger, O. L. *et al.* (2008). KLF2 primes the antioxidant transcription factor Nrf2 for activation in endothelial cells. *Arterioscler Thromb Vasc Biol*, *28*(7), 1339-1346.

Fledderus, J. O., van Thienen, J. V., Boon, R. A. *et al.* (2007). Prolonged shear stress and KLF2 suppress constitutive proinflammatory transcription through inhibition of ATF2. *Blood*, *109*(10), 4249-4257.

Forsythe, J. A., Jiang, B. H., Iyer, N. V. *et al.* (1996). Activation of vascular endothelial growth factor gene transcription by hypoxia-inducible factor 1. *Mol Cell Biol*, *16*(9), 4604-4613.

Fouquet, B., Weinstein, B. M., Serluca, F. C. *et al.* (1997). Vessel patterning in the embryo of the zebrafish: guidance by notochord. *Dev Biol*, *183*(1), 37-48.

Fournier, H. N., Dupe-Manet, S., Bouvard, D. *et al.* (2005). Nuclear translocation of integrin cytoplasmic domain-associated protein 1 stimulates cellular proliferation. *Mol Biol Cell*, *16*(4), 1859-1871.

Francalanci, F., Avolio, M., De Luca, E. *et al.* (2009). Structural and functional differences between KRIT1A and KRIT1B isoforms: a framework for understanding CCM pathogenesis. *Exp Cell Res*, *315*(2), 285-303.

Funahashi, Y., Shawber, C. J., Vorontchikhina, M. *et al.* (2010). Notch regulates the angiogenic response via induction of VEGFR-1. *J Angiogenes Res*, *2*(1), 3.

Gault, J., Shenkar, R., Recksiek, P. *et al.* (2005). Biallelic somatic and germ line CCM1 truncating mutations in a cerebral cavernous malformation lesion. *Stroke*, *36*(4), 872-874.

Gerhardt, H., Golding, M., Fruttiger, M. *et al.* (2003). VEGF guides angiogenic sprouting utilizing endothelial tip cell filopodia. *J Cell Biol*, *161*(6), 1163-1177.

Giannone, G., & Sheetz, M. P. (2006). Substrate rigidity and force define form through tyrosine phosphatase and kinase pathways. *Trends Cell Biol*, *16*(4), 213-223.

Gil-Nagel, A., Wilcox, K. J., Stewart, J. M. *et al.* (1995). Familial cerebral cavernous angioma: clinical analysis of a family and phenotypic classification. *Epilepsy Res*, *21*(1), 27-36.

Gingras, A. R., Puzon-McLaughlin, W., & Ginsberg, M. H. (2013). The structure of the ternary complex of Krev interaction trapped 1 (KRIT1) bound to both the Rap1

GTPase and the heart of glass (HEG1) cytoplasmic tail. *J Biol Chem*, *288*(33), 23639-23649.

Ginsberg, M. H., Partridge, A., & Shattil, S. J. (2005). Integrin regulation. *Curr Opin Cell Biol*, *17*(5), 509-516.

Glading, A., Han, J., Stockton, R. A. *et al.* (2007). KRIT-1/CCM1 is a Rap1 effector that regulates endothelial cell cell junctions. *J Cell Biol*, *179*(2), 247-254.

Glading, A. J., & Ginsberg, M. H. (2010). Rap1 and its effector KRIT1/CCM1 regulate beta-catenin signaling. *Dis Model Mech*, *3*(1-2), 73-83.

Goldberg, M. A., & Schneider, T. J. (1994). Similarities between the oxygen-sensing mechanisms regulating the expression of vascular endothelial growth factor and erythropoietin. *J Biol Chem*, *269*(6), 4355-4359.

Gore, A. V., Lampugnani, M. G., Dye, L. *et al.* (2008). Combinatorial interaction between CCM pathway genes precipitates hemorrhagic stroke. *Dis Model Mech*, *1*(4-5), 275-281.

Gracia-Sancho, J., Russo, L., Garcia-Caldero, H. *et al.* (2011). Endothelial expression of transcription factor Kruppel-like factor 2 and its vasoprotective target genes in the normal and cirrhotic rat liver. *Gut*, *60*(4), 517-524.

Guzeloglu-Kayisli, O., Amankulor, N. M., Voorhees, J. *et al.* (2004). KRIT1/cerebral cavernous malformation 1 protein localizes to vascular endothelium, astrocytes, and pyramidal cells of the adult human cerebral cortex. *Neurosurgery*, *54*(4), 943-9; discussion 949.

Haar, J. L., & Ackerman, G. A. (1971). Ultrastructural changes in mouse yolk sac associated with the initiation of vitelline circulation. *Anat Rec*, *170*(4), 437-455.

Harel, L., Costa, B., Tcherpakov, M. *et al.* (2009). CCM2 mediates death signaling by the TrkA receptor tyrosine kinase. *Neuron*, *63*(5), 585-591.

Hay, N., & Sonenberg, N. (2004). Upstream and downstream of mTOR. *Genes Dev*, *18*(16), 1926-1945.

He, Y., Zhang, H., Yu, L. *et al.* (2010). Stabilization of VEGFR2 signaling by cerebral cavernous malformation 3 is critical for vascular development. *Sci Signal*, *3*(116), ra26.

Helbing, T., Rothweiler, R., Ketterer, E. *et al.* (2011). BMP activity controlled by BMPER regulates the proinflammatory phenotype of endothelium. *Blood*, *118*(18), 5040-5049.

Hellstrom, M., Phng, L. K., Hofmann, J. J. *et al.* (2007). Dll4 signalling through Notch1 regulates formation of tip cells during angiogenesis. *Nature*, *445*(7129), 776-780.

Henderson, A. M., Wang, S. J., Taylor, A. C. *et al.* (2001). The basic helix-loop-helix transcription factor HESR1 regulates endothelial cell tube formation. *J Biol Chem*, *276*(9), 6169-6176.

Hergenreider, E., Heydt, S., Treguer, K. *et al.* (2012). Atheroprotective communication between endothelial cells and smooth muscle cells through miRNAs. *Nat Cell Biol*, *14*(3), 249-256.

Hilder, T. L., Malone, M. H., Bencharit, S. *et al.* (2007). Proteomic identification of the cerebral cavernous malformation signaling complex. *J Proteome Res*, *6*(11), 4343-4355.

Hodivala-Dilke, K. M., McHugh, K. P., Tsakiris, D. A. *et al.* (1999). Beta3-integrin-deficient mice are a model for Glanzmann thrombasthenia showing placental defects and reduced survival. *J Clin Invest*, *103*(2), 229-238.

Hogan, B. M., Bussmann, J., Wolburg, H. *et al.* (2008). ccm1 cell autonomously

regulates endothelial cellular morphogenesis and vascular tubulogenesis in zebrafish. *Hum Mol Genet*, *17*(16), 2424-2432.

Huang, C. H., Li, X. J., Zhou, Y. Z. *et al.* (2010). Expression and clinical significance of EGFL7 in malignant glioma. *J Cancer Res Clin Oncol*, *136*(11), 1737-1743.

Huang, C. J., Tu, C. T., Hsiao, C. D. *et al.* (2003). Germ-line transmission of a myocardium-specific GFP transgene reveals critical regulatory elements in the cardiac myosin light chain 2 promoter of zebrafish. *Dev Dyn*, *228*(1), 30-40.

Huber, T. L., Kouskoff, V., Fehling, H. J. *et al.* (2004). Haemangioblast commitment is initiated in the primitive streak of the mouse embryo. *Nature*, *432*(7017), 625-630.

Huber, W., von Heydebreck, A., Sultmann, H. *et al.* (2002). Variance stabilization applied to microarray data calibration and to the quantification of differential expression. *Bioinformatics*, *18 Suppl 1*, S96-104.

Huddleson, J. P., Ahmad, N., Srinivasan, S. *et al.* (2005). Induction of KLF2 by fluid shear stress requires a novel promoter element activated by a phosphatidylinositol 3-kinase-dependent chromatin-remodeling pathway. *J Biol Chem*, *280*(24), 23371-23379.

Humphries, J. D., Byron, A., & Humphries, M. J. (2006). Integrin ligands at a glance. *J Cell Sci*, *119*(Pt 19), 3901-3903.

Hurlstone, A. F., Haramis, A. P., Wienholds, E. *et al.* (2003). The Wnt/beta-catenin pathway regulates cardiac valve formation. *Nature*, *425*(6958), 633-637.

Huveneers, S., & Danen, E. H. (2009). Adhesion signaling - crosstalk between integrins, Src and Rho. *J Cell Sci*, *122*(Pt 8), 1059-1069.

Hynes, R. O. (2002). Integrins: bidirectional, allosteric signaling machines. *Cell*, *110*(6), 673-687.

Isogai, S., Horiguchi, M., & Weinstein, B. M. (2001). The vascular anatomy of the developing zebrafish: an atlas of embryonic and early larval development. *Dev Biol*, *230*(2), 278-301.

Jin, S. W., Beis, D., Mitchell, T. *et al.* (2005). Cellular and molecular analyses of vascular tube and lumen formation in zebrafish. *Development*, *132*(23), 5199-5209.

Jung, K. H., Chu, K., Jeong, S. W. *et al.* (2003). Cerebral cavernous malformations with dynamic and progressive course: correlation study with vascular endothelial growth factor. *Arch Neurol*, *60*(11), 1613-1618.

Just, S., Berger, I. M., Meder, B. *et al.* (2011). Protein kinase D2 controls cardiac valve formation in zebrafish by regulating histone deacetylase 5 activity. *Circulation*, *124*(3), 324-334.

Kabrun, N., Buhring, H. J., Choi, K. *et al.* (1997). Flk-1 expression defines a population of early embryonic hematopoietic precursors. *Development*, *124*(10), 2039-2048.

Kamei, M., Saunders, W. B., Bayless, K. J. *et al.* (2006). Endothelial tubes assemble from intracellular vacuoles in vivo. *Nature*, *442*(7101), 453-456.

Kaunas, R., Usami, S., & Chien, S. (2006). Regulation of stretch-induced JNK activation by stress fiber orientation. *Cell Signal*, *18*(11), 1924-1931.

Kawanami, D., Mahabeleshwar, G. H., Lin, Z. *et al.* (2009). Kruppel-like factor 2 inhibits hypoxia-inducible factor 1alpha expression and function in the endothelium. *J Biol Chem*, *284*(31), 20522-20530.

Kean, M. J., Ceccarelli, D. F., Goudreault, M. *et al.* (2011). Structure-function analysis of core STRIPAK Proteins: a signaling complex implicated in Golgi polarization. *J Biol Chem*, *286*(28), 25065-25075.

Keegan, B. R., Feldman, J. L., Begemann, G. *et al.* (2005). Retinoic acid signaling restricts the cardiac progenitor pool. *Science*, *307*(5707), 247-249.

Keegan, B. R., Meyer, D., & Yelon, D. (2004). Organization of cardiac chamber progenitors in the zebrafish blastula. *Development*, *131*(13), 3081-3091.

Kim, D. W., Langille, B. L., Wong, M. K. *et al.* (1989). Patterns of endothelial microfilament distribution in the rabbit aorta in situ. *Circ Res*, *64*(1), 21-31.

Kim, I., Moon, S. O., Kim, S. H. *et al.* (2001). Vascular endothelial growth factor expression of intercellular adhesion molecule 1 (ICAM-1), vascular cell adhesion molecule 1 (VCAM-1), and E-selectin through nuclear factor-kappa B activation in endothelial cells. *J Biol Chem*, *276*(10), 7614-7620.

Kim, S., Bell, K., Mousa, S. A. *et al.* (2000). Regulation of angiogenesis in vivo by ligation of integrin alpha5beta1 with the central cell-binding domain of fibronectin. *Am J Pathol*, *156*(4), 1345-1362.

Kimmel, C. B., Ballard, W. W., Kimmel, S. R. *et al.* (1995). Stages of embryonic development of the zebrafish. *Dev Dyn*, *203*(3), 253-310.

Kimmel, C. B., Warga, R. M., & Schilling, T. F. (1990). Origin and organization of the zebrafish fate map. *Development*, *108*(4), 581-594.

Kleaveland, B., Zheng, X., Liu, J. J. *et al.* (2009). Regulation of cardiovascular development and integrity by the heart of glass-cerebral cavernous malformation protein pathway. *Nat Med*, *15*(2), 169-176.

Kloeker, S., Major, M. B., Calderwood, D. A. *et al.* (2004). The Kindler syndrome protein is regulated by transforming growth factor-beta and involved in integrin-mediated adhesion. *J Biol Chem*, *279*(8), 6824-6833.

Kobus, K., Kopycinska, J., Kozlowska-Wiechowska, A. *et al.* (2012). Angiogenesis within the duodenum of patients with cirrhosis is modulated by mechanosensitive Kruppel-like factor 2 and microRNA-126. *Liver Int*, *32*(8), 1222-1232.

Koh, W., Mahan, R. D., & Davis, G. E. (2008). Cdc42- and Rac1-mediated endothelial lumen formation requires Pak2, Pak4 and Par3, and PKC-dependent signaling. *J Cell Sci*, *121*(Pt 7), 989-1001.

Krisht, K. M., Whitehead, K. J., Niazi, T. *et al.* (2010). The pathogenetic features of cerebral cavernous malformations: a comprehensive review with therapeutic implications. *Neurosurg Focus*, *29*(3), E2.

Krueger, J., Liu, D., Scholz, K. *et al.* (2011). Flt1 acts as a negative regulator of tip cell formation and branching morphogenesis in the zebrafish embryo. *Development*, *138*(10), 2111-2120.

Kuhnert, F., Mancuso, M. R., Hampton, J. *et al.* (2008). Attribution of vascular phenotypes of the murine Egfl7 locus to the microRNA miR-126. *Development*, *135*(24), 3989-3993.

Kumar, A., Lin, Z., SenBanerjee, S. *et al.* (2005). Tumor necrosis factor alpha-mediated reduction of KLF2 is due to inhibition of MEF2 by NF-kappaB and histone deacetylases. *Mol Cell Biol*, *25*(14), 5893-5903.

Kuo, C.T., Veseltis, M.L. Barton,K.P. *et al*. (1997). The LKLF transcription factor is required for normal tunica media formation and blood vessel stabilization during murine embryogenesis. *Genes Dev. 11,* 2996-3006

Kwan, K. M., Fujimoto, E., Grabher, C. *et al.* (2007). The Tol2kit: a multisite gateway-based construction kit for Tol2 transposon transgenesis constructs. *Dev Dyn*, *236*(11), 3088-3099.

Labauge, P., Enjolras, O., Bonerandi, J. J. *et al.* (1999). An association between

autosomal dominant cerebral cavernomas and a distinctive hyperkeratotic cutaneous vascular malformation in 4 families. *Ann Neurol*, *45*(2), 250-254.

Laberge-le Couteulx, S., Jung, H. H., Labauge, P. *et al.* (1999). Truncating mutations in CCM1, encoding KRIT1, cause hereditary cavernous angiomas. *Nat Genet*, *23*(2), 189-193.

Lampugnani, M. G., Orsenigo, F., Rudini, N. *et al.* (2010). CCM1 regulates vascular-lumen organization by inducing endothelial polarity. *J Cell Sci*, *123*(Pt 7), 1073-1080.

Lawson, N. D., Mugford, J. W., Diamond, B. A. *et al.* (2003). phospholipase C gamma-1 is required downstream of vascular endothelial growth factor during arterial development. *Genes Dev*, *17*(11), 1346-1351.

Lawson, N. D., Scheer, N., Pham, V. N. *et al.* (2001). Notch signaling is required for arterial-venous differentiation during embryonic vascular development. *Development*, *128*(19), 3675-3683.

Lawson, N. D., Vogel, A. M., & Weinstein, B. M. (2002a). sonic hedgehog and vascular endothelial growth factor act upstream of the Notch pathway during arterial endothelial differentiation. *Dev Cell*, *3*(1), 127-136.

Lawson, N. D., & Weinstein, B. M. (2002b). In vivo imaging of embryonic vascular development using transgenic zebrafish. *Dev Biol*, *248*(2), 307-318.

Lawson, N. D., & Weinstein, B. M. (2002c). Arteries and veins: making a difference with zebrafish. *Nat Rev Genet*, *3*(9), 674-682.

Lee, D. Y., Lee, C. I., Lin, T. E. *et al.* (2012). Role of histone deacetylases in transcription factor regulation and cell cycle modulation in endothelial cells in response to disturbed flow. *Proc Natl Acad Sci U S A*, *109*(6), 1967-1972.

Lee, H. S., Han, J., Bai, H. J. *et al.* (2009). Brain angiogenesis in developmental and pathological processes: regulation, molecular and cellular communication at the neurovascular interface. *FEBS J*, *276*(17), 4622-4635.

Legate, K. R., Montanez, E., Kudlacek, O. *et al.* (2006). ILK, PINCH and parvin: the tIPP of integrin signalling. *Nat Rev Mol Cell Biol*, *7*(1), 20-31.

Lelievre, E., Hinek, A., Lupu, F. *et al.* (2008). VE-statin/egfl7 regulates vascular elastogenesis by interacting with lysyl oxidases. *EMBO J*, *27*(12), 1658-1670.

Leslie, J. D., Ariza-McNaughton, L., Bermange, A. L. *et al.* (2007). Endothelial signalling by the Notch ligand Delta-like 4 restricts angiogenesis. *Development*, *134*(5), 839-844.

Leung, D. W., Cachianes, G., Kuang, W. J. *et al.* (1989). Vascular endothelial growth factor is a secreted angiogenic mitogen. *Science*, *246*(4935), 1306-1309.

Li, X., Zhang, R., Draheim, K. M. *et al.* (2012). Structural basis for small G protein effector interaction of Ras-related protein 1 (Rap1) and adaptor protein Krev interaction trapped 1 (KRIT1). *J Biol Chem*, *287*(26), 22317-22327.

Li, X., Zhang, R., Zhang, H. *et al.* (2010). Crystal structure of CCM3, a cerebral cavernous malformation protein critical for vascular integrity. *J Biol Chem*, *285*(31), 24099-24107.

Liao, Y. F., Gotwals, P. J., Koteliansky, V. E. *et al.* (2002). The EIIIA segment of fibronectin is a ligand for integrins alpha 9beta 1 and alpha 4beta 1 providing a novel mechanism for regulating cell adhesion by alternative splicing. *J Biol Chem*, *277*(17), 14467-14474.

Lin, S. C., Dolle, P., Ryckebusch, L. *et al.* (2010a). Endogenous retinoic acid regulates cardiac progenitor differentiation. *Proc Natl Acad Sci U S A*, *107*(20), 9234-9239.

Lin, Z., Kumar, A., SenBanerjee, S. *et al.* (2005). Kruppel-like factor 2 (KLF2) regulates endothelial thrombotic function. *Circ Res*, *96*(5), e48-e57.

Lin, Z., Natesan, V., Shi, H. *et al.* (2010b). Kruppel-like factor 2 regulates endothelial barrier function. *Arterioscler Thromb Vasc Biol*, *30*(10), 1952-1959.

Lindsay, M.E. and Dietz, H.C. (2011). Lessons on the pathogenesis of aneurysm from heritable conditions. *Nature*, *473,* 308-316

Liquori, C. L., Berg, M. J., Siegel, A. M. *et al.* (2003). Mutations in a gene encoding a novel protein containing a phosphotyrosine-binding domain cause type 2 cerebral cavernous malformations. *Am J Hum Genet*, *73*(6), 1459-1464.

Liu, J. J., Stockton, R. A., Gingras, A. R. *et al.* (2011). A mechanism of Rap1-induced stabilization of endothelial cell--cell junctions. *Mol Biol Cell*, *22*(14), 2509-2519.

Liu, W., Draheim, K. M., Zhang, R. *et al.* (2013). Mechanism for KRIT1 release of ICAP1-mediated suppression of integrin activation. *Mol Cell*, *49*(4), 719-729.

Liu, Y., Cox, S. R., Morita, T. *et al.* (1995). Hypoxia regulates vascular endothelial growth factor gene expression in endothelial cells. Identification of a 5' enhancer. *Circ Res*, *77*(3), 638-643.

Lobov, I. B., Renard, R. A., Papadopoulos, N. *et al.* (2007). Delta-like ligand 4 (Dll4) is induced by VEGF as a negative regulator of angiogenic sprouting. *Proc Natl Acad Sci U S A*, *104*(9), 3219-3224.

Lombardo, V. A., Otten, C., Abdelilah-Seyfried, S. (2015). Large-scale zebrafish embryonic heart dissection for transcriptional analysis. *J Vis Exp*, (95).

Londesborough, A., Vaahtomeri, K., Tiainen, M. *et al.* (2008). LKB1 in endothelial cells is required for angiogenesis and TGFbeta-mediated vascular smooth muscle cell recruitment. *Development*, *135*(13), 2331-2338.

Louvi, A., Chen, L., Two, A. M. *et al.* (2011). Loss of cerebral cavernous malformation 3 (Ccm3) in neuroglia leads to CCM and vascular pathology. *Proc Natl Acad Sci U S A*, *108*(9), 3737-3742.

Lubarsky, B., & Krasnow, M. A. (2003). Tube morphogenesis: making and shaping biological tubes. *Cell*, *112*(1), 19-28.

Ma, Q., Nie, X., Yu, M. *et al.* (2012). Rapamycin regulates the expression and activity of Kruppel-like transcription factor 2 in human umbilical vein endothelial cells. *PLoS One*, *7*(8), e43315.

Ma, X., Zhao, H., Shan, J. *et al.* (2007). PDCD10 interacts with Ste20-related kinase MST4 to promote cell growth and transformation via modulation of the ERK pathway. *Mol Biol Cell*, *18*(6), 1965-1978.

Ma, Y. Q., Qin, J., Wu, C. *et al.* (2008). Kindlin-2 (Mig-2): a co-activator of beta3 integrins. *J Cell Biol*, *181*(3), 439-446.

Mably, J. D., Chuang, L. P., Serluca, F. C. *et al.* (2006). santa and valentine pattern concentric growth of cardiac myocardium in the zebrafish. *Development*, *133*(16), 3139-3146.

Mably, J. D., Mohideen, M. A., Burns, C. G. *et al.* (2003). heart of glass regulates the concentric growth of the heart in zebrafish. *Curr Biol*, *13*(24), 2138-2147.

MacGrogan, D., Luna-Zurita, L., & de la Pompa, J. L. (2011). Notch signaling in cardiac valve development and disease. *Birth Defects Res A Clin Mol Teratol*, *91*(6), 449-459.

Maddaluno, L., Rudini, N., Cuttano, R. *et al.* (2013). EndMT contributes to the onset and progression of cerebral cavernous malformations. *Nature*, *498*(7455), 492-496.

Maharaj, A. S., & D'Amore, P. A. (2007). Roles for VEGF in the adult. *Microvasc Res*, *74*(2-3), 100-113.

Malek, A. M., Greene, A. L., & Izumo, S. (1993). Regulation of endothelin 1 gene by fluid shear stress is transcriptionally mediated and independent of protein kinase C and cAMP. *Proc Natl Acad Sci U S A*, *90*(13), 5999-6003.

McCarty, J. H., Monahan-Earley, R. A., Brown, L. F. *et al.* (2002). Defective associations between blood vessels and brain parenchyma lead to cerebral hemorrhage in mice lacking alphav integrins. *Mol Cell Biol*, *22*(21), 7667-7677.

Meadows, S. M., Salanga, M. C., & Krieg, P. A. (2009). Kruppel-like factor 2 cooperates with the ETS family protein ERG to activate Flk1 expression during vascular development. *Development*, *136*(7), 1115-1125.

Millon-Fremillon, A., Bouvard, D., Grichine, A. *et al.* (2008). Cell adaptive response to extracellular matrix density is controlled by ICAP-1-dependent beta1-integrin affinity. *J Cell Biol*, *180*(2), 427-441.

Miranti, C. K., & Brugge, J. S. (2002). Sensing the environment: a historical perspective on integrin signal transduction. *Nat Cell Biol*, *4*(4), E83-E90.

Mitra, S. K., Hanson, D. A., & Schlaepfer, D. D. (2005). Focal adhesion kinase: in command and control of cell motility. *Nat Rev Mol Cell Biol*, *6*(1), 56-68.

Montanez, E., Ussar, S., Schifferer, M. *et al.* (2008). Kindlin-2 controls bidirectional signaling of integrins. *Genes Dev*, *22*(10), 1325-1330.

Moore, M. A., & Owen, J. J. (1965). Chromosome marker studies on the development of the haemopoietic system in the chick embryo. *Nature*, *208*(5014), 956 passim.

Morton, S. U., Scherz, P. J., Cordes, K. R. *et al.* (2008). microRNA-138 modulates cardiac patterning during embryonic development. *Proc Natl Acad Sci U S A*, *105*(46), 17830-17835.

Moser, M., Nieswandt, B., Ussar, S. *et al.* (2008). Kindlin-3 is essential for integrin activation and platelet aggregation. *Nat Med*, *14*(3), 325-330.

Musiyenko, A., Bitko, V., & Barik, S. (2008). Ectopic expression of miR-126*, an intronic product of the vascular endothelial EGF-like 7 gene, regulates prostein translation and invasiveness of prostate cancer LNCaP cells. *J Mol Med (Berl)*, *86*(3), 313-322.

Nichol, D., Shawber, C., Fitch, M. J. *et al.* (2010). Impaired angiogenesis and altered Notch signaling in mice overexpressing endothelial Egfl7. *Blood*, *116*(26), 6133-6143.

Nichol, D., & Stuhlmann, H. (2012). EGFL7: a unique angiogenic signaling factor in vascular development and disease. *Blood*, *119*(6), 1345-1352.

Nicoli, S., Standley, C., Walker, P. *et al.* (2010). MicroRNA-mediated integration of haemodynamics and Vegf signalling during angiogenesis. *Nature*, *464*(7292), 1196-1200.

Nikolic, I., Stankovic, N. D., Bicker, F. *et al.* (2013). EGFL7 ligates alphavbeta3 integrin to enhance vessel formation. *Blood*, *121*(15), 3041-3050.

Noseda, M., Chang, L., McLean, G. *et al.* (2004). Notch activation induces endothelial cell cycle arrest and participates in contact inhibition: role of p21Cip1 repression. *Mol Cell Biol*, *24*(20), 8813-8822.

Notelet, L., Houtteville, J. P., Khoury, S. *et al.* (1997). Proliferating cell nuclear antigen (PCNA) in cerebral cavernomas: an immunocytochemical study of 42 cases. *Surg Neurol*, *47*(4), 364-370.

Oates, A. C., Pratt, S. J., Vail, B. *et al.* (2001). The zebrafish klf gene family. *Blood*,

98(6), 1792-1801.

Otten, P., Pizzolato, G. P., Rilliet, B. *et al.* (1989). [131 cases of cavernous angioma (cavernomas) of the CNS, discovered by retrospective analysis of 24,535 autopsies]. *Neurochirurgie*, *35*(2), 82-3, 128.

Pagenstecher, A., Stahl, S., Sure, U. *et al.* (2009). A two-hit mechanism causes cerebral cavernous malformations: complete inactivation of CCM1, CCM2 or CCM3 in affected endothelial cells. *Hum Mol Genet*, *18*(5), 911-918.

Papusheva, E., & Heisenberg, C. P. (2010). Spatial organization of adhesion: force-dependent regulation and function in tissue morphogenesis. *EMBO J*, *29*(16), 2753-2768.

Pardali, E., Goumans, M.J., and ten, D.P. (2010). Signaling by members of the TGF-beta family in vascular morphogenesis and disease. *Trends Cell Biol.*, *20*, 556-567.

Parker, L. H., Schmidt, M., Jin, S. W. *et al.* (2004). The endothelial-cell-derived secreted factor Egfl7 regulates vascular tube formation. *Nature*, *428*(6984), 754-758.

Parmar, K. M., Larman, H. B., Dai, G. *et al.* (2006). Integration of flow-dependent endothelial phenotypes by Kruppel-like factor 2. *J Clin Invest*, *116*(1), 49-58.

Pham, V. N., Lawson, N. D., Mugford, J. W. *et al.* (2007). Combinatorial function of ETS transcription factors in the developing vasculature. *Dev Biol*, *303*(2), 772-783.

Poissonnier, L., Villain, G., Soncin, F. *et al.* (2014). Egfl7 is differentially expressed in arteries and veins during retinal vascular development. *PLoS One*, *9*(3), e90455.

Reiter, J. F., Alexander, J., Rodaway, A. *et al.* (1999). Gata5 is required for the development of the heart and endoderm in zebrafish. *Genes Dev*, *13*(22), 2983-2995.

Renz, M., Otten, C., Faurobert, E. *et al.* (2015). Regulation of β1 Integrin-Klf2-mediated angiogenesis by CCM proteins. *Dev. Cell,*

Riant, F., Bergametti, F., Ayrignac, X. *et al.* (2010). Recent insights into cerebral cavernous malformations: the molecular genetics of CCM. *FEBS J*, *277*(5), 1070-1075.

Rohr, S., Otten, C., & Abdelilah-Seyfried, S. (2008). Asymmetric involution of the myocardial field drives heart tube formation in zebrafish. *Circ Res*, *102*(2), e12-e19.

Rosen, J. N., Sogah, V. M., Ye, L. Y. *et al.* (2013). ccm2-like is required for cardiovascular development as a novel component of the Heg-CCM pathway. *Dev Biol*, *376*(1), 74-85.

Sahoo, T., Johnson, E. W., Thomas, J. W. *et al.* (1999). Mutations in the gene encoding KRIT1, a Krev-1/rap1a binding protein, cause cerebral cavernous malformations (CCM1). *Hum Mol Genet*, *8*(12), 2325-2333.

Sainson, R. C., Aoto, J., Nakatsu, M. N. *et al.* (2005). Cell-autonomous notch signaling regulates endothelial cell branching and proliferation during vascular tubulogenesis. *FASEB J*, *19*(8), 1027-1029.

Scherz, P. J., Huisken, J., Sahai-Hernandez, P. *et al.* (2008). High-speed imaging of developing heart valves reveals interplay of morphogenesis and function. *Development*, *135*(6), 1179-1187.

Schmidt, M., Paes, K., De Maziere, A. *et al.* (2007). EGFL7 regulates the collective migration of endothelial cells by restricting their spatial distribution. *Development*,

134(16), 2913-2923.

Schmidt, M. H., Bicker, F., Nikolic, I. *et al.* (2009). Epidermal growth factor-like domain 7 (EGFL7) modulates Notch signalling and affects neural stem cell renewal. *Nat Cell Biol*, *11*(7), 873-880.

Schwarzbauer, J. E., & DeSimone, D. W. (2011). Fibronectins, their fibrillogenesis, and in vivo functions. *Cold Spring Harb Perspect Biol*, *3*(7).

Sehnert, A. J., Huq, A., Weinstein, B. M. *et al.* (2002). Cardiac troponin T is essential in sarcomere assembly and cardiac contractility. *Nat Genet*, *31*(1), 106-110.

Seker, A., Yildirim, O., Kurtkaya, O. *et al.* (2006). Expression of integrins in cerebral arteriovenous and cavernous malformations. *Neurosurgery*, *58*(1), 159-68; discussion 159.

SenBanerjee, S., Lin, Z., Atkins, G. B. *et al.* (2004). KLF2 Is a novel transcriptional regulator of endothelial proinflammatory activation. *J Exp Med*, *199*(10), 1305-1315.

Senger, D. R., Galli, S. J., Dvorak, A. M. *et al.* (1983). Tumor cells secrete a vascular permeability factor that promotes accumulation of ascites fluid. *Science*, *219*(4587), 983-985.

Serebriiskii, I., Estojak, J., Sonoda, G. *et al.* (1997). Association of Krev-1/rap1a with Krit1, a novel ankyrin repeat-containing protein encoded by a gene mapping to 7q21-22. *Oncogene*, *15*(9), 1043-1049.

Shattil, S. J., Kim, C., & Ginsberg, M. H. (2010). The final steps of integrin activation: the end game. *Nat Rev Mol Cell Biol*, *11*(4), 288-300.

Shenkar, R., Venkatasubramanian, P. N., Wyrwicz, A. M. *et al.* (2008a). Advanced magnetic resonance imaging of cerebral cavernous malformations: part II. Imaging of lesions in murine models. *Neurosurgery*, *63*(4), 790-7; discussion 797.

Shenkar, R., Venkatasubramanian, P. N., Zhao, J. C. *et al.* (2008b). Advanced magnetic resonance imaging of cerebral cavernous malformations: part I. High-field imaging of excised human lesions. *Neurosurgery*, *63*(4), 782-9; discussion 789.

Shi, H., Sheng, B., Zhang, F. *et al.* (2013). Kruppel-like factor 2 protects against ischemic stroke by regulating endothelial blood brain barrier function. *Am J Physiol Heart Circ Physiol*, *304*(6), H796-H805.

Shibue, T., Brooks, M. W., & Weinberg, R. A. (2013). An integrin-linked machinery of cytoskeletal regulation that enables experimental tumor initiation and metastatic colonization. *Cancer Cell*, *24*(4), 481-498.

Shweiki, D., Itin, A., Soffer, D. *et al.* (1992). Vascular endothelial growth factor induced by hypoxia may mediate hypoxia-initiated angiogenesis. *Nature*, *359*(6398), 843-845.

Siekmann, A. F., & Lawson, N. D. (2007). Notch signalling limits angiogenic cell behaviour in developing zebrafish arteries. *Nature*, *445*(7129), 781-784.

Siekmann, A. F., Standley, C., Fogarty, K. E. *et al.* (2009). Chemokine signaling guides regional patterning of the first embryonic artery. *Genes Dev*, *23*(19), 2272-2277.

Sirbu, I. O., Zhao, X., & Duester, G. (2008). Retinoic acid controls heart anteroposterior patterning by down-regulating Isl1 through the Fgf8 pathway. *Dev Dyn*, *237*(6), 1627-1635.

Slater, S. C., Ramnath, R. D., Uttridge, K. *et al.* (2012). Chronic exposure to laminar shear stress induces Kruppel-like factor 2 in glomerular endothelial cells and modulates interactions with co-cultured podocytes. *Int J Biochem Cell Biol*, *44*(9), 1482-1490.

Smith, K. A., Chocron, S., von der Hardt, S. *et al.* (2008). Rotation and asymmetric development of the zebrafish heart requires directed migration of cardiac progenitor cells. *Dev Cell*, *14*(2), 287-297.

Soncin, F., Mattot, V., Lionneton, F. *et al.* (2003). VE-statin, an endothelial repressor of smooth muscle cell migration. *EMBO J*, *22*(21), 5700-5711.

Song, Y., Eng, M., & Ghabrial, A. S. (2013). Focal defects in single-celled tubes mutant for Cerebral cavernous malformation 3, GCKIII, or NSF2. *Dev Cell*, *25*(5), 507-519.

Stainier, D. Y., Fouquet, B., Chen, J. N. *et al.* (1996). Mutations affecting the formation and function of the cardiovascular system in the zebrafish embryo. *Development*, *123*, 285-292.

Stainier, D. Y., Lee, R. K., & Fishman, M. C. (1993). Cardiovascular development in the zebrafish. I. Myocardial fate map and heart tube formation. *Development*, *119*(1), 31-40.

Stockton, R. A., Shenkar, R., Awad, I. A. *et al.* (2010). Cerebral cavernous malformations proteins inhibit Rho kinase to stabilize vascular integrity. *J Exp Med*, *207*(4), 881-896.

Storkebaum, E., Quaegebeur, A., Vikkula, M. *et al.* (2011). Cerebrovascular disorders: molecular insights and therapeutic opportunities. *Nat Neurosci*, *14*(11), 1390-1397.

Suchting, S., & Eichmann, A. (2009). Jagged gives endothelial tip cells an edge. *Cell*, *137*(6), 988-990.

Suchting, S., Freitas, C., le Noble, F. *et al.* (2007). The Notch ligand Delta-like 4 negatively regulates endothelial tip cell formation and vessel branching. *Proc Natl Acad Sci U S A*, *104*(9), 3225-3230.

Sugden, P. H., McGuffin, L. J., & Clerk, A. (2013). SOcK, MiSTs, MASK and STicKs: the GCKIII (germinal centre kinase III) kinases and their heterologous protein-protein interactions. *Biochem J*, *454*(1), 13-30.

Sumanas, S., Gomez, G., Zhao, Y. *et al.* (2008). Interplay among Etsrp/ER71, Scl, and Alk8 signaling controls endothelial and myeloid cell formation. *Blood*, *111*(9), 4500-4510.

Sumanas, S., & Lin, S. (2006). Ets1-related protein is a key regulator of vasculogenesis in zebrafish. *PLoS Biol*, *4*(1), e10.

Takeuchi, K., Yanai, R., Kumase, F. et al. (2014). EGF-Like-Domain-7 is required for VEGF-induced Akt/ERK activation and vascular tube formation in an *ex vivo* angiogenesis assay. *PLoS One*, 9(3), e91849.

Tammela, T., Zarkada, G., Wallgard, E. *et al.* (2008). Blocking VEGFR-3 suppresses angiogenic sprouting and vascular network formation. *Nature*, *454*(7204), 656-660.

Tanriover, G., Sozen, B., Seker, A. *et al.* (2013). Ultrastructural analysis of vascular features in cerebral cavernous malformations. *Clin Neurol Neurosurg*, *115*(4), 438-444.

Taylor, K. L., Henderson, A. M., & Hughes, C. C. (2002). Notch activation during endothelial cell network formation in vitro targets the basic HLH transcription factor HESR-1 and downregulates VEGFR-2/KDR expression. *Microvasc Res*, *64*(3), 372-383.

ten Klooster, J. P., Jansen, M., Yuan, J. *et al.* (2009). Mst4 and Ezrin induce brush borders downstream of the Lkb1/Strad/Mo25 polarization complex. *Dev Cell*,

16(4), 551-562.

Timmerman, L. A., Grego-Bessa, J., Raya, A. *et al.* (2004). Notch promotes epithelial-mesenchymal transition during cardiac development and oncogenic transformation. *Genes Dev*, *18*(1), 99-115.

Uhlik, M. T., Abell, A. N., Johnson, N. L. *et al.* (2003). Rac-MEKK3-MKK3 scaffolding for p38 MAPK activation during hyperosmotic shock. *Nat Cell Biol*, *5*(12), 1104-1110.

van Thienen, J. V., Fledderus, J. O., Dekker, R. J. *et al.* (2006). Shear stress sustains atheroprotective endothelial KLF2 expression more potently than statins through mRNA stabilization. *Cardiovasc Res*, *72*(2), 231-240.

Veerkamp, J., Rudolph, F., Cseresnyes, Z. *et al.* (2013). Unilateral dampening of Bmp activity by nodal generates cardiac left-right asymmetry. *Dev Cell*, *24*(6), 660-667.

Vermot, J., Forouhar, A. S., Liebling, M. *et al.* (2009). Reversing blood flows act through klf2a to ensure normal valvulogenesis in the developing heart. *PLoS Biol*, *7*(11), e1000246.

Villa, N., Walker, L., Lindsell, C. E. *et al.* (2001). Vascular expression of Notch pathway receptors and ligands is restricted to arterial vessels. *Mech Dev*, *108*(1-2), 161-164.

Villefranc, J. A., Amigo, J., & Lawson, N. D. (2007). Gateway compatible vectors for analysis of gene function in the zebrafish. *Dev Dyn*, *236*(11), 3077-3087.

Vogeli, K. M., Jin, S. W., Martin, G. R. *et al.* (2006). A common progenitor for haematopoietic and endothelial lineages in the zebrafish gastrula. *Nature*, *443*(7109), 337-339.

Wang, L., Zhang, P., Wei, Y. *et al.* (2011). A blood flow-dependent klf2a-NO signaling cascade is required for stabilization of hematopoietic stem cell programming in zebrafish embryos. *Blood*, *118*(15), 4102-4110.

Wang, S., Aurora, A. B., Johnson, B. A. *et al.* (2008). The endothelial-specific microRNA miR-126 governs vascular integrity and angiogenesis. *Dev Cell*, *15*(2), 261-271.

Wang, W., Ha, C. H., Jhun, B. S. *et al.* (2010a). Fluid shear stress stimulates phosphorylation-dependent nuclear export of HDAC5 and mediates expression of KLF2 and eNOS. *Blood*, *115*(14), 2971-2979.

Wang, X. Q., Nigro, P., World, C. *et al.* (2012). Thioredoxin interacting protein promotes endothelial cell inflammation in response to disturbed flow by increasing leukocyte adhesion and repressing Kruppel-like factor 2. *Circ Res*, *110*(4), 560-568.

Wang, Y., Kaiser, M. S., Larson, J. D. *et al.* (2010b). Moesin1 and Ve-cadherin are required in endothelial cells during in vivo tubulogenesis. *Development*, *137*(18), 3119-3128.

Wang, Y., Nakayama, M., Pitulescu, M. E. *et al.* (2010c). Ephrin-B2 controls VEGF-induced angiogenesis and lymphangiogenesis. *Nature*, *465*(7297), 483-486.

Wani, M. A., Conkright, M. D., Jeffries, S. *et al.* (1999). cDNA isolation, genomic structure, regulation, and chromosomal localization of human lung Kruppel-like factor. *Genomics*, *60*(1), 78-86.

Warga, R. M., & Kimmel, C. B. (1990). Cell movements during epiboly and gastrulation in zebrafish. *Development*, *108*(4), 569-580.

Watanabe, Y., Kokubo, H., Miyagawa-Tomita, S. *et al.* (2006). Activation of Notch1 signaling in cardiogenic mesoderm induces abnormal heart morphogenesis in

mouse. *Development*, *133*(9), 1625-1634.
Waxman, J. S., Keegan, B. R., Roberts, R. W. *et al.* (2008). Hoxb5b acts downstream of retinoic acid signaling in the forelimb field to restrict heart field potential in zebrafish. *Dev Cell*, *15*(6), 923-934.
Wegener, K. L., Partridge, A. W., Han, J. *et al.* (2007). Structural basis of integrin activation by talin. *Cell*, *128*(1), 171-182.
Weis, S. M., Lindquist, J. N., Barnes, L. A. *et al.* (2007). Cooperation between VEGF and beta3 integrin during cardiac vascular development. *Blood*, *109*(5), 1962-1970.
Westerfield, M., Doerry, E., Kirkpatrick, A. E. *et al.* (1997). An on-line database for zebrafish development and genetics research. *Semin Cell Dev Biol*, *8*(5), 477-488.
White, C. R., & Frangos, J. A. (2007). The shear stress of it all: the cell membrane and mechanochemical transduction. *Philos Trans R Soc Lond B Biol Sci*, *362*(1484), 1459-1467.
Whitehead, K. J., Chan, A. C., Navankasattusas, S. *et al.* (2009). The cerebral cavernous malformation signaling pathway promotes vascular integrity via Rho GTPases. *Nat Med*, *15*(2), 177-184.
Wu, C., Li, F., Han, G. *et al.* (2013). Abeta(1-42) disrupts the expression and function of KLF2 in Alzheimer's disease mediated by p53. *Biochem Biophys Res Commun*, *431*(2), 141-145.
Wu, F., Yang, L. Y., Li, Y. F. *et al.* (2009). Novel role for epidermal growth factor-like domain 7 in metastasis of human hepatocellular carcinoma. *Hepatology*, *50*(6), 1839-1850.
Wu, W., Xiao, H., Laguna-Fernandez, A. *et al.* (2011). Flow-Dependent Regulation of Kruppel-Like Factor 2 Is Mediated by MicroRNA-92a. *Circulation*, *124*(5), 633-641.
Wustehube, J., Bartol, A., Liebler, S. S. *et al.* (2010). Cerebral cavernous malformation protein CCM1 inhibits sprouting angiogenesis by activating DELTA-NOTCH signaling. *Proc Natl Acad Sci U S A*, *107*(28), 12640-12645.
Xie, P., Tang, Y., Shen, S. *et al.* (2011). Smurf1 ubiquitin ligase targets Kruppel-like factor KLF2 for ubiquitination and degradation in human lung cancer H1299 cells. *Biochem Biophys Res Commun*, *407*(1), 254-259.
Xu, X., Wang, X., Zhang, Y. *et al.* (2013). Structural basis for the unique heterodimeric assembly between cerebral cavernous malformation 3 and germinal center kinase III. *Structure*, *21*(6), 1059-1066.
Yelon, D., Horne, S. A., & Stainier, D. Y. (1999). Restricted expression of cardiac myosin genes reveals regulated aspects of heart tube assembly in zebrafish. *Dev Biol*, *214*(1), 23-37.
You, C., Sandalcioglu, I. E., Dammann, P. *et al.* (2013). Loss of CCM3 impairs DLL4-Notch signalling: implication in endothelial angiogenesis and in inherited cerebral cavernous malformations. *J Cell Mol Med*, *17*(3), 407-418.
Young, A., Wu, W., Sun, W. *et al.* (2009). Flow activation of AMP-activated protein kinase in vascular endothelium leads to Kruppel-like factor 2 expression. *Arterioscler Thromb Vasc Biol*, *29*(11), 1902-1908.
Zawistowski, J. S., Stalheim, L., Uhlik, M. T. *et al.* (2005). CCM1 and CCM2 protein interactions in cell signaling: implications for cerebral cavernous malformations pathogenesis. *Hum Mol Genet*, *14*(17), 2521-2531.
Zhang, J., Basu, S., Rigamonti, D. *et al.* (2008). Krit1 modulates beta 1-integrin-

mediated endothelial cell proliferation. *Neurosurgery*, *63*(3), 571-8; discussion 578.

Zhang, J., Clatterbuck, R. E., Rigamonti, D. *et al.* (2001). Interaction between krit1 and icap1alpha infers perturbation of integrin beta1-mediated angiogenesis in the pathogenesis of cerebral cavernous malformation. *Hum Mol Genet*, *10*(25), 2953-2960.

Zhang, M., Dong, L., Shi, Z. *et al.* (2013a). Structural mechanism of CCM3 heterodimerization with GCKIII kinases. *Structure*, *21*(4), 680-688.

Zhang, Y., Tang, W., Zhang, H. *et al.* (2013b). A network of interactions enables CCM3 and STK24 to coordinate UNC13D-driven vesicle exocytosis in neutrophils. *Dev Cell*, *27*(2), 215-226.

Zheng, X., Xu, C., Di Lorenzo, A. *et al.* (2010). CCM3 signaling through sterile 20-like kinases plays an essential role during zebrafish cardiovascular development and cerebral cavernous malformations. *J Clin Invest*, *120*(8), 2795-2804.

Zheng, X., Xu, C., Smith, A. O. *et al.* (2012). Dynamic regulation of the cerebral cavernous malformation pathway controls vascular stability and growth. *Dev Cell*, *23*(2), 342-355.

Zhu, Y., Wu, Q., Xu, J. F. *et al.* (2010). Differential angiogenesis function of CCM2 and CCM3 in cerebral cavernous malformations. *Neurosurg Focus*, *29*(3), E1.

Ziegler, W. H., Liddington, R. C., & Critchley, D. R. (2006). The structure and regulation of vinculin. *Trends Cell Biol*, *16*(9), 453-460.

Acknowledgement

First and foremost, I would like to thank Prof. Dr. Salim Seyfried for the valuable guidance and advice and for giving me this exiting project. I would also like to thank Prof. Harald Saumweber for being my supervisor at the Humboldt University Berlin. Special thanks go to all former and current members of the Seyfried lab, including Cecile Otten, Jana Richter, Robby Fechner, Björn Fiege, Stefan Donat, Veronica Lombardo, Marta Rocha Lourenco, Justus Veerkamp, Florian Priller and Ann-Christin Dietrich.

Finally, I am forever indebted to my family and Pia for their understanding, endless love and encouragement during my studies and my PhD.

Publications

Renz, M., Otten, O., Faurobert, E., Rudolph, F., Zhu, Y., Boulday, G., Duchene, J., Mickoleit, M., Abdelilah-Seyfried, S. *et al.* (2015). Regulation of β1 Integrin-Klf2-mediated angiogenesis by CCM proteins. *Dev. Cell*, 32:181-190.

Veerkamp, J., Rudolph, F., Cseresnyes, Z., Priller, F., Otten, C., **Renz, M.**, Schaefer, L. and Abdelilah-Seyfried, S. (2013). Unilateral dampening of BMP activity by Nodal generates cardiac left-right asymmetrie. *Dev. Cell*, 24(6):660-7.

Date

Signature

Selbständigkeitserklärung

Hiermit erkläre ich, dass ich die vorliegende Arbeit selbständig und nur unter Verwendung der angegebenen Hilfsmittel angefertigt habe. Diese Arbeit wurde keiner anderen Prüfungsbehörde vorgelegt. Die Promotionsordnung der Mathematisch-Naturwissenschaftlichen Fakultät I der Humboldt-Universität zu Berlin vom 06. Juli 2009 habe ich gelesen und akzeptiert.

Datum

Unterschrift